



1977

Missile employment from fast patrol boats : a computer-based analysis of the search-sector parameters.

Lehmann, Bernd, Dipl-Geol

Monterey, California. Naval Postgraduate School

<http://hdl.handle.net/10945/18205>



Calhoun is a project of the Dudley Knox Library at NPS, furthering the precepts and goals of open government and government transparency. All information contained herein has been approved for release by the NPS Public Affairs Officer.

Dudley Knox Library / Naval Postgraduate School
411 Dyer Road / 1 University Circle
Monterey, California USA 93943

<http://www.nps.edu/library>

NAVAL POSTGRADUATE SCHOOL

Monterey, California



THESIS

MISSILE EMPLOYMENT FROM FAST PATROL BOATS.
COMPUTER-BASED ANALYSIS OF THE
SEARCH-SECTOR PARAMETERS

by

Bernd Lehmann
Lieutenant Commander, Federal German Navy

June 1977

Thesis Advisor:

D. E. Harrison

Approved for public release; distribution unlimited.

T178042

REPORT DOCUMENTATION PAGE		READ INSTRUCTIONS BEFORE COMPLETING FORM
1. REPORT NUMBER	2. GOVT ACCESSION NO.	3. RECIPIENT'S CATALOG NUMBER
4. TITLE (and Subtitle) MISSILE EMPLOYMENT FROM FAST PATROL BOATS. A COMPUTER-BASED ANALYSIS OF THE SEARCH-SECTOR PARAMETERS		5. TYPE OF REPORT & PERIOD COVERED Master's Thesis; June 1977
7. AUTHOR(s) Bernd Lehmann, Lieutenant Commander, Federal German Navy		6. PERFORMING ORG. REPORT NUMBER
9. PERFORMING ORGANIZATION NAME AND ADDRESS Naval Postgraduate School Monterey, California 93940		8. CONTRACT OR GRANT NUMBER(s)
11. CONTROLLING OFFICE NAME AND ADDRESS Naval Postgraduate School Monterey, California 93940		10. PROGRAM ELEMENT, PROJECT, TASK AREA & WORK UNIT NUMBERS
14. MONITORING AGENCY NAME & ADDRESS (if different from Controlling Office) Naval Postgraduate School Monterey, California 93940		12. REPORT DATE June 1977
		13. NUMBER OF PAGES 137
		15. SECURITY CLASS. (of this report) Unclassified
		15a. DECLASSIFICATION/DOWNGRADING SCHEDULE
16. DISTRIBUTION STATEMENT (of this Report) Approved for public release; distribution unlimited.		
17. DISTRIBUTION STATEMENT (of the abstract entered in Block 20, if different from Report)		
18. SUPPLEMENTARY NOTES		
19. KEY WORDS (Continue on reverse side if necessary and identify by block number) target motion analysis, sensitivity of missile search parameters, improvement of probability of acquisition by shift of the aimpoint, unassisted targeting, and assisted targeting		
20. ABSTRACT (Continue on reverse side if necessary and identify by block number) The objective of this computer-based analysis is to investigate the effect of target evasive maneuvers on the probability of acquisition by the seeker of the surface-to-surface missile MM 38 "Exocet" employed from Federal German Navy Fast Patrol Boats. Two different targeting methods, the unassisted and the assisted (by helicopter or remotely piloted vehicle) are analyzed with respect to the dependence of the probability of acquisition upon sensor capabilities, missile characteristics, and the motion of the target, in		

20. (Continued)

particular the interdependence between the various missile search-sector parameters, the target range, and the target aspect-angle. The influence of the radar cross-section at different aspect-angles of the various Warsaw Pact Navy surface vessels are not considered in this unclassified analysis. The most effective measures to significantly improve the probability of acquisition are the shift of the point of aim and the minimization of the target reaction-time.

Approved for public release; distribution unlimited.

MISSILE EMPLOYMENT FROM FAST PATROL BOATS.
A COMPUTER-BASED ANALYSIS OF THE SEARCH-SECTOR PARAMETERS

by

Bernd Lehmann
Lieutenant Commander, Federal German Navy

Submitted in partial fulfillment of the
requirements for the degree of

MASTER OF SCIENCE IN OPERATIONS RESEARCH

from the
NAVAL POSTGRADUATE SCHOOL

June 1977

ABSTRACT

The objective of this computer-based analysis is to investigate the effect of target evasive maneuvers on the probability of acquisition by the seeker of the surface-to-surface missile MM 38 "Exocet" employed from Federal German Navy Fast Patrol Boats. Two different targeting methods, the unassisted and the assisted (by helicopter or remotely piloted vehicle) are analyzed with respect to the dependence of the probability of acquisition upon sensor capabilities, missile characteristics, and the motion of the target, in particular the interdependence between the various missile search-sector parameters, the target range, and the target aspect-angle. The influence of the radar cross-section at different aspect-angles of the various Warsaw Pact Navy surface vessels are not considered in this unclassified analysis. The most effective measures to significantly improve the probability of acquisition are the shift of the point of aim and the minimization of the target reaction-time.

TABLE OF CONTENTS

I.	INTRODUCTION.....	11
A.	OBJECTIVES OF THE ANALYSIS.....	11
B.	PRESENTATION OF THE TARGETING-SCHEMES.....	14
C.	PATTERN OF THE ANALYSIS.....	16
II.	DESCRIPTION OF RELATED WEAPON-SYSTEMS.....	17
A.	FPBG-CLASSES 143/148.....	17
1.	Technical Data.....	17
2.	Performance Variables.....	20
B.	EXTENDED PLATFORM.....	21
1.	Performance Variables.....	21
C.	MM 38 "EXOCET" MISSILE-SYSTEM.....	23
1.	Technical Data.....	23
2.	The Missile Trajectory.....	25
a.	The Vertical Missile Trajectory.....	25
b.	The Horizontal Missile Trajectory....	26
3.	Performance Variables.....	28
III.	GENERAL ASSUMPTIONS.....	30
A.	ENVIRCNMENTAL FACTORS.....	30
B.	TACTICAL CONDITIONS ASSUMED FOR OWN FORCES...	32
C.	TACT. CONDITIONS ASSUMED FOR HOSTILE FORCES..	33
1.	Enemy Surface-Combattants.....	33
2.	Enemy Reaction-Time.....	34
3.	Enemy Countermeasures.....	36
a.	Speed/Course-Changes.....	36
b.	Electronic-Warfare.....	38
D.	SUMMARY OF RELEVANT VARIABLES.....	38
IV.	TARGETING REQUIREMENTS.....	40
A.	SEARCH-PATTERN DIMENSIONS.....	40
B.	SHIFT OF THE POA.....	45
V.	MEASURE OF EFFECTIVENESS/STATIST. REQUIREMENTS...	48

A.	MEASURE OF EFFECTIVENESS.....	48
B.	SAMPLE SIZE.....	49
C.	VALIDATION.....	50
VI.	UNASSISTED TARGETING-SCHEME.....	51
A.	TARGETING GEOMETRY.....	51
B.	RESULTS.....	54
1.	PA w/r to Wind Effects.....	55
2.	PA w/r to Target Range.....	55
3.	PA w/r to Target Aspect-Angle.....	61
4.	PA w/r to POA-Shift.....	80
5.	PA w/r to Detection-Delay.....	82
C.	CONCLUSIONS AND RECOMMENDATIONS.....	83
1.	Conclusions.....	83
2.	Recommendations.....	85
VII.	ASSISTED TARGETING-SCHEME.....	86
A.	RESULTS.....	88
1.	PA w/r to HC-Location.....	89
2.	PA w/r to HC-Sensor Data.....	92
3.	PA w/r to POA-shift.....	98
B.	CONCLUSIONS/RECOMMENDATIONS.....	101
1.	Conclusions.....	101
2.	Recommendations.....	102
Appendix A:	TARGET-MOTION-ANALYSIS.....	103
Appendix B:	ELECTROMAGNETIC RADIATION RANGE PREDICTION.	110
Appendix C:	SIMULATION-MODEL MM38-UAT.....	113
Appendix D:	SIMULATION-MODEL MM38-OTH.....	123
	LIST OF REFERENCES.....	135
	INITIAL DISTRIBUTION LIST.....	136
	LIST OF TABLES.....	7
	LIST OF FIGURES.....	9

LIST OF TABLES

I	Relevant Data for the Analysis.....	39
II	CR/DR-Dimensions.....	44
III	Relation Search Pattern/Aspect-angle Maximum Target Range for PA=0.99 DDG Krivak-Class (Low Speed).....	56
IV	Relation Search Pattern/Aspect-angle Maximum Target Range for PA=0.99 PFG Nanuchka-Class.....	57
V	Relation Search Pattern/Aspect-angle Maximum Target Range for PA=0.99 FPBG Osa-Class.....	58
VI	Relation Search Pattern/Aspect-angle Maximum Target Range for PA=0.99 LSM Polnocny-Class.....	59
VII	Relation Search Pattern/Aspect-angle Maximum Target Range for PA=0.99 DDG Krivak-Class (High Speed).....	60
VIII	PA-Results for Different DETDEL-Values DDG Krivak-Class.....	81
IX	PA-Results for Low/High Initial Speed for DDG Krivak-Class with 30° Aspect.....	82
X	PA-Results for BLPEP of 10°.....	90
XI	PA-Results for BLPEP of 20°.....	91
XII	PA-Results for SIGBE of 10°.....	

	BLPEP 10°/Aspect-Angle -30°.....	94
XIII	PA-Results for SIGBE of 2°	
	BLPEP 10°/Aspect-Angle -30°.....	95
XIV	PA-Results for SIGBE of 3°	
	BLPEP 10°/Aspect-Angle -30°.....	96
XV	PA-Results for SIGBE of 1°	
	BLPEP 10°/Aspect-Angle 0°.....	97
XVI	PA-Results w/r to POA-Shift	
	SIGBE 1°/BLPEP 10°/Aspect-Angle -30°.....	99
XVII	PA-Results w/r to POA-Shift	
	SIGBE 2°/BLPEP 10°/Aspect-Angle -30°.....	100

LIST OF FIGURES

1.	Targeting-Schemes.....	15
2.	FPBG-Classes 143/148.....	19
3.	MM 38 EXOCET-SSM.....	23
4.	Missile Trajectory in the Vertical Plane.....	26
5.	Missile Trajectory in the Horizontal Plane.....	27
6.	Approximation of the Search Pattern.....	41
7.	Relation Search-Angle/Scan-Angle.....	42
8.	Reduction of the Search Pattern.....	43
9.	Construction of the POA-Shift.....	46
10.	Relation of Search-Pattern and POA-Shift.....	47
11.	Targeting Geometry for Model MM38-UAT (without POA-Shift).....	52
12.	Targeting Geometry for Model MM38-UAT (with POA-Shift).....	53
13.	Relation PA - Target Aspect-Angle w/o POA-Shift DDG Target (Low Speed) - RP9 -.....	62
14.	Relation PA - Target Aspect-Angle w/o POA-Shift DDG Target (High Speed) - RP9 -.....	63
15.	Relation PA - Target Aspect-Angle w/o POA-Shift LSM Target - RP9 -.....	64
16.	Relation PA - Target Aspect-Angle w/o POA-Shift DDG Target (Low Speed) - RP5 -.....	66

17.	Relation PA - Target Aspect-Angle w/o POA-Shift DDG Target (High Speed) - RP5 -.....	67
18.	Relation PA - Target Aspect-Angle w/o POA-Shift LSM Target - RP5 -.....	68
19.	Relation PA - Target Aspect-Angle w/o POA-Shift DDG Target (Low Speed) - RP1 -.....	70
20.	Relation PA - Target Aspect-Angle w/o POA-Shift DDG Target (High Speed) - RP1 -.....	71
21.	Relation PA - Target Aspect-Angle w POA-Shift LSM Target - RP1 -.....	72
22.	Relation PA - Target Aspect-Angle w POA-Shift DDG Target (Low Speed) - RP9 -.....	74
23.	Relation PA - Target Aspect-Angle w POA-Shift DDG Target (High Speed) - RP9 -.....	75
24.	Relation PA - Target Aspect-Angle w POA-Shift DDG Target (Low Speed) - RP5 -.....	76
25.	Relation PA - Target Aspect-Angle w POA-Shift DDG Target (High Speed) - RP5 -.....	77
26.	Relation PA - Target Aspect-Angle w POA-Shift DDG Target (Low Speed) - RP1 -.....	78
27.	Relation PA - Target Aspect-Angle w POA-Shift DDG Target (High Speed) - RP1 -.....	79
28.	Targeting-geometry for the OTH-scheme.....	87
29.	The Construction of the Outer Boundary.....	106
30.	The Comparison of Two Position Areas and a Search-Sector.....	108
31.	Outer Boundary for DDG Krivak-Class.....	109

I. INTRODUCTION

A. OBJECTIVES OF THE ANALYSIS

This computer-based analysis provides preliminary tactical recommendations for the employment of the MM 38 "EXOCET" Surface-to-Surface-Missile (SSM) from Federal German Navy (FGN) Fast Patrol Boats (FPBG) Class 143 (10 boats) and Class 148 (20 boats). These boats have a displacement of less than 400 tons, and their main operation area is the Baltic Sea and its approaches.

The successful employment of a missile against a target is primarily dependent on its target-aquisition (TA) capability, measured by the probability of acquisition (PA). A significant characteristic of any SSM of the present generation is, that due to the technological limitations, its seeker can not discriminate between several targets in the assigned search-area.

The solution of the problem of target-discrimination (TD) - the seeker acquires only the selected target - is very desirable in multiship naval engagements. TD can be improved by decreasing the search area of the missile, but this also decreases the probability that the desired target will be acquired, a result which normally can not be accepted.

These two competing requirements, TA and TD, require a thorough investigation of the various missile search-sector

parameters' influence on the targeting-scheme chosen in an assumed tactical scenario.

The search-sector area, which is defined by three variable parameters, must

1. ensure a PA of 0.99 - a specification required by the FGN. The very high probability is chosen to compensate for uncertainties of the system reliability and target-data related errors like course and speed, range and bearing. This requirement results in maximizing the possible search-sector area with the consequence that almost all target discrimination is lost.

2. achieve an improved target discrimination. This requirement can be achieved by minimizing the search-sector area.

3. prevent premature detection and identification of own missiles in flight and therefore minimize effective enemy Anti-Ship-Missile-Defense (ASMD). This can be only achieved by minimizing the missile seeker activation-distance, which would decrease the actual search-area, and thereby improve the target discrimination.

In the view of these three requirements, the analysis investigates the dependence of PA upon sensor capabilities, missile characteristics, and the motion of the target, in particular the interdependence between the various search-sector parameters, the target range, and the target aspect-angle. Eight hypotheses with respect to TA and TD result from "improvement-considerations":

1.Target-Acquisition (TA)

(1) TA can be improved by reducing the missile launching-distance.

(2) TA can be improved by a proper choice of the aspect-angle to the target.

(3) TA can be improved by shifting the aim-point in the direction of the expected target-motion.

(4) TA can be improved by any combination of (1), (2), and (3).

2.Target-Discrimination (TD)

(5) TD can be improved by reducing the missile seeker activation-distance,

(6) TD can be improved by reducing the missile-scan-angle.

(7) TD can be improved by reducing the missile-seeker search-depth.

(8) TD can be improved by any combination of (5), (6) and/or (7).

Although TD considerations will be included where appropriate, this analysis deals with one-on-one scenarios, and the multiship-engagement is not analyzed.

B. PRESENTATION OF THE TARGETING-SCHEMES

The analysis examines two scenarios which correspond to two anticipated targeting-schemes:

- * Unassisted Targeting (UAT),

- * Over-the-Horizon Targeting (OTH).

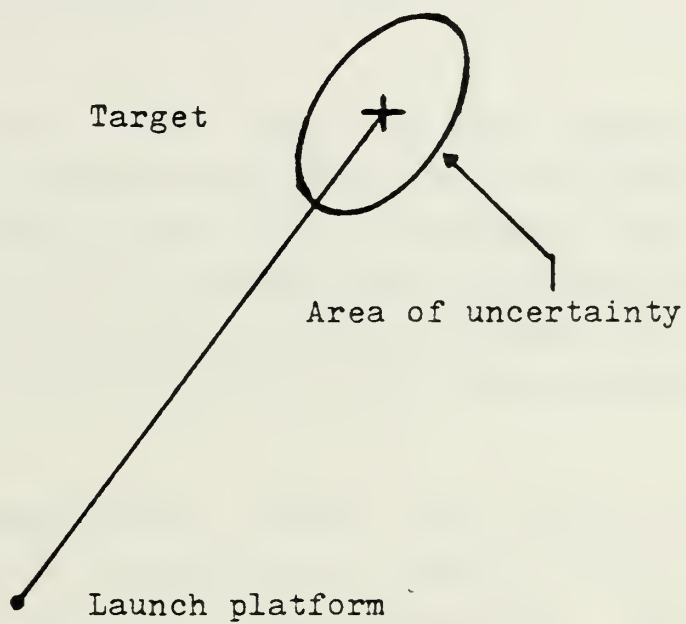
Fig 1 depicts these two schemes.

1. UAT - The single ellipse in the first box indicates that UAT has one source of targeting error - the launch-platform's sensor error. The attack range is limited to the line-of-sight horizon.

2. OTH - This procedure has an additional source of error - the uncertainty of position of the extended platform - which also contributes to the final target position error. The upper bound for the attack range is the missile range itself.

The computer simulations are similar, and share many common features, but the OTH analysis is more complex. In each case the engagement is followed until the missile is in position to achieve Lock-on. Target ASMD-options other than maneuvers are not considered; it is assumed that the target accelerates to maximum speed when aware of the "threat" and maneuvers in a fashion to evade the missile seeker search area.

Unassisted Targeting-scheme (UAT)



Assisted Targeting-scheme (OTH)

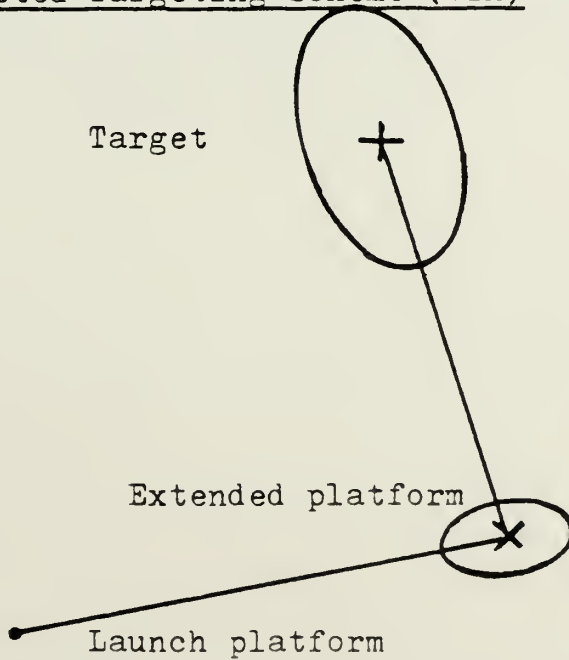


Figure 1 - TARGETING-SCHEMES

C. PATTERN OF THE ANALYSIS

A description of the related weapon systems and the introduction of relevant variables for the simulation, based on the performance characteristics, precedes the statement of necessary general assumptions, targeting requirements, and the evaluation of the targeting-schemes as one-on-one engagements. Finally, conclusions and recommendations are presented.

The recommendations reflect only generalized scenario situations due to a suppression of complete data about own and hostile forces and their capabilities. Two appendices illustrate the target-motion analysis and sensor performance prediction. The simulation models for both targeting-schemes are provided as a computer printout. Results and recommendations for the real systems are available as a classified appendix.

II. DESCRIPTION OF RELATED WEAPONS-SYSTEMS

The performance characteristics of the three weapon systems and their degree of sensitivity dominate the successful missile employment. Relevant variables are introduced to describe and represent these characteristics in the simulation models for both targeting-schemes..

A. FPBG-CLASSES 143/148

These two FPBG-Classes are the launch platforms for the missile MM 38 in both targeting-schemes; there is no distinction between their different capabilities in the simulation model.

1. Technical Data

Both classes have a displacement hull-design, and their propulsion-system consists of four diesels delivering a total of 16000 HP (143), 12000 HP (148).

The armament of Class 143 consists of

- Four SNIAS MM38 EXOCET missiles
- Two 76 mm OTO-MELARA general-purpose gun mounts
- Two tubes with wire-guided torpedoes

The armament of Class 148 is similar to that of

Class 143 and consists of

- Four SNIAS MM38 EXOCET missiles
- One 76 mm OTO-MELARA general-purpose gun mount
- One 40 mm BOFORS anti-aircraft gun
- Eight mines

The Class 143 carries a fully integrated command and fire-control system - data automation system AGIS. Target data can be almost immediately analyzed by AGIS, a capability, which is not provided on the Class 148 [1].

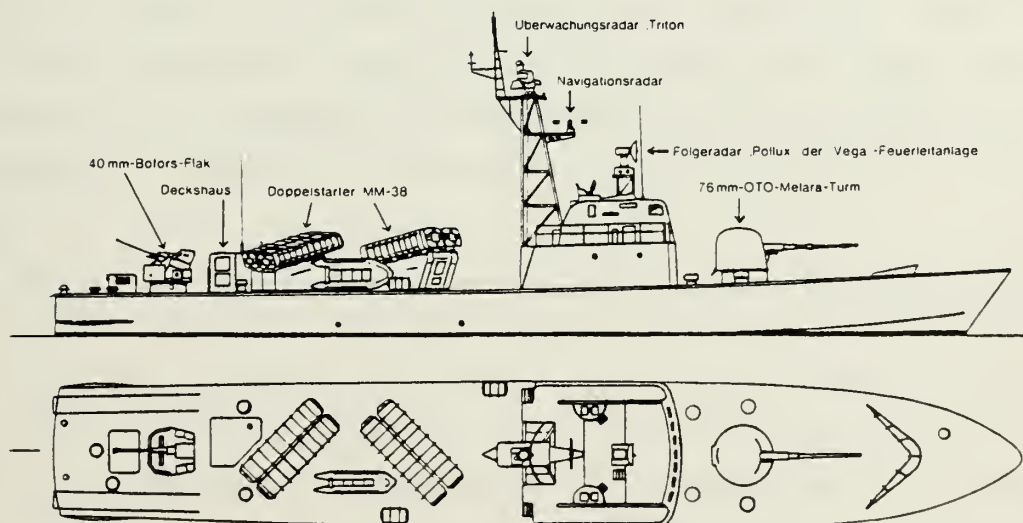
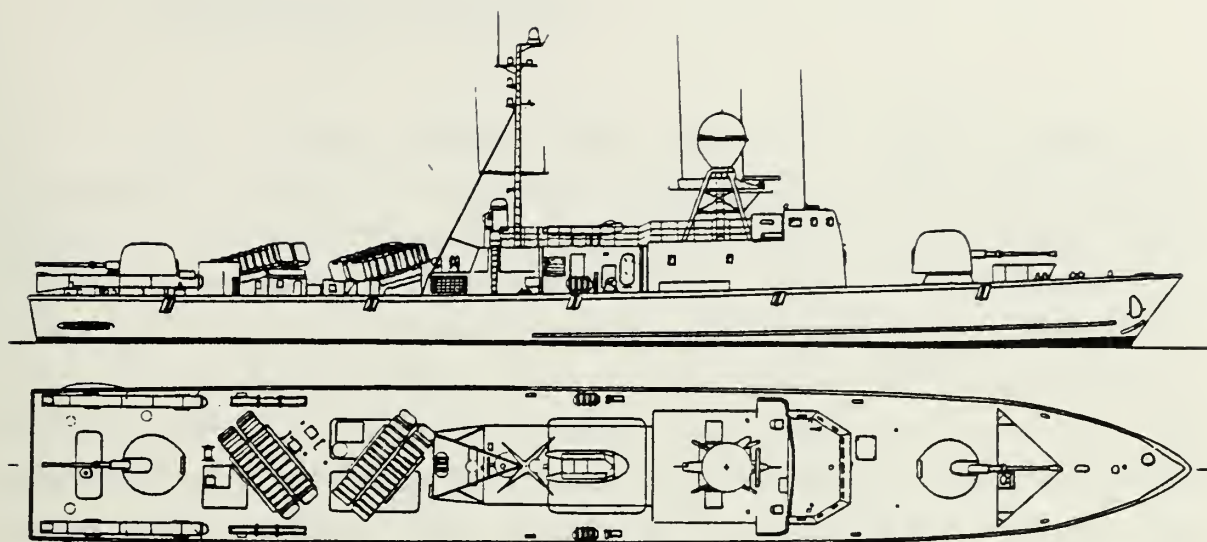


Figure 2 - FPBG CLASSES 143/148

2. Performance Variables

At least intermittent use of active radar is required to provide reliable target-data. The performance data of the active sensors are pertinent for the simulation model. The surface search radar on both FPBG-Classes is used to detect the target and to obtain further target data; its use is suggested for the unassisted targeting-scheme. The assisted targeting-scheme requires the use of the fire-control radar to establish a radar-fix on the extended platform. Target data evaluation is performed without the use of AGIS, which results in a degraded quality of the data - larger inaccuracy - and in an increase of the delaytime. The bearing and range errors are normally distributed random variables with mean-values of 0 and standard deviations (SIGBL, SIGRL) of 0.25° and 120 m respectively. The errors in the evaluated target data for course and speed are also assumed to be normally distributed with mean-values of 0 and respective standard deviations (SIGCL, SIGSL) of 3.5° and 0.4 kts.

σ_{BL} = standard deviation of the sensor bearing error,

σ_{RL} = standard deviation of the sensor range error,

σ_{CL} = standard deviation of the target-course error, and

σ_{SL} = standard deviation of the target-speed error.

B. EXTENDED PLATFORM

In this analysis extended platforms are considered to be either a helicopter (HC) or a remotely piloted vehicle (RPV). Both are means to extend the "information-range" of the launch platform, which is limited to the radar horizon without this support.

At the present time the FGN deploys only the land-based "Seaking" Mk 41 HC in its Search and Rescue-version. Until the introduction of a HC or RPV more suitable for this purpose it is reasonable to assume that the present HC might be used as an extended platform in cooperation with the FPBG-force, if appropriate conditions - geographical factors as well as the degree of air-threat - prevail. Because no suitable HC is presently being procured, detailed performance data are not available. Here the technical description of the HC are characteristics of the "Seaking" Mk 41 and the "Lamps" Mk 2. Electronic/optronic detection and communications are postulated. The HC or the RPV is used as a "Third Party" for the assisted targeting-scheme.

1. Performance Variables

The sensor performance data are also the standard deviations (SIGBE, SIGRE) of the normally distributed random errors in bearing and range. The mean-values of these errors are also assumed to be 0. The sensor inaccuracies will be 30 m in range, and from 1° to 3° in bearing. The target data for course and speed, which are a combination of measurement and human evaluation, contain errors which are also assumed to be normally distributed with mean-values of

0 and standard deviations (SIGCE, SIGSE) of 5° and 1.5 kts.

σ_{BE} = standard deviation of the sensor bearing error,

σ_{RE} = standard deviation of the sensor range error,

σ_{CE} = standard deviation of the target-course error, and

σ_{SE} = standard deviation of the target-speed error.

σ_{BL} , σ_{BE} , σ_{RL} , and σ_{RE} are solely sensor-related. whereas

σ_{CL} , σ_{CE} , σ_{SL} , and σ_{SE} have an additional error due to human

performance for the 148-Class boats, and, in the case of the use of an extended platform, because these two data sets are not directly evaluated by AGIS.

C. MM 38 "EXOCET" MISSILE-SYSTEM

The following technical presentation of this SSM and the trajectory description in the vertical and horizontal plane was partially drawn from an unclassified report [2]. It provides a good presentation of the general trajectory characteristics of the MM 38.

1. Technical Data

The missile was developed in the late sixties, and its first successful launch was recorded in June 1971. The air-tight container, in which the missile is stored, also serves as the launcher. The warhead is a classic fragmentation type with blast effect and a weight of 165 kg; it has a delayed impact fuze and a proximity fuze controlled by the autopilot.

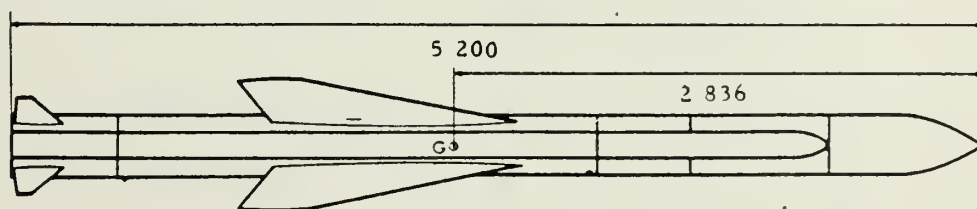


Figure 3 - MM 38 EXOCET-SSM

The missile with its sea-skimming trajectory has a maximum range of 22.7 nm (42000 m), a practical range of 20.5 nm (38000 m), and a minimum range of 2.5 nm (4500 m). Its cruise speed is specified as 315 m/sec (Mach 0.93), The midcourse flight altitude is 10-15 m, the final phase altitude is 2-5 m. The trajectory launch-phase covers about 2.2 nm (4000 m), the midcourse phase about 11.9 nm (22000 m), and the final phase about 6.4 nm (12000 m). Target information is normally provided by radar (active/passive), but visual bearing and estimated range can be set manually.

The variable size of the search-area is primarily dependent on 3 different parameters, which have to be determined/set before launch:

- Missile seeker-activation-distance ACTIV (m), related to the target-distance at launch-time,
- Missile seeker-scan-angle \pm PHI (deg), centered on the point-of-aim (POA), and
- Missile seeker-search-depth \pm L (m), related to the target-distance at launch-time.

The parameter-settings are assumed as follows:

- small (K), and
- large (G).

The resulting parameter combinations are KKK, KKG, KGK, and KGG for the small activation-distance, and GKK, GKG, G GK, and GGG for the large activation-distance. The second letter refers to the scan-angle, and the third letter determines the size of the search-depth. Additionally, the search-sector size is dependent on the lobe-width of the missile radar.

2. The Missile Trajectory

It should be pointed out that the following description of the missile trajectory reflects a particular parameter combination which is necessary to assure a very high PA. The homing-head search-area is always ground-stabilized, and adjusted in size to cover aiming and system errors and to allow for almost all possible target-motions. The largest values of all adjustable parameters assure a large PA, but lead to very poor TD.

a. The Vertical Missile Trajectory

For the following description refer to Fig 4. At the end of the launch phase the missile is stabilized in the direction of the target at the midcourse altitude H_1 . This altitude H_1 satisfies a dual requirement: while being low enough to avoid detection by the target until the missile is a given distance from it, the missile is still high enough to allow its seeker head to rapidly acquire the target after activation. At the end of the midcourse phase, the missile descends to an altitude ($H_2 < H_1$), chosen to meet the same requirements as H_1 but at a shorter distance from the target. Finally, the missile covers the final approach phase at the lowest altitude ($H_3 < H_2$) permitted by the sea state. The search phase, which follows the activation of the seeker head, can take place either at the end of the midcourse phase, or during the approach phase, depending on the launch range. Normally the altitude H_3 guarantees the impact on the target, otherwise the proximity fuze will detonate.

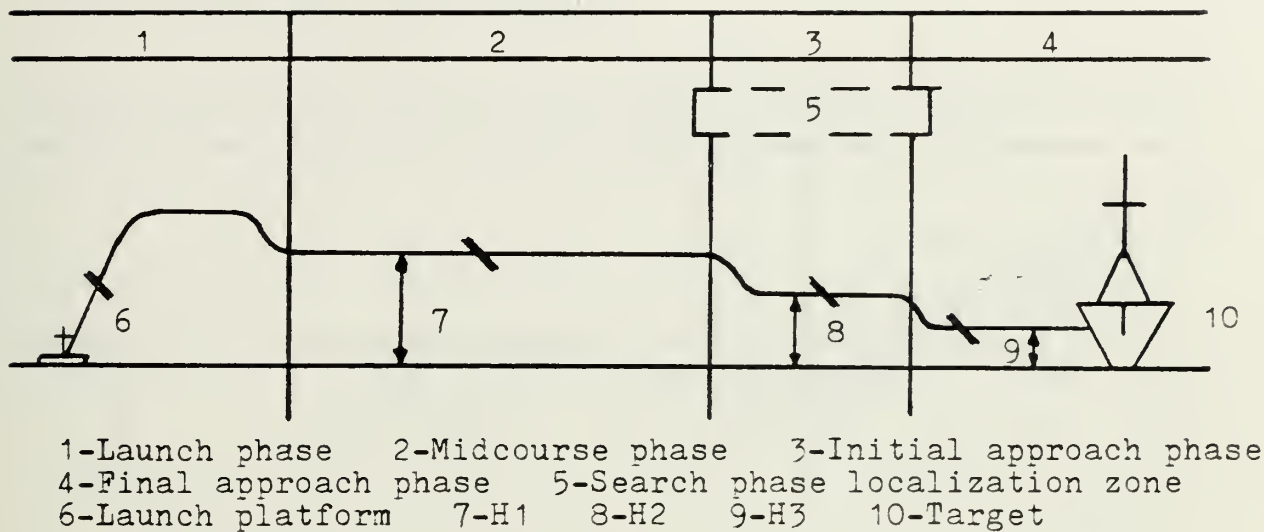
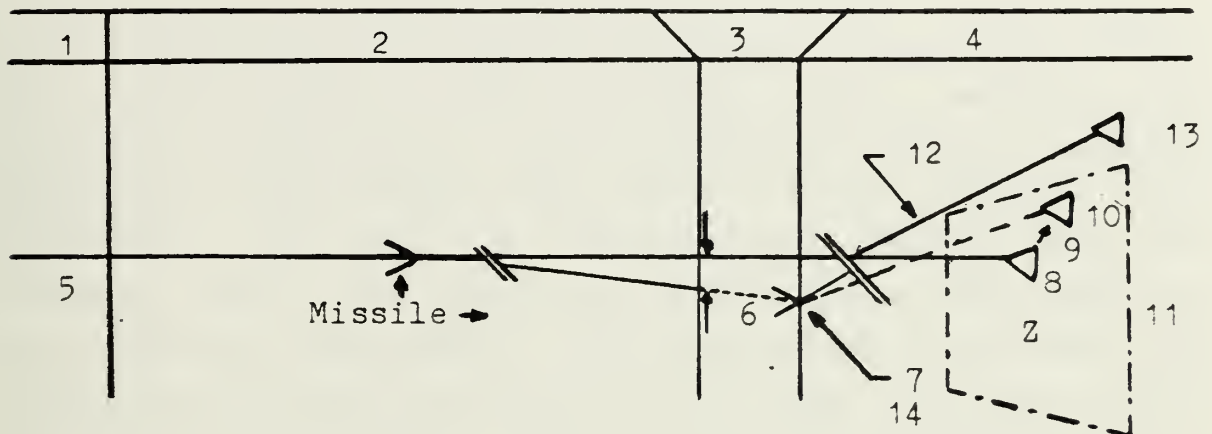


Figure 4 - MISSILE TRAJECTORY IN THE VERTICAL PLANE

b. The Horizontal Missile Trajectory

For the following description refer to Fig 5. The horizontal trajectory shows that the missile flies (at altitude H1) towards the target's position B1, which is designated at the instant of launching. Regardless of the surface wind, the missile's inertial platform maintains it on its path to a within a small error, until the end of the midcourse phase. At a given distance, D, from B1, the seeker is activated, and sweeps a predetermined zone, Z, sufficient to compensate for any navigational errors, any launching errors in target designation, and particularly any changes in the target's course during the missile flight. The target is detected at B3, at the end of a short search phase. Immediately, there is an exchange of data between the seeker and the inertial platform to determine the target's motion, counter any possible maneuvers, overcome

any ECM, and under the surveillance of the radar altimeter, choose the best point of impact.



- | | | |
|----------------|---------------------------|------------------------|
| 1-Launch phase | 2-Midcourse phase | 3-Search phase |
| 4-Homing phase | 5-Launch platform | 6-Error |
| 7-Detection | 8-B1 | 9-B2 |
| 10-B3 | 11-Search pattern | |
| 12-Homing | 13-Actual target position | 14-Activation distance |

Figure 5 - MISSILE TRAJECTORY IN THE HORIZONTAL PLANE

3. Performance Variables

The search parameter settings - chosen just before the actual launch - are constants; they reflect the evaluated target-data. Wind direction and speed are both variables, established just prior to the launch, and therefore are built as deterministic values into the computer model. The choice of the activation time dominates the missile performance. When activation is delayed, the target has a greater time in which to react, and the PA of the system is degraded. Prior to the actual missile launch, a time of 12 sec is necessary for the missile gyro stabilisation (MISRED). This delay is included in the assisted targeting-scheme. The unassisted targeting-scheme simulation is initiated with the launch command. It takes 2.5 sec (T_{LAUN}) on an average, until the missile has actually left the launcher.

The missile speed of 315 m/sec plus a normally distributed random variable with a mean-value of 0 and a standard deviation (SIGVM) of 1.5 m/sec determines the flight time until the expected Lock-on. This flight time can be influenced by the downrange component of the prevailing wind.

The missile seeker will be activated at the preprogrammed activation-distance, and it is fully operational after 3 sec (T_{OP}). The search for the target is terminated with the Lock-on of the homing head which occurs after 0.4 sec or 2.4 sec (T_{SCAN}) as a function of the choice

of the scan-angle, ϕ , the number of scans necessary to lock-on, and the scan-speed of the seeker. It is evident that this delay caused by T_{OP} and T_{SCAN} will significantly influence the size of the actual search area. These three defined times are summed to the variable T_{DEL} , which has a value of 5.90 sec or 7.90 sec, dependent on the scan-angle ϕ .

The actual missile flight-time (T_{FLIT}) until the Lock-on is a function of the target range and the actual missile speed, the selected activation-distance, and the scan-angle. The actual Time of Lock-on (T_{LOCK}) is given by

$$T_{LOCK} = T_{FLIT} + T_{LAUN}.$$

The value of T_{LOCK} also determines the navigation error of the missile, which is circular normally distributed with a mean-value of 0 and a standard deviation ($SLOKB$, $SLOKR$) of $T_{LOCK} * 1.62$ m/sec.

III. GENERAL ASSUMPTIONS

Due to the number of factors involved in a complete "time development" from the first detection of enemy units, their classification, the decision to engage with missiles until the actual missile impact on the selected target, assumptions are necessary to simplify the simulation and the resulting analysis. These assumptions cannot oversimplify; the simulation must remain credible. To avoid any obvious bias by overemphasizing some factors (i.e. abnormal ducting conditions, heavy sea-state, stationary target), and to obtain an insight into the significance of the different factors, a standard scenario was built. This includes assumptions concerning environmental factors as well as tactical factors which describe the behavior of both own and hostile forces. It seems to be evident, that with the knowledge of the significance of the factors any actual deviation from the standard scenario can be thoroughly evaluated for its influence on the missile employment.

A. ENVIRONMENTAL FACTORS

Environmental factors influence the planning and execution of surface warfare operations. They may help or hinder the platforms, the sensors, and weapons; they include

- Meteorological Factors,
- Oceanographical Factors,
- Ionospheric Factors, and

- Geographical Factors.

The following assumptions were made:

- System performance is not degraded until sea-state is reached.

- Wind-direction: 300 degrees.

- Wind-speed: 0.0 m/sec, or 7.7 m/sec (15 kts).

- Detection range is limited by the radar horizon (line of sight); no surface radar ducting conditions. Relevant detection ranges of FGN FPGB-units against prospective WPN Surface-units are provided in Appendix B which also includes assumptions about hostile detection ranges against the MM 38 missile. The wind speed was included in the computer simulation, but preliminary analysis of the output indicated that at these speeds its effect is negligible.

B. TACTICAL CONDITIONS ASSUMED FOR OWN FORCES

The most important factors of this group refer to the "time development" of the missile employment for either targeting-scheme. The following assumptions were made:

- System reliability of 1.0 for all components on board the launch-platform/HC/RPV.

- Time development for the unassisted targeting-scheme extends from the actual launch-command (all necessary data were already fed into the missile computer) until the final Lock-on of the missile on the selected target.

- HC/RPV availability without delay, if necessary.

- Time development for the assisted targeting-scheme extends from the target-data report by HC/RPV to the launch-platform until the final Lock-on of the missile on the selected target. This procedure will be more inaccurate due to the greater time-delay and because different sensor-types are required.

- No distinction in capabilities between FPBG-Classes.

C. TACTICAL CONDITIONS ASSUMED FOR HOSTILE FORCES

This group of factors depends on the characteristics of various types of Warsaw-Pact Navy (WPN)-Forces, and the countermeasures available to each vessel.

1. Enemy Surface-Combattants

For the one-on-one engagement four target-types were chosen:

- 1.Guided missile destroyer (DDG) : Krivak-Class
- 2.Guided missile corvette (PFG) ..: Nanuchka-Class
- 3.Guided missile FPB (FPBG): Osa-Class
- 4.Amphibious ship (LSM): Polnocny-Class

Detailed descriptions of these different surface-ship types are provided in [3].

2. Enemy Reaction-Time

The enemy reaction-time defines a second set of variables, which also significantly contribute to the time development of the launch-sequence; the reaction-time also depends on the type of engagement (UAT/OTH).

For the UAT-scheme, the first variable is the delaytime prior to missile detection (DETDEL), which is a function of the sensor type operated on board the target. The second variable is the delaytime before an actual response can be initiated by evasive maneuvers (TRNDEL). For the four target types the following mean-values in seconds are assumed for DETDEL and TRNDEL, respectively:

- DDG...: 10/10
- PFG...: 10/10
- FPBG...: 12/8
- LSM...: 15/15

The values for DETDEL assume a high level of maintenance and operator skill, but it is reasonable to believe that the WPN have sophisticated sensors and trained personnel available, which justify these assumptions. The values for TRNDEL are based on personal experience, and also seem applicable to the WPN.

For the OTH-scheme, four delaytimes affect the reaction-time. They are defined as follows:

1. Delaytime due to transmission of the enemy contact report (RELAY) from the H/C to the launch-platform.

2. Delaytime onboard the launch-platform for the evaluation of the transmitted target data (DELEVA).

3.Delaytime due to missile gyro stabilisation, necessary for the launch (MISRED), and the

4.Delaytime TRNDEL.

The delaytime DETDEL, defined for the UAT-scheme, is included in the three delaytimes RELAY, DELEVA, and MISRED, because it is reasonable to assume, that the HC and/or its UHF-transmission will be detected by the target and interpreted as an imminent SSM attack. Therefore this time-variable is discarded in this targeting-scheme.

The respective times in seconds are

- RELAY...: 10
- DELEVA.: 10
- MISRED.: 12
- TRNDEL.: equivalent to the UAT-scheme.

The reaction-time is also assumed to be normally distributed with mean-value formed by the sum of the respective delaytimes, and the standard deviation σ_{Del} of 1.5 sec.

This reaction-time (REACT) is further influenced by the detection-range of the WPN surface-combattants against the attacking missile. Appendix B provides the pertinent data, defined as RNG5. If the range to the target is less than the given values, the reaction-time (the time from the first detection until the attacked ship actually starts changing its motion by manueuvring) keeps its original value. If this range is larger than the limiting value, an additional time is obtained by dividing the difference (actual range - RNG5) by the missile speed, and adding the result to the original value of REACT. Until this time the target course and speed are assumed to remain constant.

3. Enemy Countermeasures

The analysis is based on the "worst case" assumption, namely, that the enemy forces have available and in operation appropriate electronic or infrared support measures to detect characteristic FC-radar emissions and/or attacking missiles. Under these conditions the missile attack might be detected as early as 10 seconds after the launch (DETDEL). This time includes the sensor-system lag-time as well as the human reaction-time, until the required counter action is taken. These sensors require line-of-sight conditions, and are limited by the radar-horizon. The maximum range at which a target can be detected depends on the sensor height and target height.

Once a threat radar or the missile-launch has been detected, the enemy forces initiate suitable defensive measures to counter the attack. In addition to the alteration of speed and course considered in this analysis electronic warfare (EW) countermeasures are also to be expected.

a. Speed/Course-Changes

Some of the target vessels have a gas-turbine or high-power diesel propulsion system, which can produce rapid and major speed changes within the expected missile flight-time. This capability combined with maximum course changes is a very effective countermeasure. The search pattern can be evaded if the target can maneuver out of the area pre-programmed into the missile prior to launch. These effects are described in detail in Appendix A "Target-Motion Analysis". Two evasive maneuver options are available to

the target: the "choices" of the turn-direction and of the number of degrees the target intends to turn in the specified direction, before it will straighten to its new course. Each option is an independently generated random event in the simulation. The direction chosen is Bernoulli event, while the angle chosen is uniformly distributed (0°-90°). This is a "best" case assumption from the target's viewpoint, because preliminary analysis also showed that any turning angle greater than 90° reduces its probability of evasion. The model determines the final course from a randomly chosen time variable as a function of the time necessary to turn 90°.

In the UAT-simulation the initial target course is defined as 360°; the target course in the OTH-simulation is 180°. The target speed change capabilities were taken from [3]:

- DDG...: 14 - 30 kts in 50 sec
- PFG...: 18 - 30 kts in 75 sec
- FPBG...: 18 - 36 kts in 60 sec
- LSM...: 12 - 16 kts in 60 sec.

The first number refers to the target initial speed assumed in the simulation, the second number to the final speed, which can be achieved with maximum acceleration in the time specified by the third number. The simulation investigated the indicated speed capabilities and also analyzed the effect of high initial speed, 28 kts, for the DDG target. The estimated acceleration-data are the same as evaluated above. The response time for course and speed changes (TRNDEL) is assumed to have an average value of approximately 10 sec.

b. Electronic-Warfare

Both passive and active measures are employed to counter the anti-ship missile threat. WPN ships probably have basic informations about NATO sensor-characteristics and relate them to their EW-measures.

Although employment of decoys and active jamming is probable and ASMD with SAMs and rapid-firing guns is certain, this analysis is restricted to enemy countermeasures by speed/course alterations.

D. SUMMARY OF RELEVANT VARIABLES

Table I lists all variables used in either targeting scenario.

LAUNCH PLATFORM:

SENSOR BEARING ERROR	-SIGBL-	(15)	0.25°
SENSOR RANGE ERROR	-SIGRL-	(15)	120 M
SENSOR BEARING ERROR (FC)	-SIGBLE-		0.14°
SENSOR RANGE ERROR (FC)	-SIGRLE-		10 M
TARGET COURSE ERROR	-SIGCL-	(15)	3.5°
TARGET SPEED ERROR	-SIGSL-	(15)	0.4 KN

MISSILE:

ACTIVATION-DISTANCE	K	-ACTIV-	6000	M
ACTIVATION-DISTANCE	G	-ACTIV-	12000	M
SCAN-ANGLE	K	-PFI-	+/-1.5	°
SCAN-ANGLE	G	-PFI-	+/-9.0	°
LOBEWIDTH	-PSI-		11	
SEARCH-DEPTH	K	-L-	+/-1000	M
SEARCH-DEPTH	G	-L-	+/-2000	M
GYRC-STABILISATION		-MISREC-	12.0	SEC
LAUNCH-DELAY		-TLAUN-	2.5	SEC
SEEKER OPERATIONAL		-TOP-	3.0	SEC
SEARCH-TIME UNTIL LOCK-ON	K	-TSCAN-	0.4	SEC
SEARCH-TIME UNTIL LOCK-ON	G	-TSCAN-	2.4	SEC
DETECTION-TIME		-DETDEL-	10-15	SEC
RESPONSE-TIME COURSE/SPEED		-TRNDEL-	8-15	SEC
SPEED	-VMISS-		315	M/SEC
STANDARD DEVIATION SPEED		-SIGVM-	1.5	M/SEC
STANDARD DEVIATION DELAYTIME		-SIGDEL-	1.5	SEC
STANDARD DEVIATION NAVIGATION		-SLOKB-	TLCK*1.62	
STANDARD DEVIATION NAVIGATION		-SLOKR-	TLCK*1.62	

EXTENDED PLATFORM:

SENSOR BEARING ERROR	-SIGBE-	(10)	1.0-3.0°
SENSOR RANGE ERROR	-SIGRE-	(15)	30 M
TARGET COURSE ERROR	-SIGCE-	(15)	5.0°
TARGET SPEED ERROR	-SIGSE-	(1)	1.5 KN

TARGET:

DETECTION-TIME	-DETDEL-	10-15	SEC
RESPONSE-TIME COURSE/SPEED	-TRNDEL-	8-15	SEC
STANDARD DEVIATION DELAYTIME	-SIGDEL-	1.5	SEC

Table I - RELEVANT DATA FOR THE ANALYSIS

IV. TARGETING REQUIREMENTS

The two major targeting requirements are that the target must be within the attack-range of the missile, and that the crossrange and downrange errors must be sufficiently small, that the missile seeker has a high target-acquisition probability. These requirements apply to both targeting-schemes investigated.

A. SEARCH-PATTERN DIMENSIONS

As already pointed out, the search-pattern of the "Exocet" missile is a function of the three parameters, the activation-distance ACTIV, the scan-angle PHI, and the search-depth L, each assumed with two different settings, which yield 8 search-pattern combinations. The simulation investigates the possibility that some of the 8 combinations are less useful than others, particularly when TD is a consideration.

Two variables, CR and DR, are determined by these three parameters. CR is defined as the crossrange halfwidth search dimension, measured in (\pm) meters, and DR is defined as the downrange halfwidth search dimension, also measured in (\pm) meters.

The search pattern of the seeker is part of an annulus, where CR represents the maximum halfwidth of the sector, and DR the distance from its inner to its outer boundary. The pattern can be approximated by a rectangle with dimensions $2*CR$ and $2*DR$, with the downrange (y)-axis in the launch direction (parallel to DR).

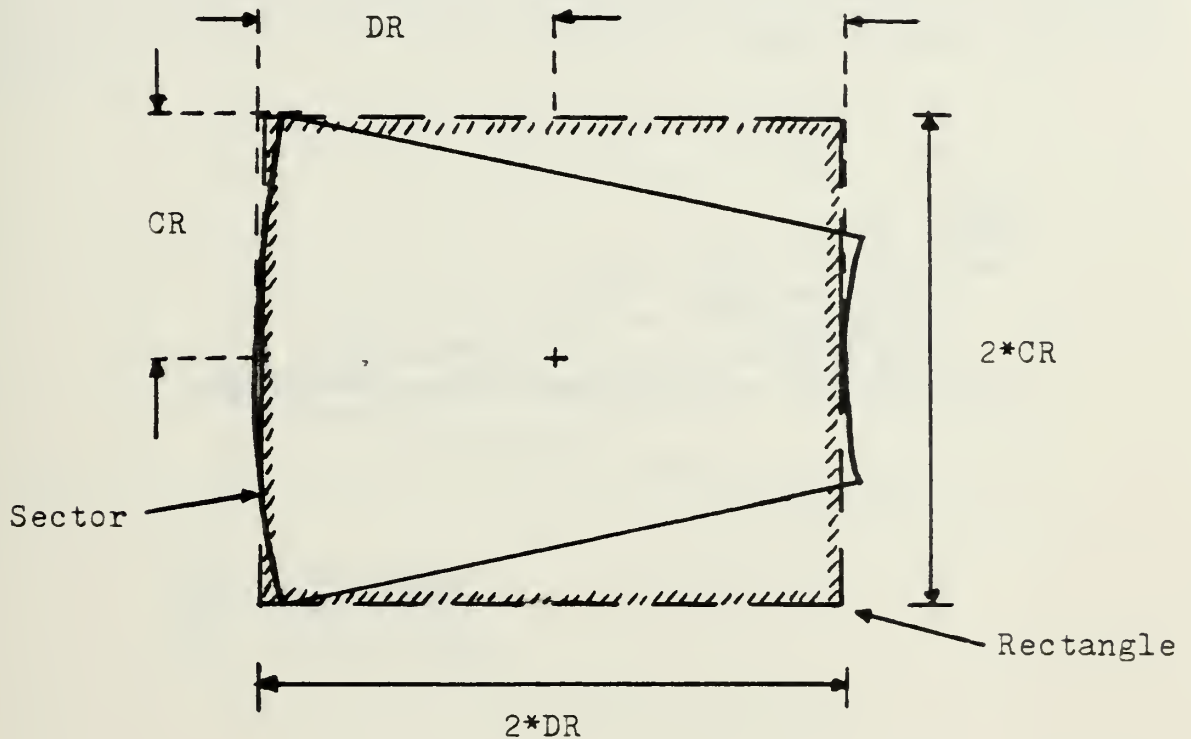
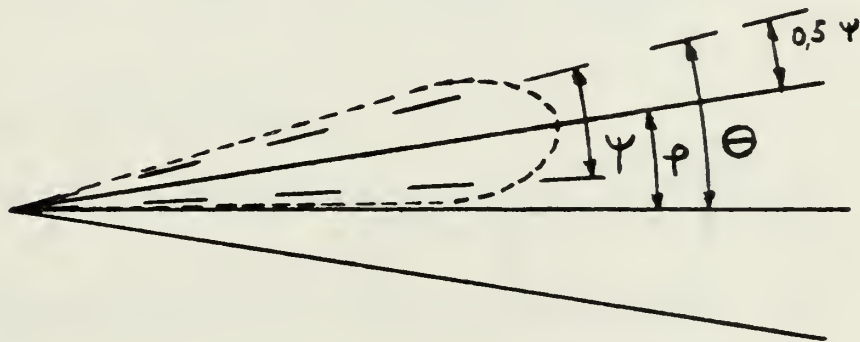


Figure 6 - APPROXIMATION OF THE SEARCH PATTERN

CR is a function of the search-angle, THETA, which is the sum of the scan-angle and half the antenna lobe-width PSI.

$$\text{Search-angle THETA } (\Theta) = \pm (\text{PHI} + 0.5 * \text{PSI})$$

PSI is the antenna lobewidth with respect to the 3 db-line. Fig 7 shows the relation search-angle/scan-angle for PHI of 9.00° and PSI of 11.00°. The complete search-width is then 29.00°.



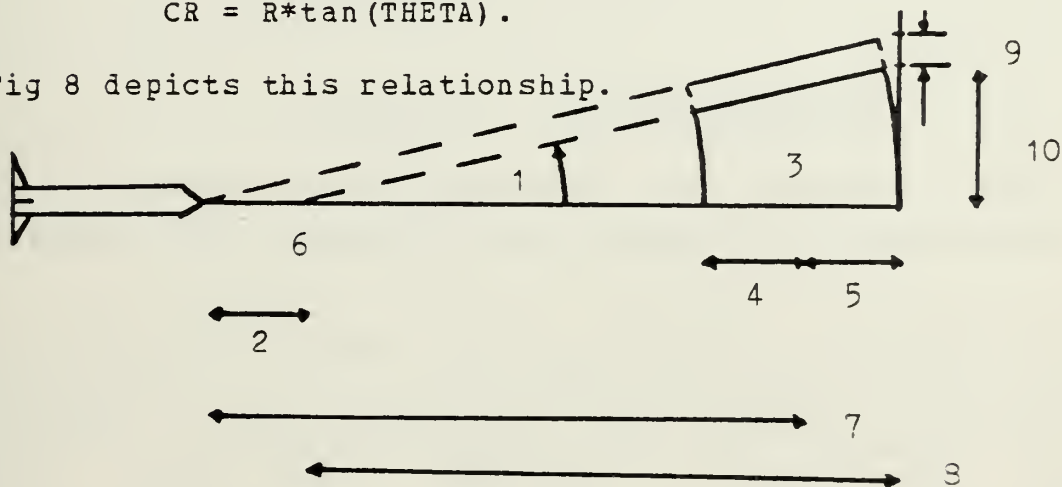
- ϕ - Scan angle
- ψ - Lobe width
- Θ - Search angle

Figure 7 - RELATION SEARCH-ANGLE/SCAN-ANGLE

The downrange dimension, DR , is determined by the search-depth, L , chosen in the parameter combination.

$$R = (ACTIV + L) - (T_{OP} + T_{SCAN}) * v_{MISS}$$

$$CR = R * \tan(\text{THETA}) .$$



- 1-Search angle (G) 2- $(T_{OP}+T_{SCAN}) \cdot v_{MISS}$ 3-POA
4-(-)L (K) 5-(+)L (K) 6-Missile position after (2)
7-Activation-distance (K) 8-R 9-CR difference due to (2)
10-Actual CR-dimension

Figure 8 - REDUCTION OF THE SEARCH PATTERN

The following table provides CR/DR-dimension values for the "Exocet" search system.

PARAMETER COMBINATICN	CR	DR
KKK	718.7	1000.0
KKG	840.6	2000.0
KGK	1318.8	1000.0
KGG	1569.2	2000.0
GKK	1449.9	1000.0
GKG	1571.8	2000.0
GGK	2821.1	1000.0
GGG	3071.5	2000.0

DIMENSION: M

Table II - CR/DR-DIMENSIONS

In the computer model the search area dimensions, CR and DR, determine the maximum allowed bearing and range errors.

The attack-ranges (launch distance) investigated vary from 14000 m, which is the effective gunnery range for 76 mm caliber, to the radar-horizon range (RP1) characteristic of each target-type. Appendix B provides the detailed derivation of these ranges. The effective RP1-values are approximated as follows:

- DDG...: 32500 m
- PFG...: 29000 m
- FPBG...: 26000 m
- LSM...: 29500 m

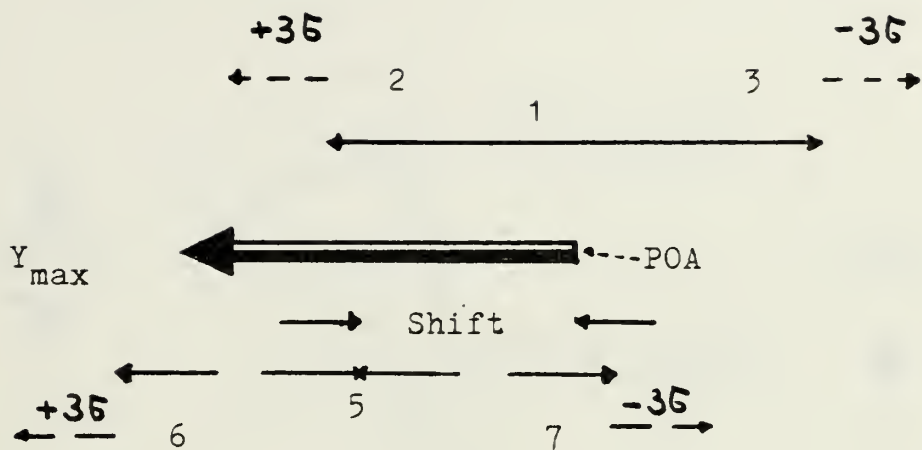
These limits are used in the UAT-simulation. The attack ranges investigated for the OTH-model vary from the characteristic RP1-range up to 40000 m, which exceeds the practical range of the MM 38 missile.

B. SHIFT OF THE POA

Appendix A "Target-Motion Analysis" reveals that it is unrealistic to assume that the target has no limitations on its course alternatives from its initial course. This perception leads to the idea that the POA should be shifted to a new point which is displaced in the direction of the predicted initial course. This displacement Y_{\max} is a function of the estimated target-speed, and the requirement that $2*DR$ bracket the maximum straight distance travelled (including a 3σ sensor range error) by the target during the time to Lock-on. In this case, it seems evident that the PA might be improved by this procedural change. The shift is calculated as

$$POA\text{-shift} = Y_{\max} - DR + 3*\sigma_R$$

where σ_R is the SIGRL-value for the UAT-simulation, and the SIGRE-value for the OTH-model. If a negative value for the POA-shift is computed, then no shift will be applied. Both models compare the PA for the shifted and unshifted POA-cases. This shift of the POA assures the complete cover of the "forward" portion of the straight target-track within the time to Lock-on, and an improved partial cover even when the target makes a radical (up to 180°) course change to either side. Fig 9 depicts the construction of this shift, while Fig 10 shows the actual offset of the search pattern caused by the shift. The model shows that the potential decrease in FA is much smaller than the improvement obtained when the POA is shifted.



1-Search depth $2 \cdot DR$ of sector without POA-shift

2-Sector offset in DR-direction caused by $+35_R$

3-Sector offset in DR-direction caused by -35_R

4-Search depth $2 \cdot DR$ of sector with POA-shift

5-Sector offset in DR-direction caused by $+35_R$

6-Sector offset in DR-direction caused by -35_R

Figure 9 - CONSTRUCTION OF THE POA-SHIFT

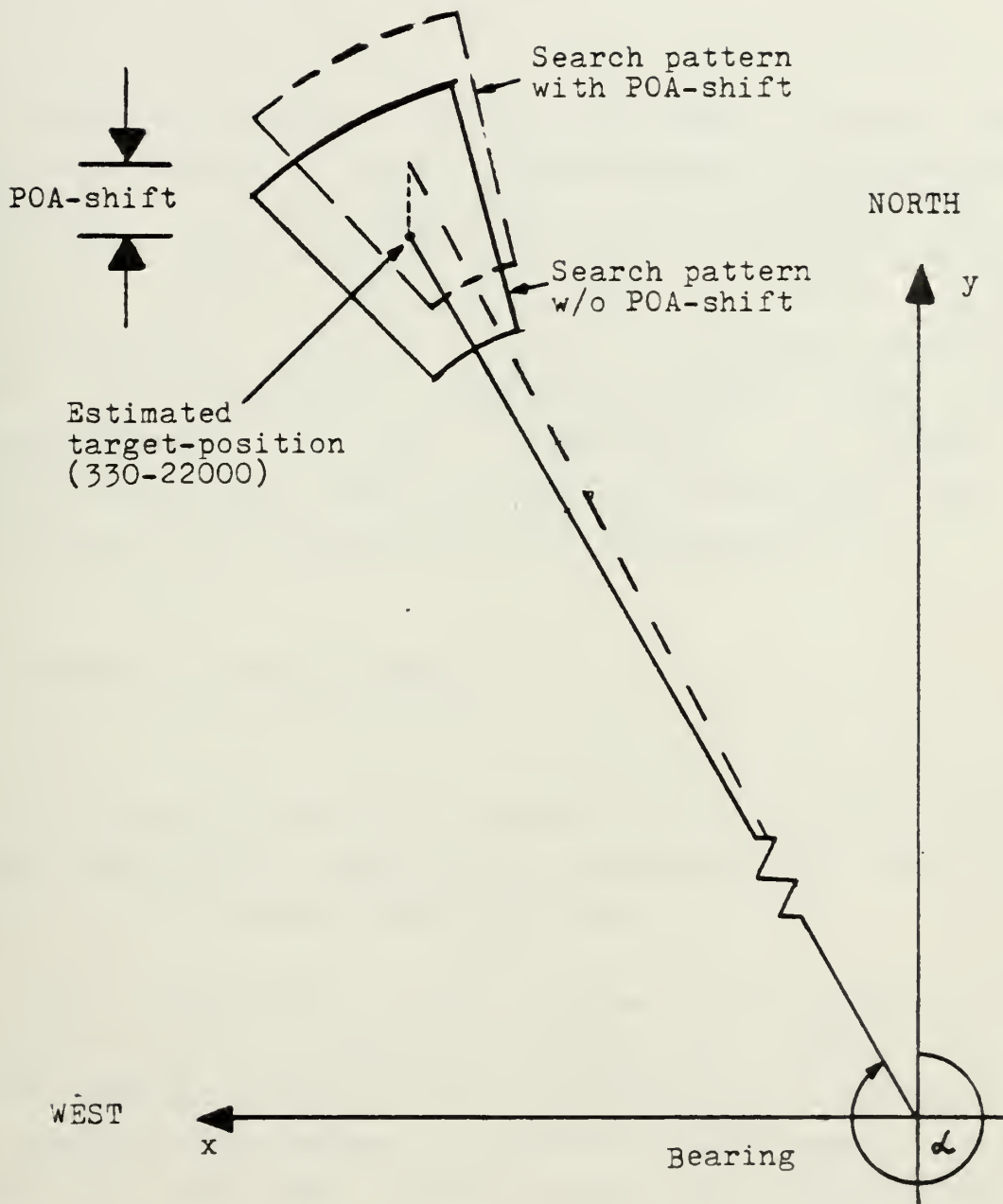


Figure 10 - RELATION OF SEARCH-PATTERN AND POA-SHIFT

V. MEASURE OF EFFECTIVENESS/STATISTICAL REQUIREMENTS

Computer simulation becomes a legitimate research tool, when known analytical methods cannot supply a solution for a model [4]. Given the complexity of this problem and the stochastic characteristics introduced by the many potential decision points (launch-platform) and the various evasive-maneuver options (target), a stochastic simulation model is appropriate. Simulation models place three responsibilities on the investigator: a measure of effectiveness (MOE) must be defined, a sample size must be established, and the model must be validated [4].

A. MEASURE OF EFFECTIVENESS

The missile-attack is a success if the target's actual final position is such that the missile can acquire the target in the assigned search-pattern.

This acquisition of the target is equivalent to the Lock-on; in the real world the success is defined by the radar Lock-on, whereas in the simulation world generated by the computer the success is defined by the presence of the target in the radar search area; its determination is obtained by geometrical calculations. Each run of the simulation is tested for all possible search-pattern combinations, and evaluated as a part of a binomial experiment (success or failure).

The MOE for each parameter combination is defined as

$$\text{MOE} = p = \frac{\text{\# of successes}}{\text{\# of trials}}$$

The second experiment calculates the same MOE for each parameter combination when the POA is shifted forward along the initial target-course.

B. SAMPLE SIZE

Computer simulation allows multiple replication of an experiment. Independent replications mean that an experiment is rerun with selected changes in parameters, in operating conditions, or in the sequence of random numbers used to drive the model. All three are used in this simulation model.

To determine the sample size for replications required to estimate the true parameter p for the PA with a specified limit of error in both directions (accuracy), the following formula is applied [5]:

$$n = \frac{(z_{1-a/2})^2 * p(1-p)}{e^2}$$

A sample of size n guarantees a probability not greater than a , that the estimate of p is in error by more than e . Since the true parameter p is unknown, and no prior information about p is available, then a value of $p' = 0.5$ is used because it leads to a "worst case" value of n .

The formula then simplifies to

$$n = \frac{(z_{1-a/2})^2}{4e^2}$$

For the purpose of this analysis, the confidence coefficient $1-a$ to be associated with the resulting estimate is chosen to be equal to 0.95, that means $a=0.05$ and $a/2=0.025$; the related two-sided value $z_{0.975}$ of the standard normal variable is 1.960; the error e permitted in the estimate was set at 0.05. The sample size was then fixed at 400. This value is used for the number of replications in both simulation models.

C. VALIDATION

The computer model output was compared with ship performance data (FGN-DDG, Hamburg-Class), and with actual flight-test data obtained from the manufacturer and the FGN. These references are included in the classified Appendix. Validation is discussed further at that point.

VI. UNASSISTED TARGETING-SCHEME

The simulation model MM38-UAT is used to model engagements in which the attack range is within the FPBG radar-horizon and no target information is available from an extended platform. Use of intermittent radiation of the relevant surface search radar provides information about target-position and target-motion, and by the use of ESM, visual means and/or intelligence reports, a target classification is possible.

A. TARGETING GEOMETRY

The simulation comprises the time development from the initiation of the missile launch - "press the button" - until the expected Lock-on time. This assumes that the target is already in the launch-sector, and the missile gyros are stabilized. The delaytimes were discussed in section III.C.2. In Fig 11 and 12, the actual position at Lock-on-time is shown, and all sources of errors have been considered. Fig 11 depicts the targeting geometry without a shift of the POA; whereas Fig 12 shows the geometry including this shift.

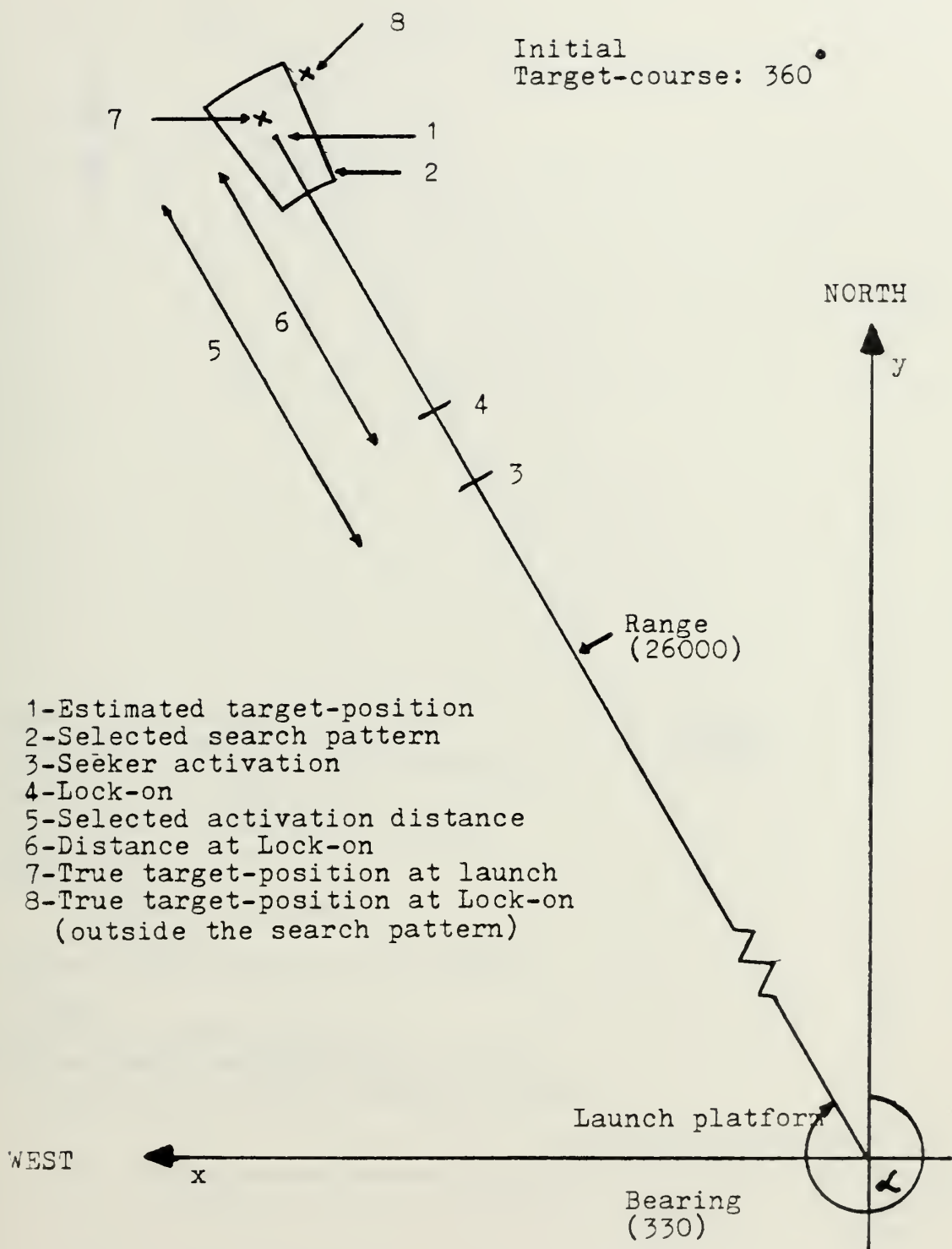


Figure 11 - TARGETING GEOMETRY FOR MODEL MM38-UAT
(WITHOUT POA-SHIFT)

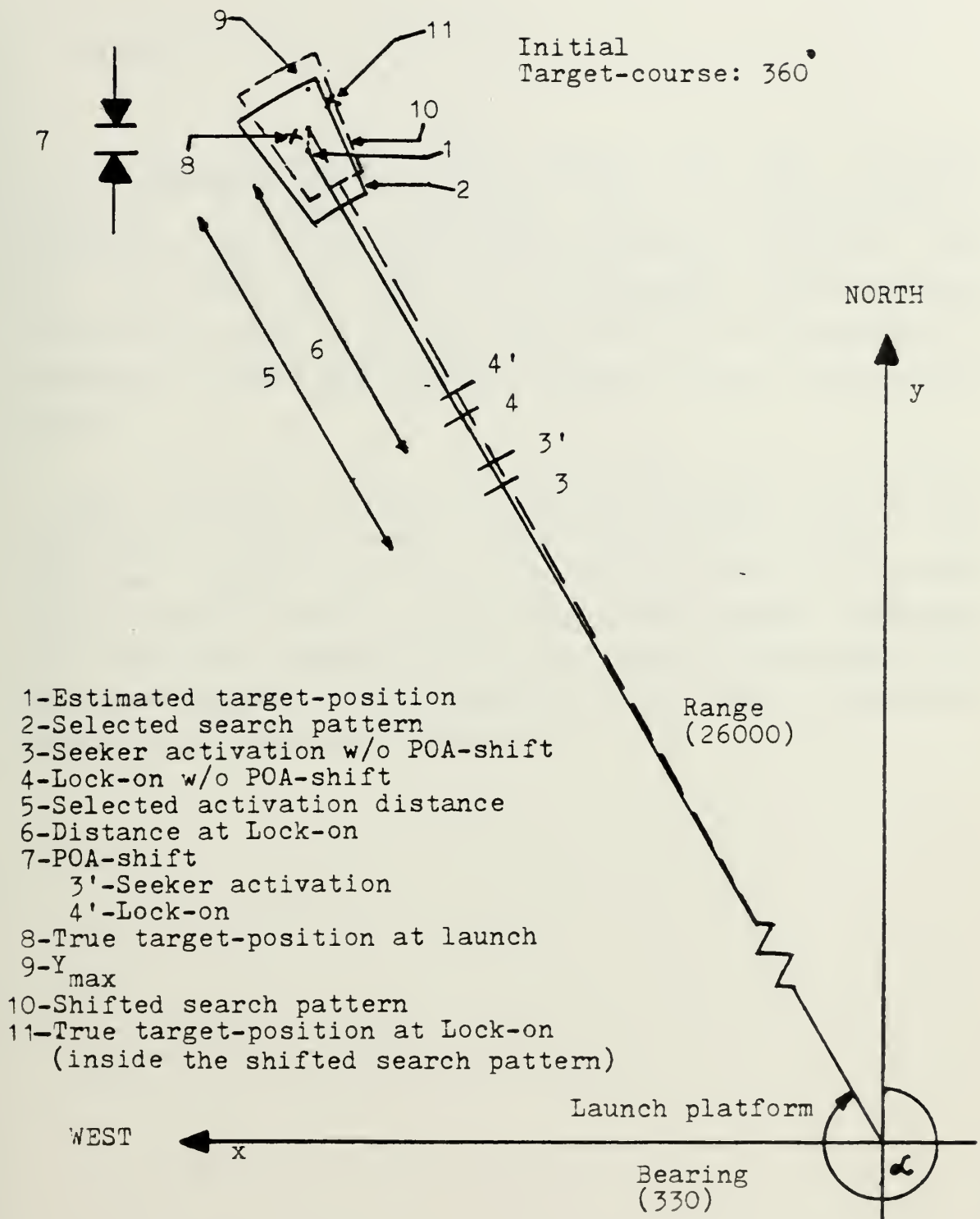


Figure 12 - TARGETING GEOMETRY FOR MODEL MM38-UAT
(WITH POA-SHIFT)

B. RESULTS

An analysis of variance (ANOVA) for all involved variables of the simulation model was performed to investigate their influence on the dependent variable, the PA. It turned out that all independent variables have significant effect on the PA, and also it is not possible to establish a linear relationship between any one variable and the PA.

The following tables and figures present the MOE as a function of target aspect-angle and target range. The indicated ranges are the upper bound limits to which the missile can be launched with the specified search pattern, and obtain the required PA of 0.99. Due to the symmetry of the aspect-angles only the positive angle-data (target-bow points to the right) are presented.

1. PA w/r to Wind Effects

The component of the wind in the direction of the missile's trajectory does not significantly affect - less than 3% - the PA for all target types, parameter combinations, target ranges, and aspect-angles.

2. PA w/r to Target Range

Tables III to VI refer to the four different target types and the ranges from 14000 m to the respective RP1-range. When the equivalent RP1-range is given as an entry in the table, in most of the cases this is an indication that a PA of at least 0.99 is also given beyond the specified range. The first value (1) is calculated without the FOA-shift, the second value (2) takes this shift into account. Otherwise, the tables are self-explanatory.

Not surprisingly, the results support the hypothesis that the PA can be improved by reducing the missile launching distance, the range to the target. For all parameter combinations, decreasing the target range can increase the PA to 1.0. This is valid for all target types, but at different ranges and with different search patterns. Table VII for the high initial speed case of the DDG target shows the same tendency.

PATTERN ANGLE	KKK	KKG	KGK	KGG	GKK	GKG	GKK	GGG
(1)	22000	23000	22000	28000	30000	32000	31000	32000
(2)	22000	23000	26000	32000	32000	32000	32000	32000
30	20000	21000	22000	28000	30000	32000	31000	32000
60	18000	18000	25000	27000	32000	32000	32000	32000
90	17000	17000	26000	32000	32000	32000	32000	32000
120	19000	19000	27000	28000	32000	32000	32000	32000
150	22000	22000	28000	29000	32000	32000	32000	32000
180	25000	25000	30000	32000	32000	32000	32000	32000

RF1: 32000 M

Table III - RELATION SEARCH PATTERN/ASPECT-ANGLE
 MAXIMUM TARGET RANGE FOR PA=0.99
 DDG KRIVAK-CLASS (LOW SPEED)

PATTERN ANGLE	KKK	KKG	KGK	KGG	GKK	GKG	GCK	GGG
0	(1) 21000	23000	20000	25000	27000	29000	26000	29000
	(2) 21000	23000	20000	25000	29000	29000	29000	29000
30	19000	19000	20000	28000	27000	29000	27000	29000
	19000	19000	20000	29000	25000	29000	29000	29000
60	17000	17000	24000	27000	29000	29000	29000	29000
	17000	17000	29000	29000	25000	29000	29000	29000
90	16000	16000	26000	26000	29000	29000	29000	29000
	16000	16000	29000	29000	25000	29000	25000	29000
120	18000	18000	27000	27000	29000	29000	29000	29000
	18000	18000	29000	29000	25000	29000	25000	29000
150	22000	22000	28000	29000	25000	29000	29000	29000
	22000	22000	29000	25000	25000	29000	29000	29000
180	25000	25000	29000	29000	29000	29000	25000	29000
	25000	25000	29000	29000	29000	29000	29000	29000

RFL: 29000 M

Table IV - RELATION SEARCH PATTERN/ASPECT-ANGLE
 MAXIMUM TARGET RANGE FOR PA=0.99
 PFG NANUCHKA-CLASS

PATTERN ANGLE	KKK	KKG	KGK	KGG	GKK	GKG	GKK	GGG
0	(1) 21000	21000	22000	26000	26000	26000	26000	26000
	(2) 21000	21000	26000	26000	26000	26000	26000	26000
30	18000	18000	22000	26000	26000	26000	26000	26000
	18000	18000	26000	26000	26000	26000	26000	26000
60	16000	16000	24000	24000	26000	26000	26000	26000
	16000	16000	26000	26000	26000	26000	26000	26000
90	17000	17000	24000	26000	26000	26000	26000	26000
	17000	17000	26000	26000	26000	26000	26000	26000
120	17000	17000	24000	26000	26000	26000	26000	26000
	17000	17000	26000	26000	26000	26000	26000	26000
150	20000	20000	22000	26000	26000	26000	26000	26000
	20000	20000	26000	26000	26000	26000	26000	26000
180	22000	22000	22000	26000	26000	26000	26000	26000
	22000	22000	26000	26000	26000	26000	26000	26000

RFL: 26000 M

Table V - RELATION SEARCH PATTERN/ASPECT-ANGLE
 MAXIMUM TARGET RANGE FOR PA=0.99
 FPBG OSA-CLASS

PATTERN ANGLE	KKK	KKG	KGK	KEG	GKK	GKE	GKG	GGG
(1)	27000	29000	27000	29000	29000	29000	29000	29000
(2)	27000	29000	27000	29000	29000	29000	29000	29000
30	24000	25000	27000	29000	29000	29000	29000	29000
60	21000	21000	27000	29000	29000	29000	29000	29000
90	20000	20000	27000	29000	29000	29000	29000	29000
120	22000	22000	27000	29000	29000	29000	29000	29000
150	27000	27000	27000	29000	29000	29000	29000	29000
180	29000	29000	27000	29000	29000	29000	29000	29000

RFL: 29000 M

Table VI - RELATION SEARCH PATTERN/ASPECT-ANGLE
 MAXIMUM TARGET RANGE FOR PA=0.99
 LSM POLNOCNY-CLASS

PATTERN ANGLE	KKK	KKG	KGK	KGK	GKK	GKG	GKK	GKG
(1)	15000	20000	15000	25000	22000	32000	21000	32000
(2)	15000	20000	15000	28000	32000	32000	21000	32000
30	15000	16000	16000	23000	22000	32000	23000	32000
	16000	16000	16000	30000	32000	32000	32000	32000
60	-	-	20000	21000	26000	30000	25000	32000
	-	-	23000	32000	32000	32000	32000	32000
90	-	-	21000	21000	30000	30000	32000	32000
	-	-	26000	32000	32000	32000	32000	32000
120	14000	14000	23000	23000	32000	32000	32000	32000
	14000	14000	28000	32000	32000	32000	32000	32000
150	18000	18000	22000	26000	28000	32000	28000	32000
	19000	19000	28000	28000	32000	32000	32000	32000
180	21000	23000	21000	32000	28000	32000	28000	32000
	22000	22000	30000	30000	32000	32000	32000	32000

RFI: 32000 N

Table VII - RELATION SEARCH PATTERN/ASPECT-ANGLE
 MAXIMUM TARGET RANGE FOR PA=0.99
 DDG KRIVAK-CLASS (HIGH SPEED)

3. PA w/r to Target Aspect-Angle

Fig 13 to 21 describe the PA as a function of the various aspect-angles and the three ranges RP9, RP5, and RP1, which are defined for each target type in Appendix B. The graphs depict this relation for only two target types, the DDG and the LSM, as significant proxies for a rapidly and a slowly reacting ship. The variant of the high initial speed for the DDG target is also analyzed.

Almost the same tendency can be observed in the various PA-curves over the whole aspect-angle set for the other two target types. The parameter combinations KKK and KKG are the most sensitive to a change of the aspect-angle for the target types DDG, PFG and FPBG, at their respective RP9-range. The PA-values decrease from a maximum of 1.0 at the aspect-angle 0° to their respective minima (0.88, 0.83, 0.83) at the aspect-angle 90° and then follow an increasing trend back to the maximum value of 1.0 at 180° .

The PA-curves in the LSM family are similar, but differ from the curves in the DDG, PFG, and FPBG family. They also show a minimum for all search patterns at 90° . For the search patterns KKK and KKG the high initial speed case for the DDG generates PA-curves which are very distinct from the curves generated by the low initial speed case. The PA-values at aspect-angle 0° are 0.66 and 0.95 respectively, they both decrease to a minimum value of 0.09 at aspect-angle 90° , and reach their maximum value of 0.99 and 1.00 at 180° . The curve for the search pattern KGG has a very different shape; at aspect-angle 0° it has its minimum of 0.64. The PA increases with the aspect-angle to 60° (0.94); then it follows the same trend of the other patterns, namely PA-values between 0.95 and 1.0.

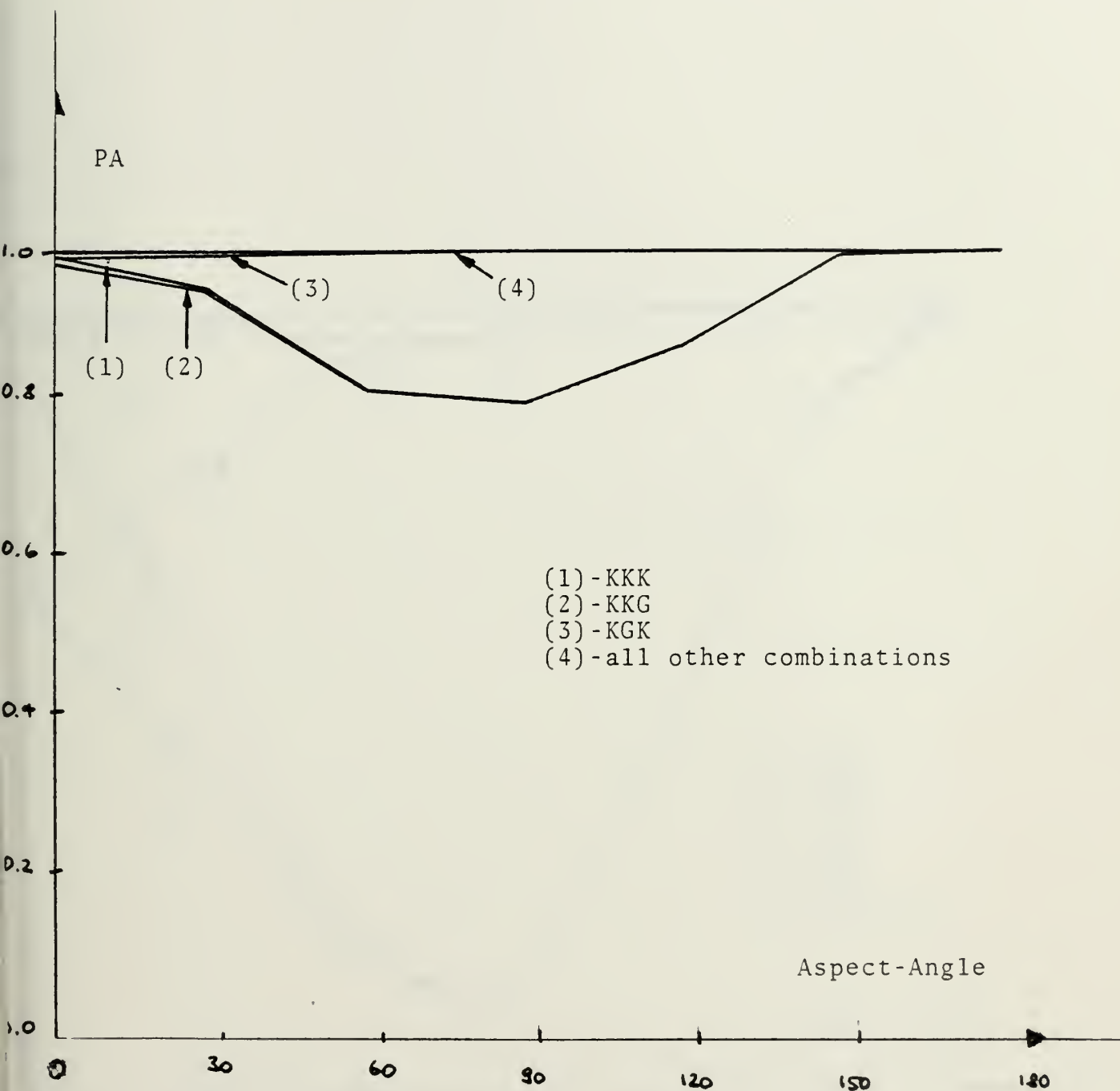


Figure 13 - RELATION PA - TARGET ASPECT-ANGLE W/O POA-SHIFT
DDG TARGET (LOW SPEED) - RP9 -

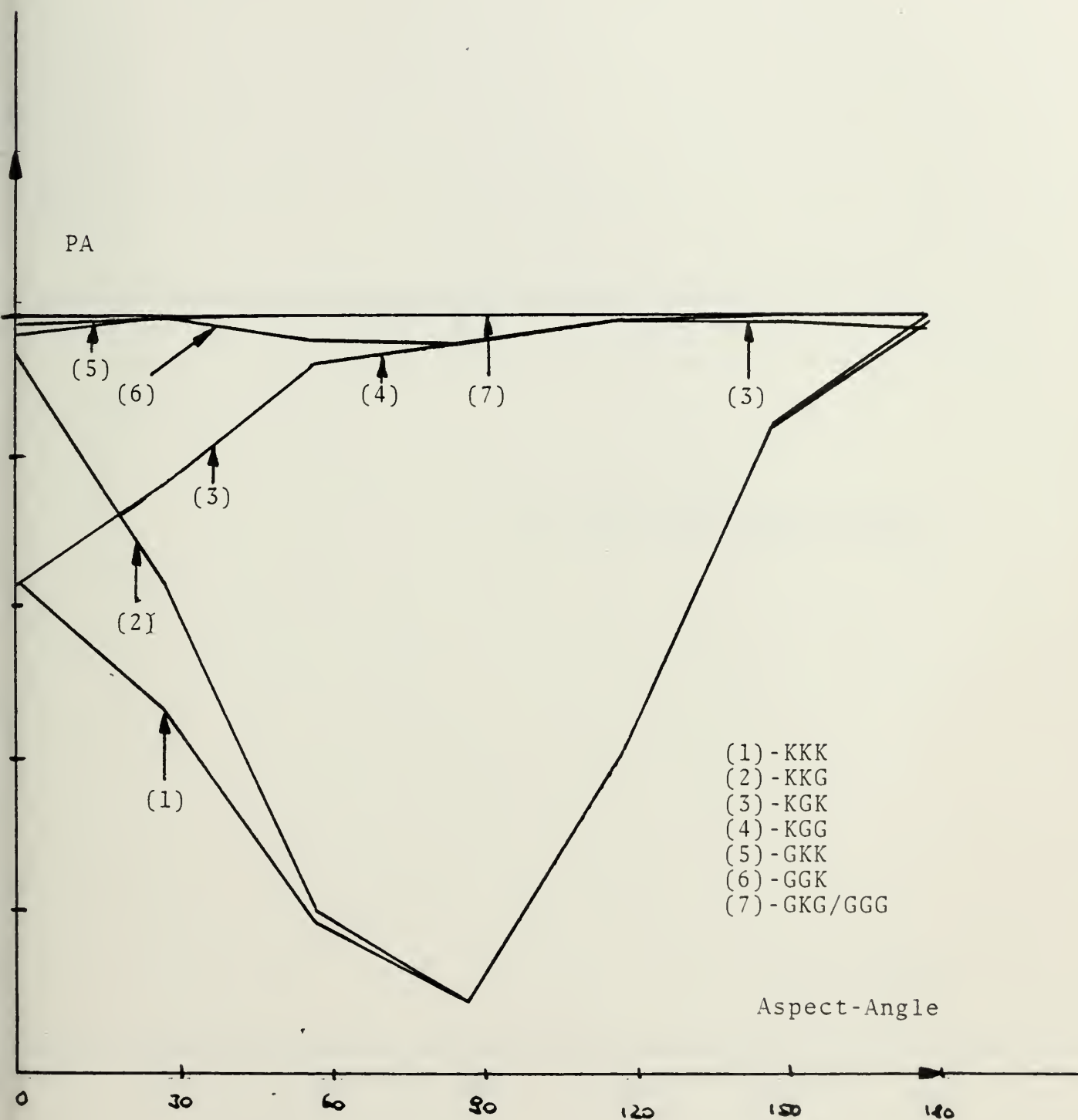


Figure 14 - RELATION PA - TARGET ASPECT-ANGLE W/O POA-SHIFT
 DDG TARGET (HIGH SPEED) - RP9 -

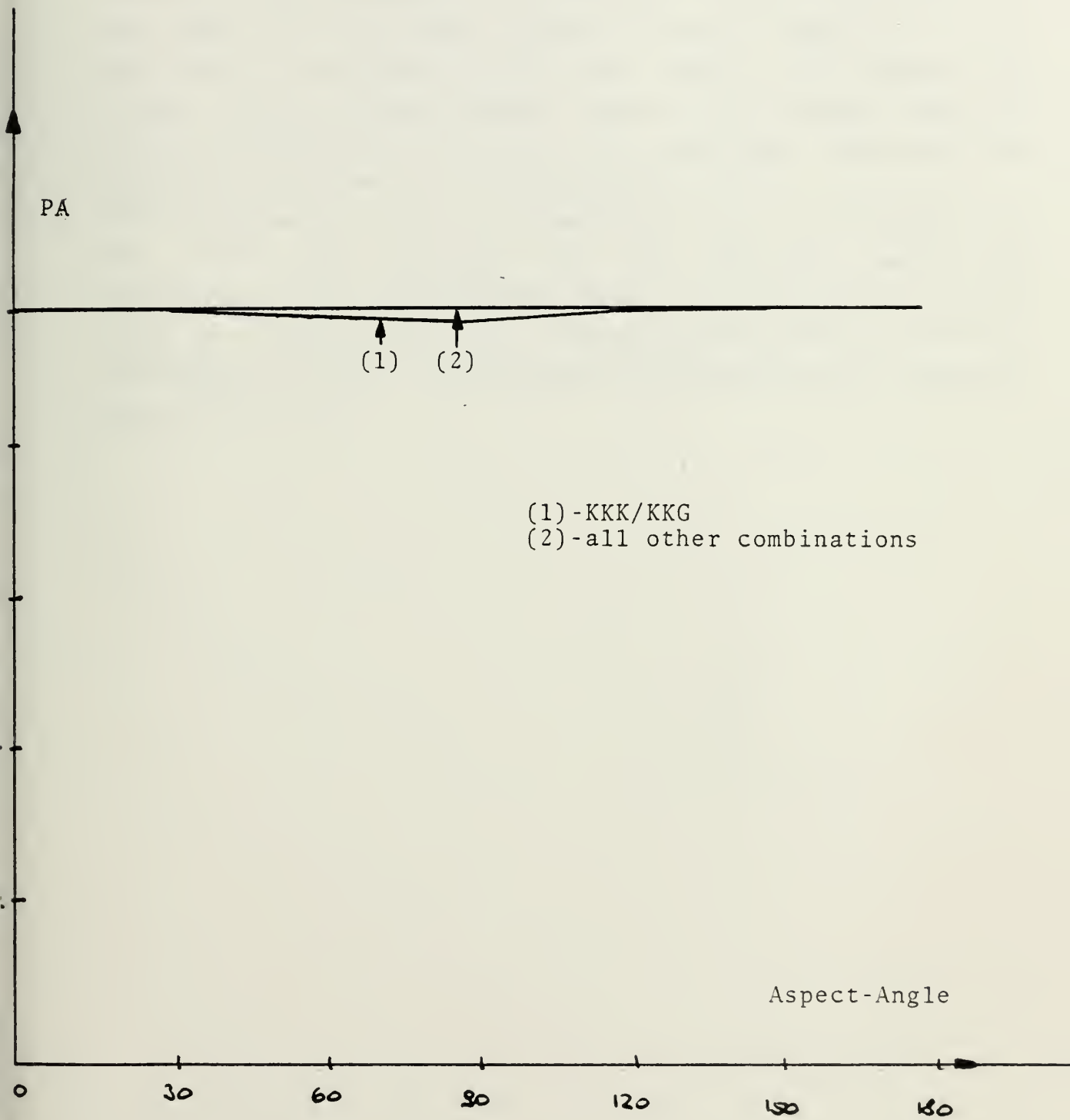


Figure 15 - RELATION PA - TARGET ASPECT-ANGLE W/O POA-SHIFT
LSM TARGET - RP9 -

For the RP5-range the same PA-curve characteristic holds for all parameter combinations. The patterns KKK and KKG have an increased absolute slope, compared to the RP9-range. The curves for the LSM target are similar to those of the other target types at this range. The KGK curves decrease more sharply, but generally approach the limiting 1.0 value at an aspect-angle of 90° .

The PA-curves for the high speed DDG target correspond to the same three patterns for the RP9-range, with the distinction, that the maximum values at aspect-angles 0° and 180° are less than 1.0, and the minimum value at 90° is decreased by 0.02. the patterns GKG and GGG do not deviate from 0.99 or 1.0.

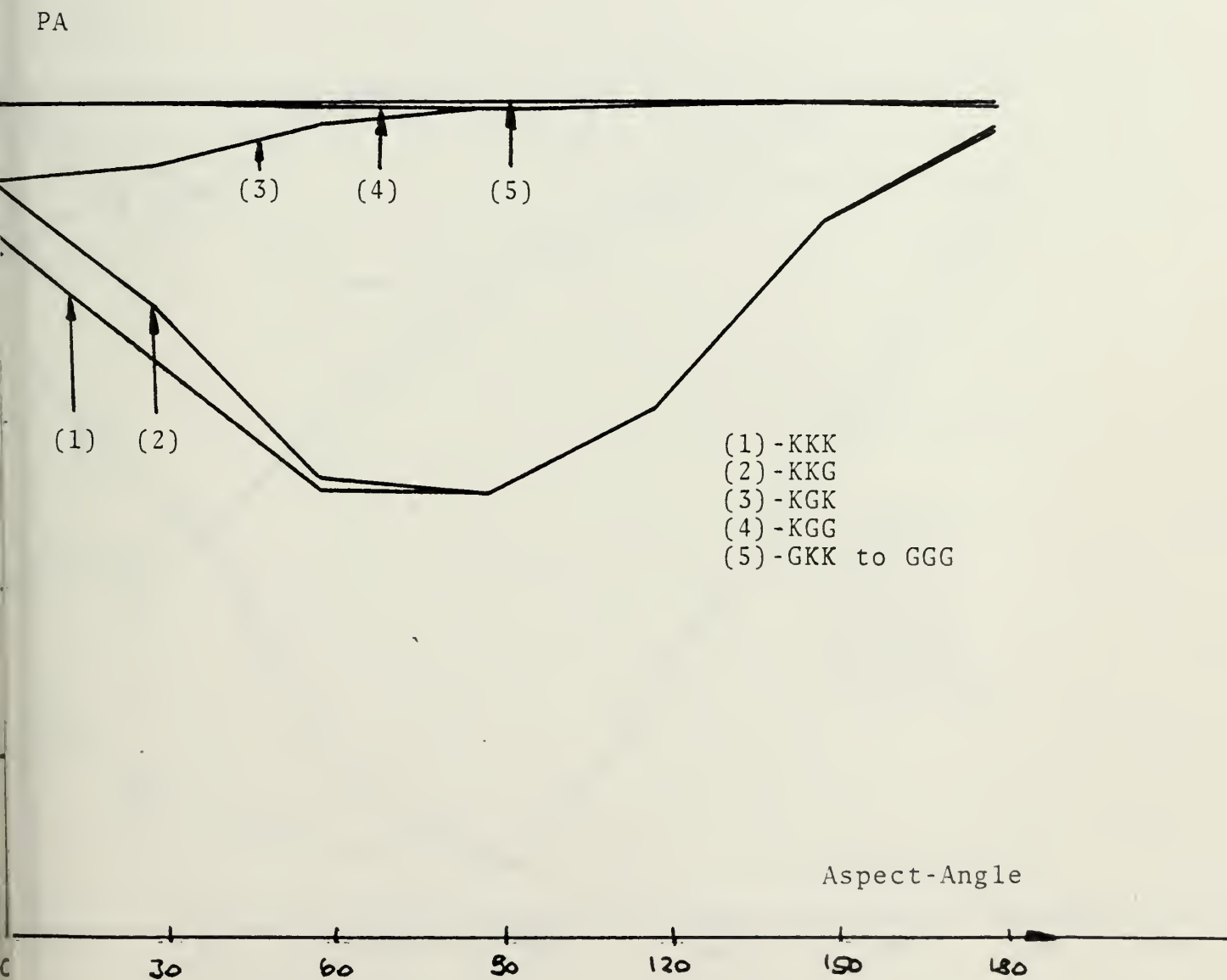


Figure 16 - RELATION PA - TARGET ASPECT-ANGLE W/O POA-SHIFT
 DDG TARGET 'LOW SPEED' - RP5 -

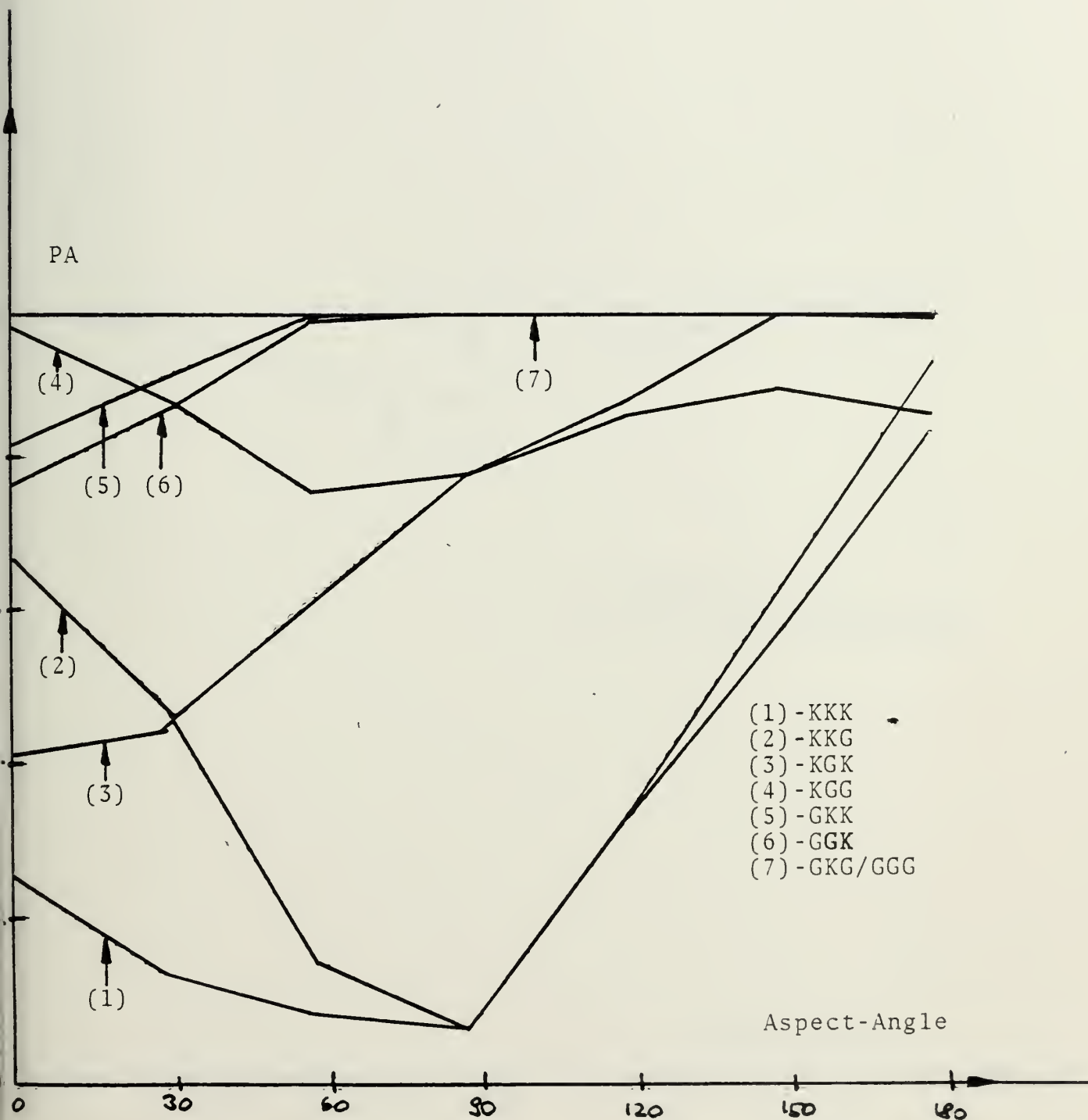


Figure 17 - RELATION PA - TARGET ASPECT-ANGLE W/O POA-SHIFT
 DDG TARGET 'HIGH SPEED' - RP5 -

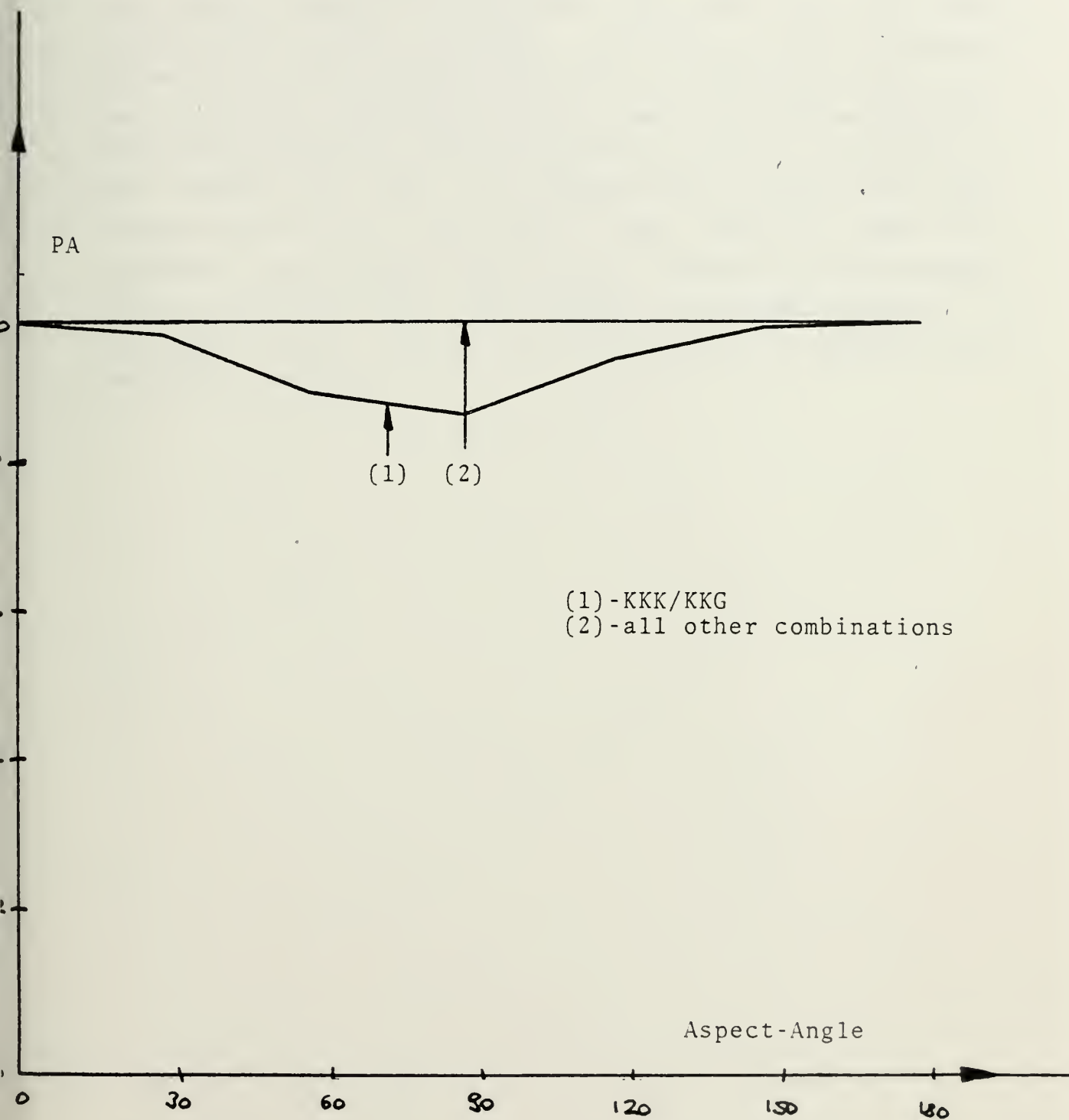


Figure 18 - RELATION PA - TARGET ASPECT-ANGLE W/O POA-SHIFT
LSM TARGET - RP5 -

For the RP1-range the PA-curves for the target types PFG, FPEG, and LSM follow the same general behavior as for the previous ranges RP9 and RP5. The graph for the high acceleration DDG, however, reveals a very distinct dependence on the aspect-angle and a different shape for each parameter combination at the small activation-distance. The minimum PA-value varies from 30° to 90° but returns to the maximum at 180° . The patterns GKK and GKG have their minimum value at 0° (0.92, 0.89) with positive slope and approach the limiting value of 1.0 reached by the patterns GKG and GGG at 90° . The slopes increased further in absolute values. Almost the same trend can be observed for the high speed DDG.

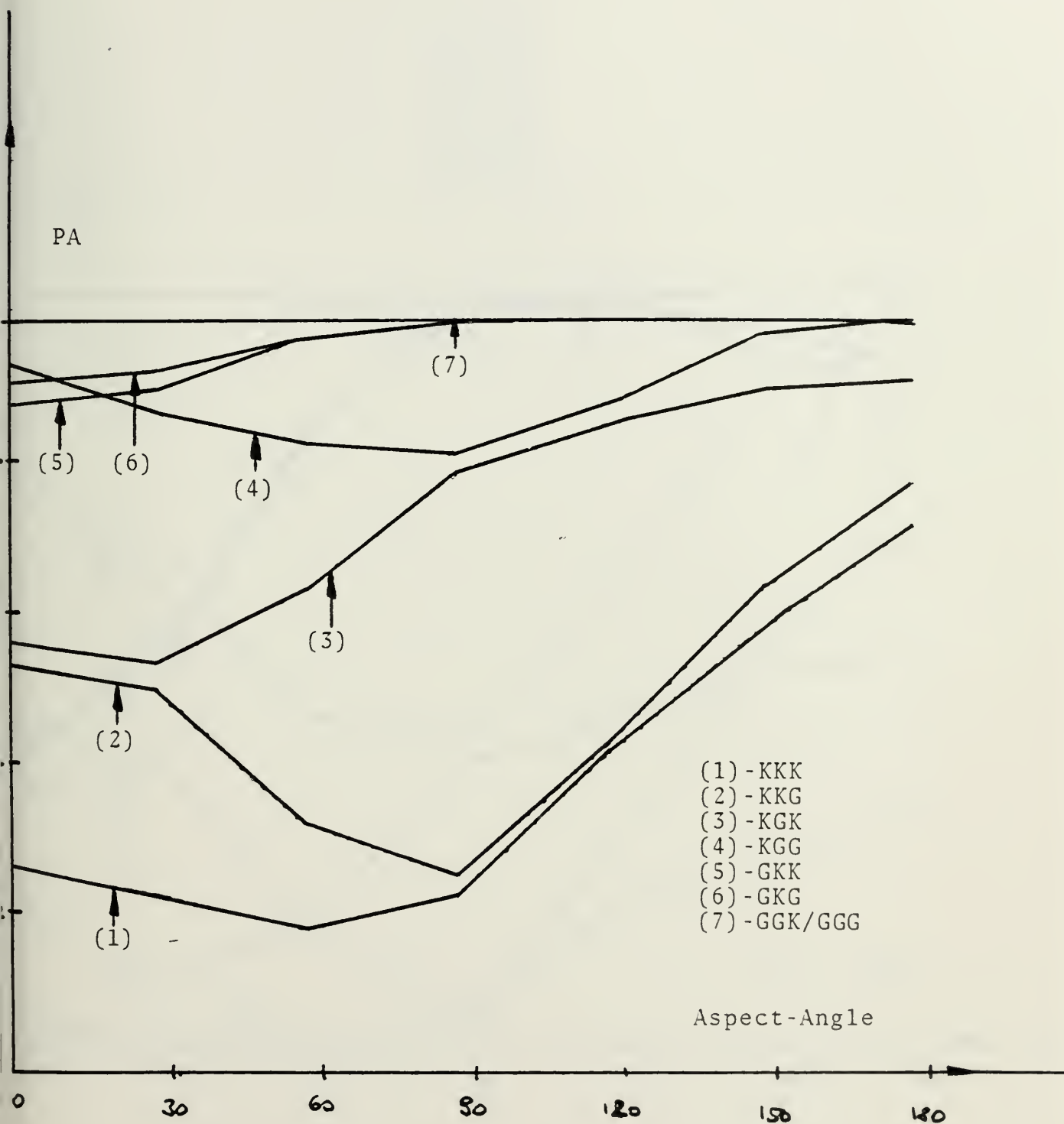


Figure 19 - RELATION PA - TARGET ASPECT-ANGLE W/O POA-SHIFT
 DDG TARGET (LOW SPEED) - RP1 -

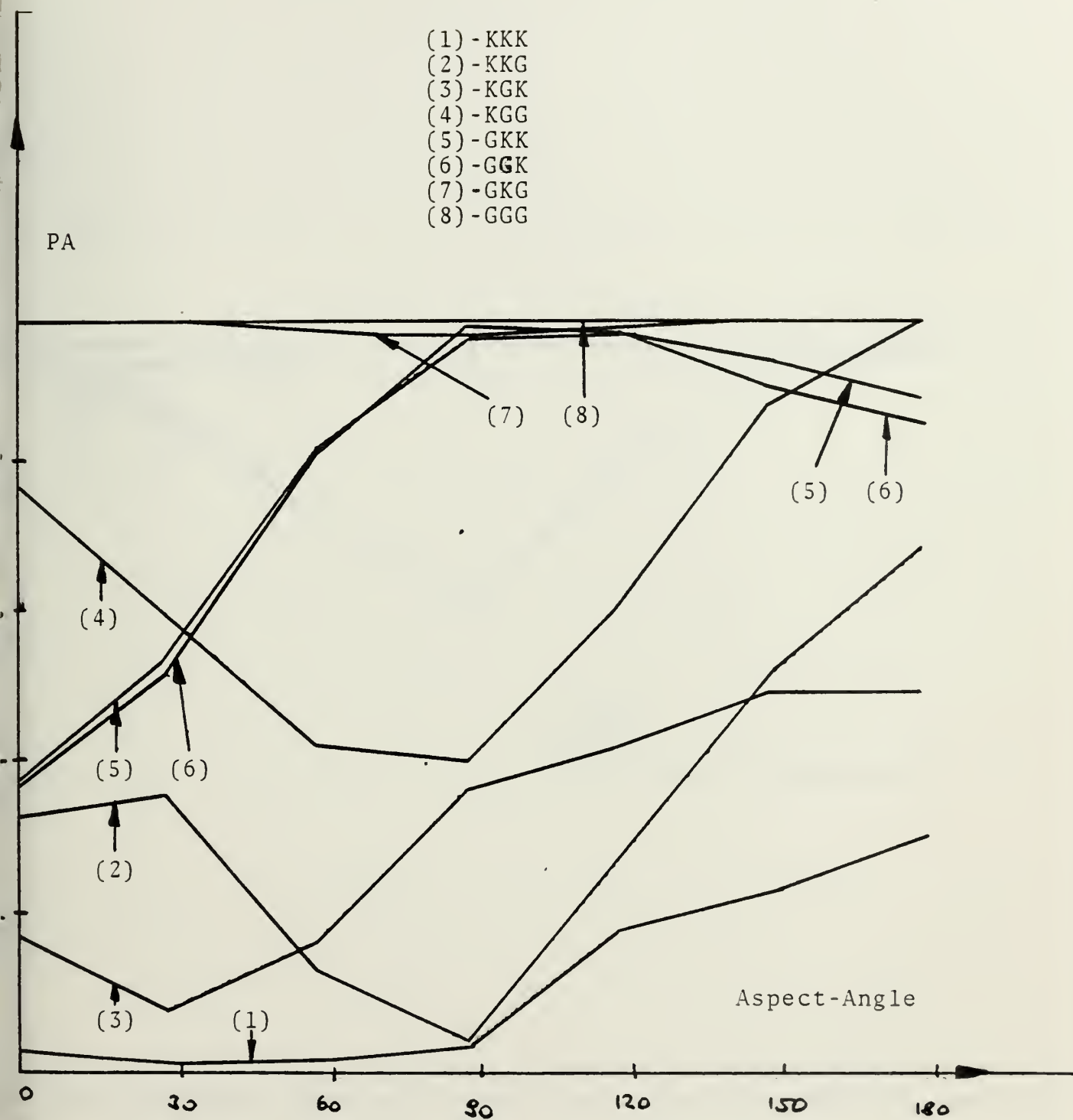


Figure 20 - RELATION PA - TARGET ASPECT-ANGLE W/O POA-SHIFT
 DDG TARGET (HIGH SPEED) - RP1 -

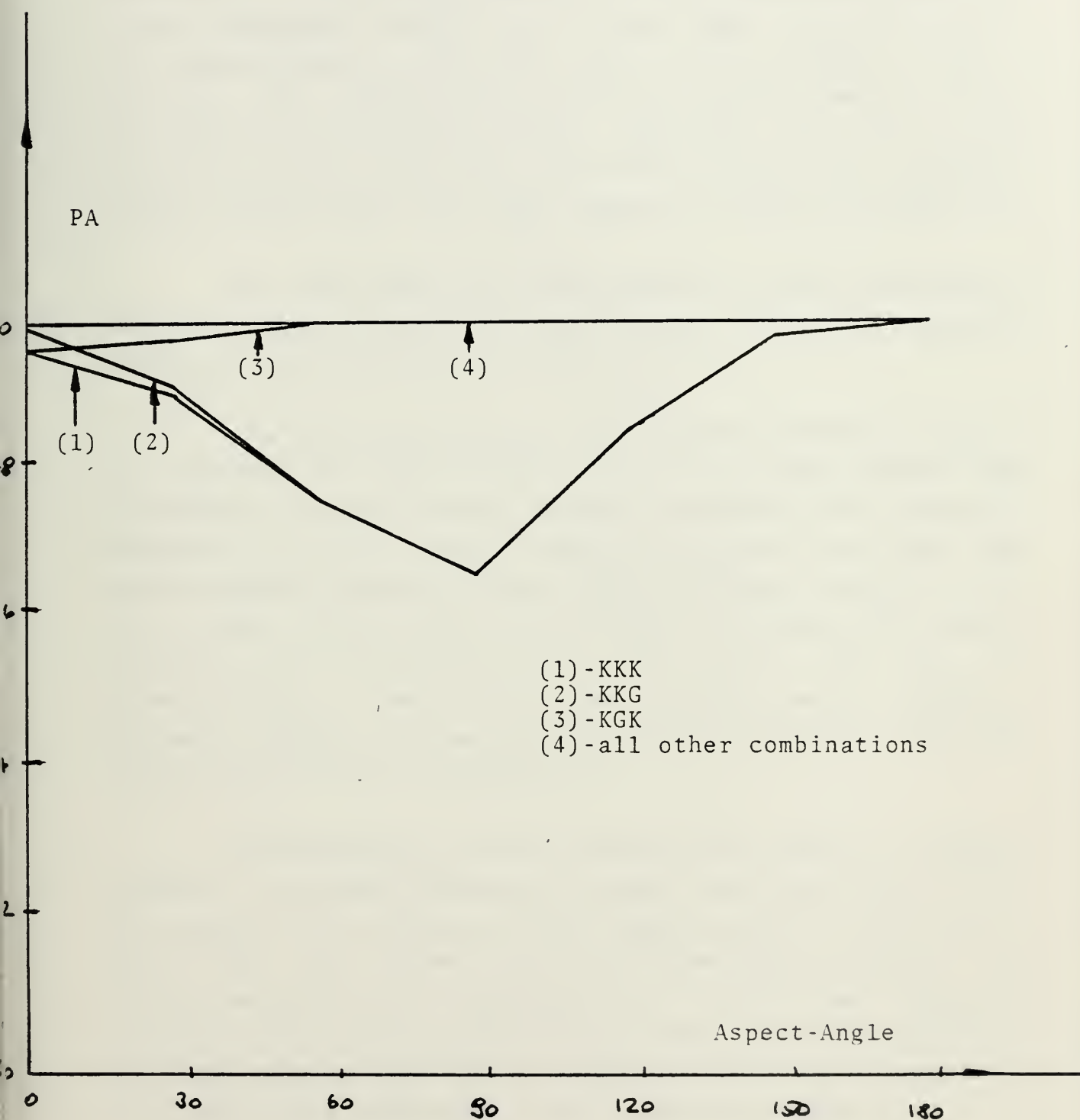


Figure 21 - RELATION PA - TARGET ASPECT-ANGLE W/O POA-SHIFT
LSM TARGET - RP1 -

The inclusion of the POA-shift for the LSM target produces no change in the behavior of the PA-curves over all three RP-ranges, because the the magnitude of the POA-shift is insignificant. For the other three target types, however, the graphs reveal similar behavior over all three RP-ranges; the PA-curves for the RP9-range show the same trend as for the LSM target; the POA-shift for this range is almost negligible for all target types, see Fig 22 and Fig 23.

The RP5-range with the related POA-shift produces a flatter PA-curve for all aspect-angles with the minimum still at 90° , see Fig 24 and Fig 25.

The RP1-range PA-curves for the PFG and FPBG targets are similar to each other, and to the curves without the POA-shift. The DDG target, however, generates very distinct PA-curves for the search pattern KKK and KKG, which now their maximum between 60° and 120° , and their minimum at 0° and 180° . The other four search pattern are almost identical with a PA-value of not less than 0.98 for all aspect-angles, see Fig 19 and 26. Even more distinct, although similar, is the trend of the PA-curves for the high speed DDG, see Fig 20 and Fig 27.

Interpretation of the graphs shows that the results support the second hypothesis, which states that the PA can be improved by a properly chosen aspect-angle to the target. Note that this is not the radar cross section effect. It occurs because of the dependence of PA on the target's mobility. The convolution of this effect with the variation in cross section with aspect-angle has not been explored. This problem is addressed in the classified appendix.

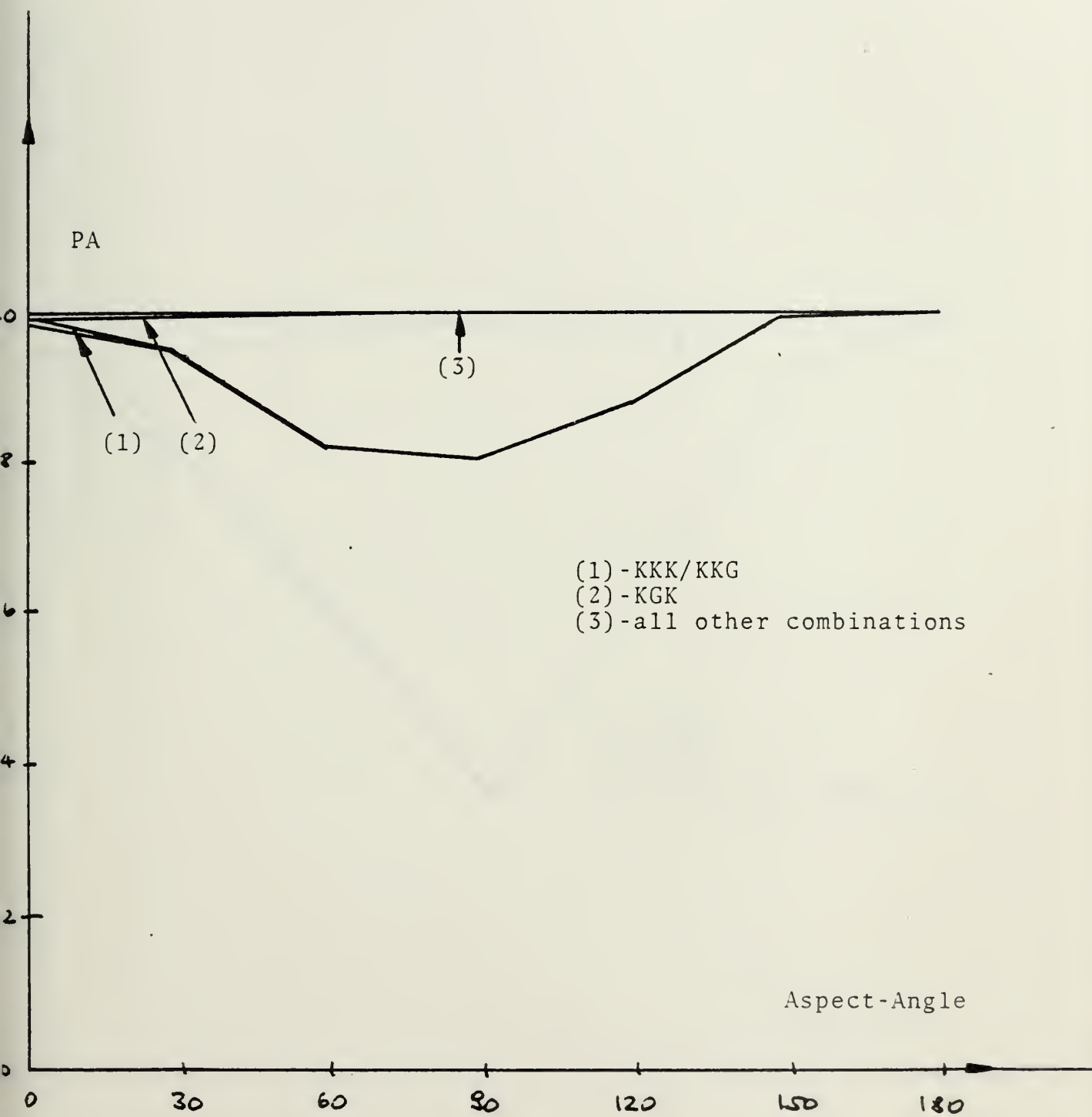


Figure 22 - RELATION PA - TARGET ASPECT-ANGLE W POA-SHIFT
DDG TARGET (LOW SPEED) - RP9 -

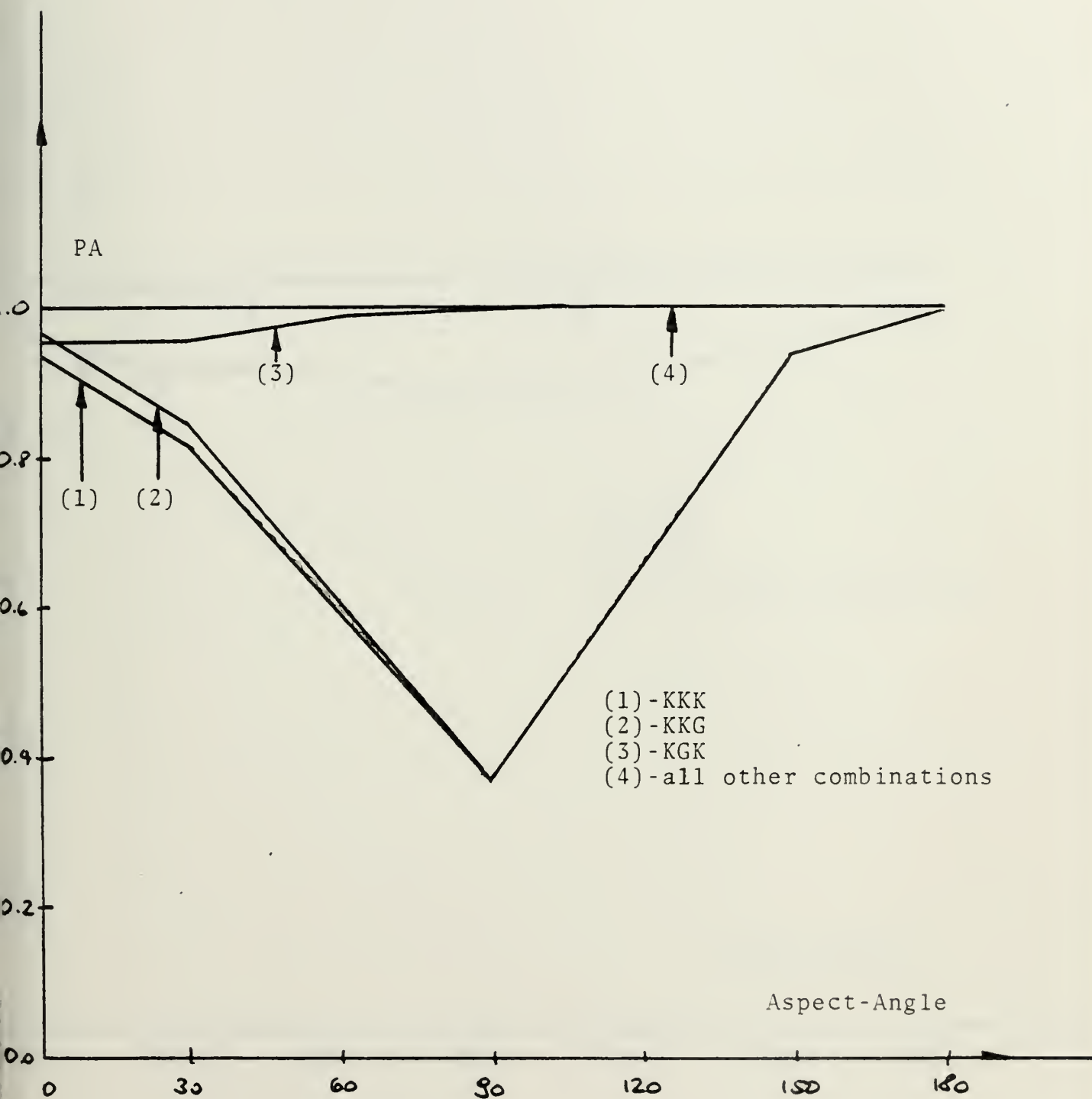


Figure 23 - RELATION PA - TARGET ASPECT-ANGLE W POA-SHIFT
DDG TARGET (HIGH SPEED) - RP9 -

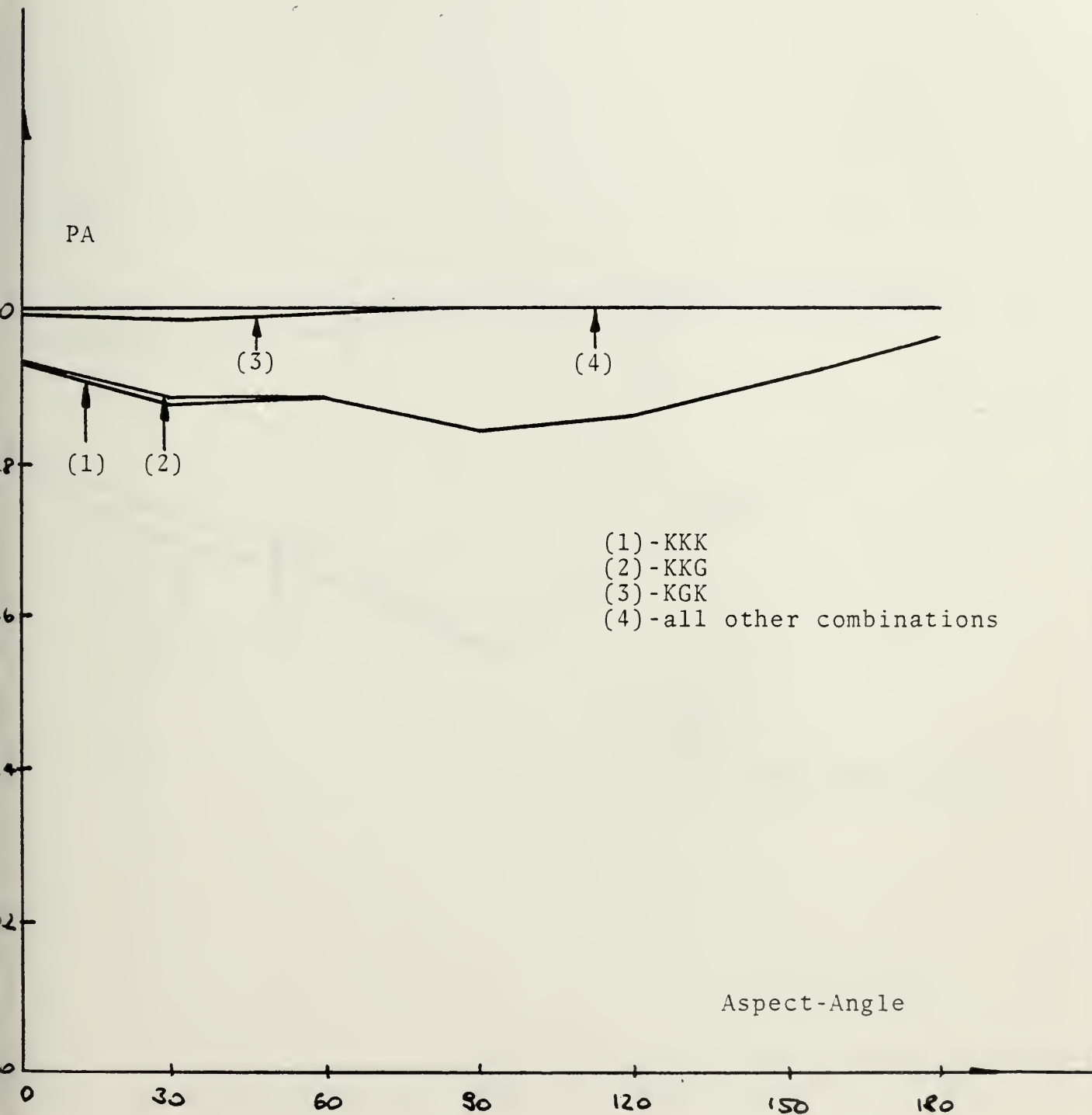


Figure 24 - RELATION PA - TARGET ASPECT-ANGLE W POA-SHIFT
DDG TARGET 'LOW SPEED' - RP5 -

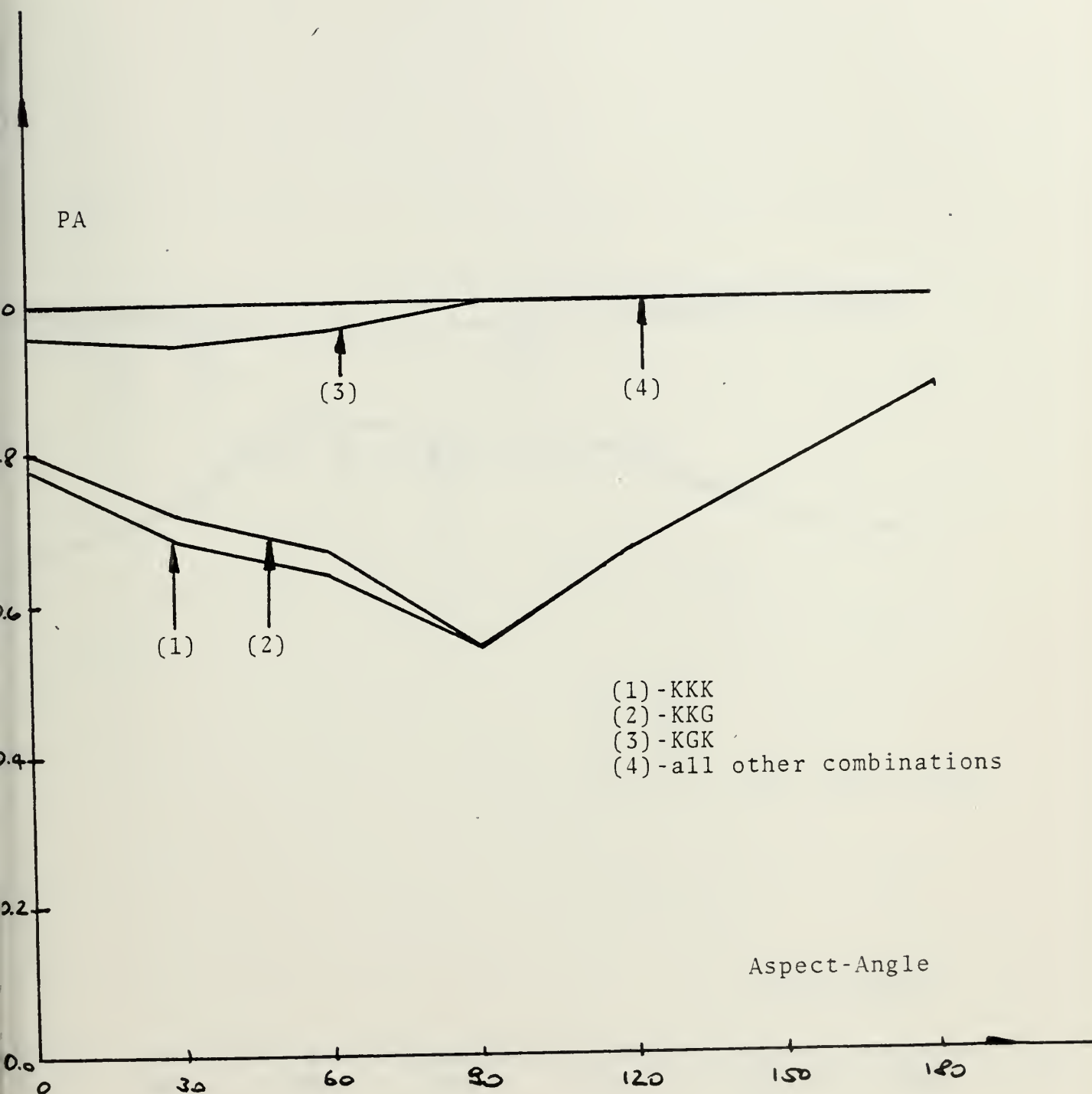


Figure 25 - RELATION PA - TARGET ASPECT-ANGLE W POA-SHIFT
 DDG TARGET (HIGH SPEED) - RP5 -

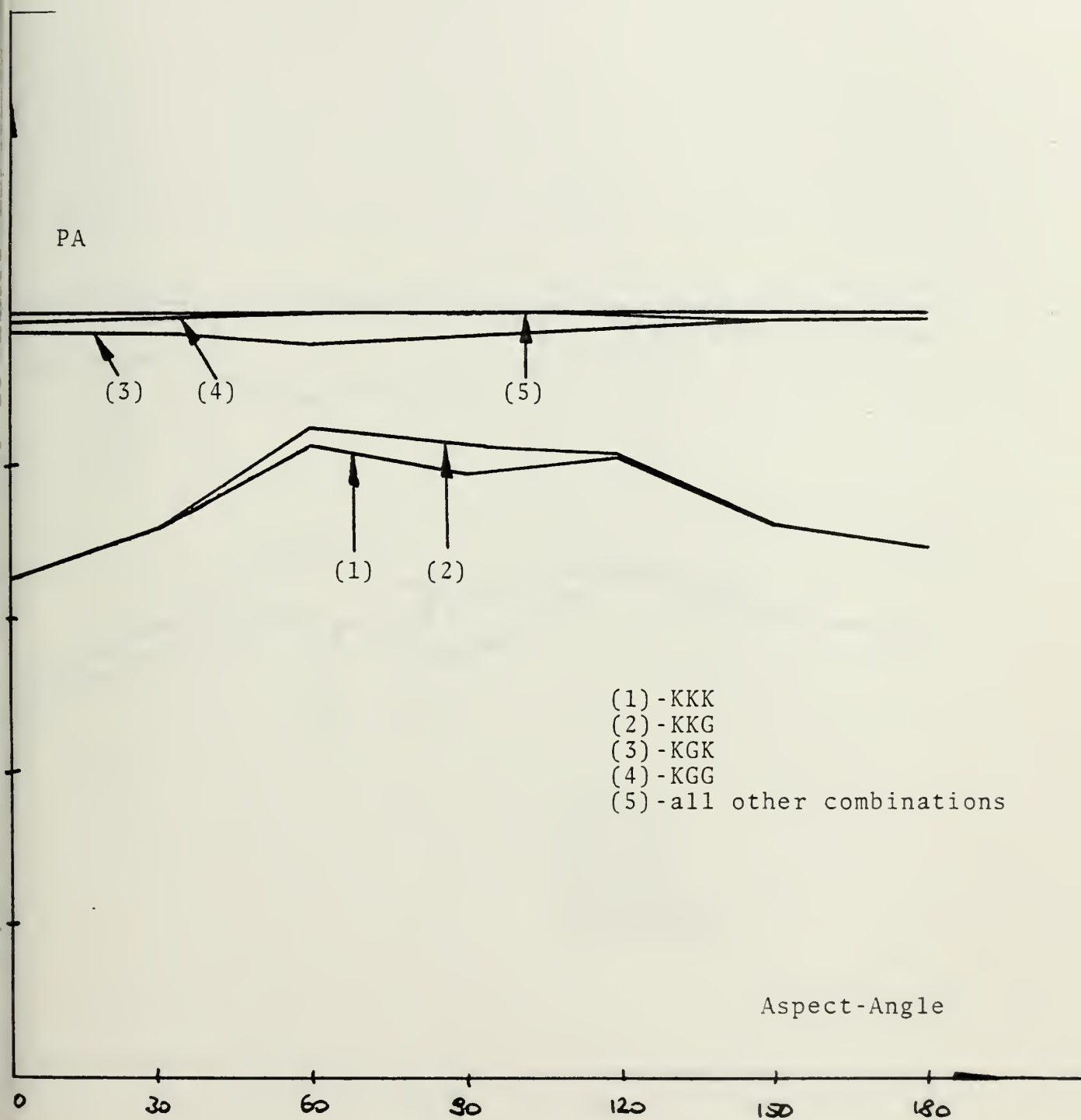


Figure 26 - RELATION PA - TARGET ASPECT-ANGLE W POA-SHIFT
DDG TARGET (LOW SPEED) - RP1 -

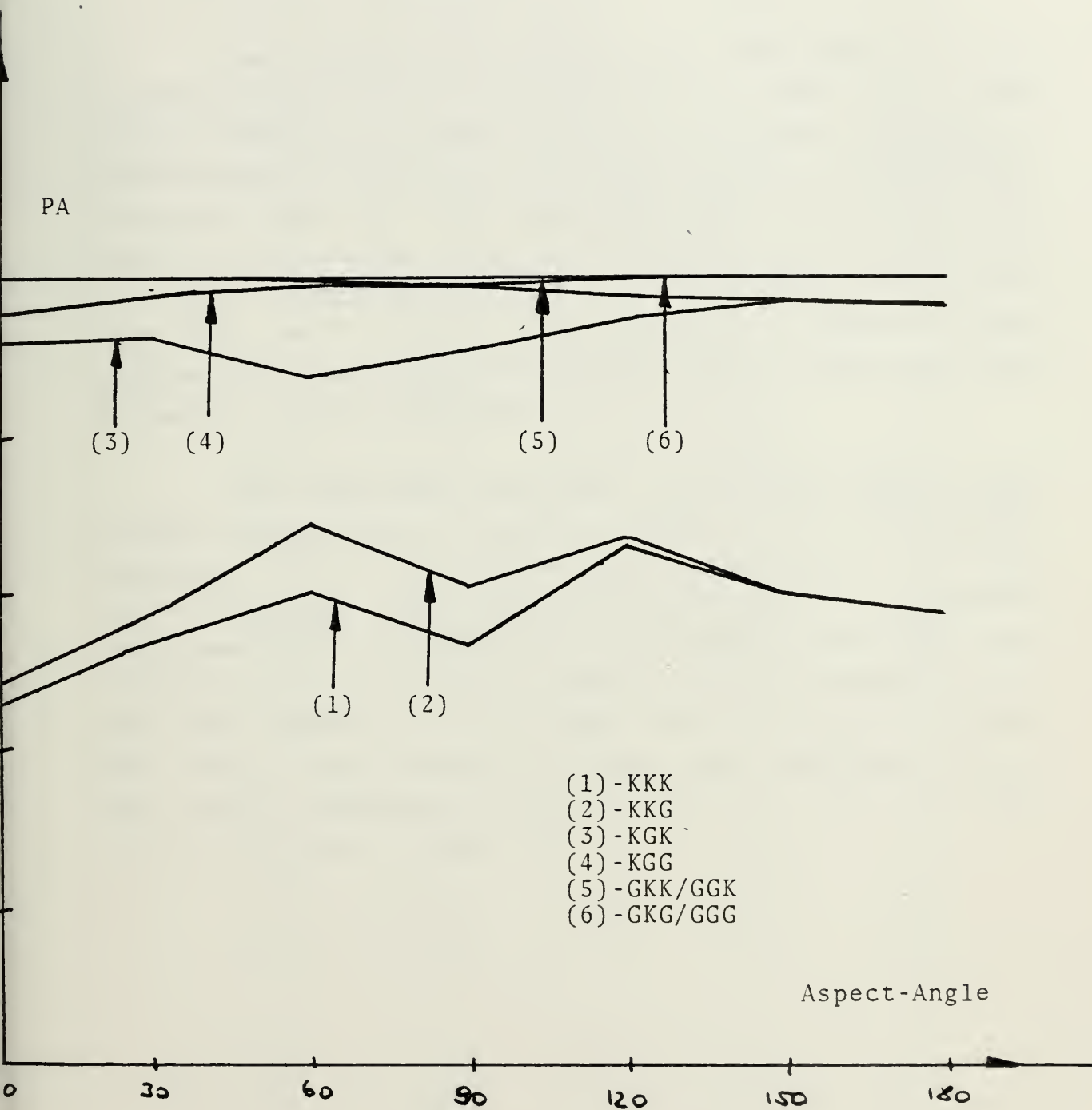


Figure 27 - RELATION PA - TARGET ASPECT-ANGLE W POA-SHIFT
 DDG TARGET (HIGH SPEED) - RP1 -

4. PA w/r to POA-Shift

The previous two subsections, which dealt with the interdependence of PA and target range as well as PA and target aspect-angle, reveal that an intentional POA-shift in the direction of the projected target-motion significantly increased the PA. The only exception was the LSM, the slowly reacting ship, where the POA-shift did not affect the PA. These results support the third hypothesis. The fourth hypothesis, which stated, that the PA can be improved by any combination of an appropriate target range, aspect-angle and POA-shift, is also verified.

The additional experiment for the DDG target, where a high initial speed is assumed, revealed its significant influence on the PA for all search patterns at the three range variants, and therefore emphasized the potential importance of the POA-shift. It turned out that with this POA-shift the search patterns GKK and GGK in addition to GKG and GGG assure a PA of at least 0.99 over the whole range set, which is not the case without the implementation of this shift. Excerpts of the PA-results for an aspect-angle of 30° are shown in Table VIII.

1. 14-30 KTS NO POA-SHIFT

RANGE	KKK	KKG	KGK	KGG
15000	1.0000	1.0000	1.0000	1.0000
18000	1.0000	1.0000	1.0000	1.0000
21000	0.9825	0.9875	0.9962	1.0000
24000	0.8487	0.8675	0.9650	1.0000
26000	0.6800	0.7625	0.9175	0.9987
32000	0.2287	0.5137	0.5237	0.8775

RANGE	GKK	GKG	GGK	GGG
15000	1.0000	1.0000	1.0000	1.0000
18000	1.0000	1.0000	1.0000	1.0000
21000	1.0000	1.0000	1.0000	1.0000
24000	1.0000	1.0000	1.0000	1.0000
26000	0.9962	1.0000	0.9975	1.0000
32000	0.9337	1.0000	0.9212	1.0000

2. 28-30 KTS NO POA-SHIFT

RANGE	KKK	KKG	KGK	KGG
15000	0.9987	1.0000	0.9975	1.0000
18000	0.8912	0.9250	0.9600	1.0000
21000	0.5950	0.7275	0.8287	1.0000
24000	0.2625	0.5350	0.6325	0.9687
26000	0.1225	0.4837	0.4350	0.8937
32000	0.0112	0.3925	0.1000	0.5950

RANGE	GKK	GKG	GGK	GGG
15000	1.0000	1.0000	1.0000	1.0000
18000	1.0000	1.0000	1.0000	1.0000
21000	0.9987	1.0000	0.9975	1.0000
24000	0.9687	1.0000	0.9537	1.0000
26000	0.9037	1.0000	0.8637	1.0000
32000	0.5637	0.9975	0.5400	1.0000

3. 28-30 KTS W POA-SHIFT

RANGE	KKK	KKG	KGK	KGG
15000	0.9987	1.0000	0.9975	1.0000
18000	0.8912	0.9250	0.9600	1.0000
21000	0.8337	0.8637	0.9537	1.0000
24000	0.7462	0.7787	0.9437	1.0000
26000	0.6887	0.7337	0.9550	1.0000
32000	0.5437	0.5775	0.9237	0.9737

RANGE	GKK	GKG	GGK	GGG
15000	1.0000	1.0000	1.0000	1.0000
18000	1.0000	1.0000	1.0000	1.0000
21000	1.0000	1.0000	1.0000	1.0000
24000	1.0000	1.0000	1.0000	1.0000
26000	1.0000	1.0000	1.0000	1.0000
32000	0.9975	1.0000	0.9962	1.0000

Table VIII - PA-RESULTS FOR LOW/HIGH INITIAL SPEED
FOR DDG KRIVAK-CLASS WITH 30° ASPECT

5. PA w/r to Detection-Delay

Another important assumption of the model refers to the delaytimes DETDEL and TRNDEL. TRNDEL is a relatively constant variable, which can be assessed from own-data. There seems no risk of underestimating this value. This, however, is not the case for DETDEL, the time before target reaction begins. If it turns out, that DETDEL with 10 seconds as the "worst" assumption is an underestimation, then the PA will increase, especially for the search patterns with the small activation-distance. This fact should be kept in mind, when the results are analyzed further. Table IX shows as an example the effect of two different values for DETDEL (10/20sec) on the PA for a DDG target with slow initial speed at an aspect-angle of 30°.

1. 28-30 KTS W POA *TDEL: 10 SEC*

RANGE	KKK	KKG	KGK	KGK
15000	0.9987	1.0000	0.9975	1.0000
18000	0.8912	0.9250	0.9600	1.0000
21000	0.8337	0.8637	0.9537	1.0000
24000	0.7462	0.7787	0.9437	1.0000
26000	0.6887	0.7337	0.9550	1.0000
28000	0.6687	0.7112	0.9275	0.9975
32000	0.5437	0.5775	0.9237	0.9737

2. 28-30 KTS W POA *TDEL: 20 SEC*

RANGE	KKK	KKG	KGK	KGK
15000	0.9975	0.9987	0.9975	1.0000
18000	0.9512	0.9625	0.9750	1.0000
21000	0.9037	0.9237	0.9650	1.0000
24000	0.8287	0.8525	0.9500	1.0000
26000	0.7575	0.8000	0.9487	0.9987
28000	0.7525	0.7725	0.9637	0.9987
32000	0.6375	0.6700	0.9337	0.9912

Table IX - PA-RESULTS FOR DIFFERENT DETDEL-VALUES
DDG KRIVAK-CLASS

C. CONCLUSIONS AND RECOMMENDATIONS

Remember that the sensor and missile performance data used for the simulation do not reflect the actual performance characteristics of the systems used on FPBG-classes 143 and 148 (which are German classified). The following conclusions and recommendations are based on modified data, and it should not be inferred that they would have significance for an actual missile employment.

1. Conclusions

1. The discussion of the interdependence between PA and the target range revealed that the missile seeker activation-distance predominantly governs the range at which a PA of 0.99 is guaranteed. For all target types the choice of the larger activation-distance assures a larger engagement range and therefore reduces the own-risk; but the target discrimination capability is also significantly decreased. If the large activation-distance is not chosen for tactical reasons, then the size of the missile search-angle dominates the PA.

It also turned out that the acceleration capability of the target has a significant influence on the range at which it can be acquired by the missile seeker with a PA of at least 0.99. One can choose a larger engagement range when the target accelerates slowly and still have an acceptable own-risk.

2. The interdependence between PA and target aspect-angle generally showed that aspect-angles between 60° and 120° yield less favorable PA-values for the sector

combinations with the small activation-distance, and in particular for the patterns KKK and KKG. This behavior opposes the degradation of performance which occurs near 0° and 180° because the target radar cross section is minimum at these angles. The objective of this analysis was to investigate the effect of target evasive maneuvers on the PA of the missile seeker. At aspect-angles around 90° the search patterns KKK and KKG cover less of the target-motion envelope than for the other aspect-angles. This is of particular significance for fast reacting targets, as the Figures show. See the classified summary for a further discussion and recommendation.

3.The results for the POA-shifted PA as a function of the target range and the aspect-angles revealed a significant impact on the PA for all search patterns when the target range exceeded the RP5-range. This is especially true for the search pattern with the small activation-distance.

4.One of the assumptions of the simulation model referred to the "standard scenario", which excluded any effect on the detection range caused by ducting. If evaporation ducting conditions exist, then their effect on the engagement range can be exploited to advantage with this POA-shift. In this context see Tables III to VII.

5.The patterns GKG and GGG will always meet PA condition, but at the expense of TD; with the POA-shift GKK and GKG also meet the criterion, and the potential for TD is greatly improved.

6.Several variables, notably DETDEL have been conservatively estimated so that the conclusions are appropriate for the "worst case" scenario. To the extent that the variables have been underestimated, improvements in PA can be anticipated.

2. Recommendations

1. In all engagements use a POA-shift based on the estimated target performance data at ranges at and beyond the RP5-range. Tables of this shift are provided in the classified summary.

2. Avoid, if possible, target aspect-angles in the vicinity of 90° , if the small activation-distance is chosen, and if the target cross section is not a strong function of the aspect-angle.

3. If target range is appropriate, use the small activation-distance in multiship engagements.

4. Make realistic assessments of enemy's detection capabilities, because they strongly affect the PA.

VII. ASSISTED TARGETING-SCHEME

The simulation model MM38-OTH is used to model engagements in which the target range is outside the FPBG radar horizon range, but within the practical attack range of the missile and when an extended platform (HC or RPV) is available to provide target data. The additional time delay for reporting data via UHF is included in the simulation model. The model MM38-OTH allows for the procedures which are appropriate for the engagement ranges investigated. The launch-platform, with the known range and bearing to the extended platform, can then calculate the target's position and the targeting solution. The position data for the extended platform are very accurate. The fire control radar is used for this purpose, which has the additional advantage, that its radiation might not be detected by hostile sensors due to the narrow beam characteristics. Therefore the presence of the launch platform might be concealed longer.

The previous sections illustrated the necessary assumptions for the general simulation model; some specific characteristics for this variant (MM38-OTH) already have been introduced in section V. and VI. The model determines the MOE for both the shifted and unshifted POA cases. Fig 28 depicts the geometry used for this model, and indicates the use of a POA-shift. The relevant data are presented in Table I.

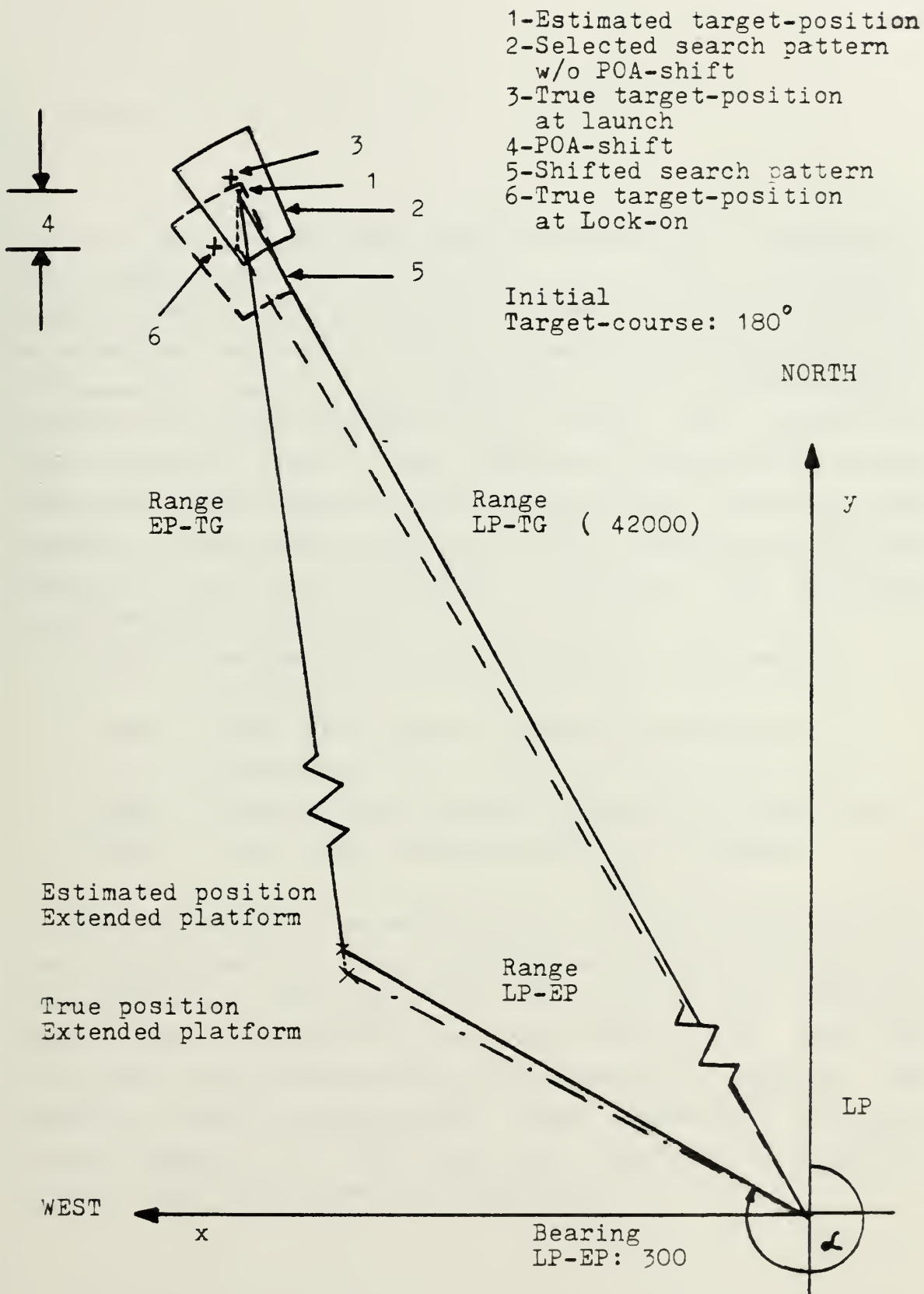


Figure 28 - TARGETING-GEOMETRY FOR THE OTH-SCHEME

A. RESULTS

This part of the analysis investigates the influence of the extended platform location and sensor performance characteristics on the PA for the various search patterns. As expected, the factors which strongly affect the PA in the UAT-scenario also are dominant in the OTH-scenario. Therefore it seems unnecessary to discuss the effects of these factors again. Two additional factors also become important; they define the extended platform location with respect to the launch platform, and the target position with respect to the extended platform location. The following variables are introduced:

- BLPEP - bearing from launch platform to extended platform,
- RLPEP - range from launch platform to extended platform,
- BEPTG - bearing from extended platform to target, and
- REPTG - range from extended platform to target.

The UAT-scheme also showed that the DDG Krivak-Class, the rapidly reacting ship, illustrates all of the effects of the additional variables upon PA; so in the OTH-model results are reported only for this target type. Runs with the other target types would show a similar behavior. The possible target aspect-angles were restricted to three forward angles, 0° , 30° , and 60° , measured as negative angles, i.e. target bow is to the left.

1. PA w/r to HC-Location

Generally, for a given scenario, the smallest REPTG-value provides the best PA-value, because the HC-sensor is more accurate at shorter ranges. The estimated target ranges of 36000 and 40000 m provide trends similar to the results for 32000 m, but the PA is gradually decreasing, so that at an engagement range of about 40000 m only the GGG search pattern assures a PA of at least 0.99 for all HC-locations. The GKG pattern meets this requirement only for the BLPEP-values of 5° and 10° and the two closest target locations. Tables X and XI provide excerpts of PA-results for BLPEP-values of 10° and 20° as a comparison. In these tables no POA-shift is assumed. The aspect-angle is -30° , and SIGBE is constant at 1° .

DDG KRIYAK-CLASS 14-30 KTS NO PCA-SHIFT

1. RLPTG: 32000 M

REFTG	BEPTG	RLPEP	KKK	KKG	KGK	KGK
10000	306	23200	0.55	0.64	0.76	0.92
14000	317	18660	0.57	0.67	0.75	0.90
18000	322	14400	0.51	0.61	0.74	0.88
22000	325	10230	0.49	0.60	0.72	0.87

REPTG	BEPTG	RLPEP	GKK	GKG	GGK	GGG
10000	306	23200	0.99	1.00	0.99	1.00
14000	317	18660	0.99	1.00	0.99	1.00
18000	322	14400	0.99	1.00	0.99	1.00
22000	325	10230	0.99	1.00	0.99	1.00

2. RLPTG: 36000 M

REPTG	BEPTG	RLPEP	KKK	KKG	KGK	KGK
10000	301	27650	0.30	0.55	0.50	0.83
15000	315	21820	0.29	0.52	0.48	0.82
20000	322	16460	0.29	0.49	0.50	0.79
25000	326	11250	0.30	0.49	0.45	0.75

REPTG	BEPTG	RLPEP	GKK	GKG	GGK	GGG
10000	301	27650	0.93	1.00	0.89	1.00
15000	315	21820	0.91	0.99	0.91	1.00
20000	322	16460	0.90	0.99	0.89	1.00
25000	326	11250	0.89	0.96	0.91	1.00

3. RLPTG: 40000 M

REPTG	BEPTG	RLPEP	KKK	KKG	KGK	KGK
10000	296	32200	0.13	0.46	0.29	0.71
17000	316	23900	0.13	0.39	0.31	0.68
24000	323	16420	0.17	0.41	0.27	0.66
31000	327	9180	0.14	0.39	0.28	0.65

REPTG	BEPTG	RLPEP	GKK	GKG	GGK	GGG
10000	296	32200	0.71	0.99	0.71	1.00
17000	316	23900	0.72	0.97	0.71	1.00
24000	323	16420	0.73	0.94	0.75	1.00
31000	327	9180	0.66	0.90	0.71	1.00

Table X - PA-RESULTS FOR BLPEP OF 100

DDG KRIVAK-CLASS 14-30 KTS NO POA-SHIFT

1. RLPTG: 32000 M

REPTG	BEPTG	RLPEP	KKK	KKG	KGK	KGG
14C00	299	21340	0.59	0.66	0.76	0.92
16C00	307	18400	0.53	0.63	0.75	0.90
18C00	313	15800	0.55	0.66	0.74	0.89
20C00	317	13330	0.51	0.60	0.75	0.87

REPTG	BEPTG	RLPEP	GKK	GKG	GGK	GGG
14000	299	21340	0.99	1.00	0.99	1.00
16C00	307	18400	0.99	1.00	0.99	1.00
18C00	313	15800	0.99	1.00	0.99	1.00
20C00	317	13330	0.99	1.00	1.00	1.00

2. RLPTG: 36000 M

REPTG	BEPTG	RLPEP	KKK	KKG	KGK	KGG
14C00	288	27170	0.30	0.51	0.49	0.82
16C00	307	20700	0.30	0.50	0.50	0.82
22C00	316	15600	0.30	0.51	0.49	0.80
26000	322	10930	0.30	0.49	0.48	0.76

REPTG	BEPTG	RLPEP	GKK	GKG	GGK	GGG
14C00	288	27170	0.90	1.00	0.89	1.00
18000	307	20700	0.92	0.99	0.90	1.00
22000	316	15600	0.92	0.99	0.90	1.00
26C00	322	10930	0.90	0.96	0.91	1.00

3. RLPTG: 40000 M

REPTG	BEPTG	RLPEP	KKK	KKG	KGK	KGG
14C00	272	34620	0.13	0.40	0.30	0.71
20C00	307	23000	0.12	0.40	0.25	0.67
26000	318	15500	0.16	0.41	0.29	0.66
32C00	325	8700	0.14	0.38	0.27	0.64

REPTG	BEPTG	RLPEP	GKK	GKG	GGK	GGG
14000	272	34620	0.72	0.98	0.74	1.00
20C00	307	23000	0.74	0.97	0.72	1.00
26C00	318	15500	0.70	0.93	0.72	1.00
32000	325	8700	0.68	0.92	0.70	1.00

Table XI - PA-RESULTS FOR BLPEP OF 20°

2. PA w/r to HC-Sensor Data

The HC was deployed at four different bearings, 5°, 10°, 15°, and 20°, and at four different ranges from the launch platform (RLPEP). The range error of the HC-sensor is relative small, and has a insignificant influence on the degree of overall uncertainty. Given a SIGBE of 10, an estimated target range of 32000 m, a BLPEP-value of 5° and a decrease of the aspect-angle from -60° to 0°, the simulation results showed that the search patterns with the small activation-distance yield maximum PA-values. Increases from 0.56 to 0.75, 0.41 to 0.83, and from 0.62 to 0.75 are recorded for the patterns KKK, KKG, and KGG. The parameter combination KGG showed an almost opposite trend; its PA-value increased from 0.715 to 0.87, with the decrease of the aspect-angle from -60° to 0°. Similar trends for these four search pattern are reported for the BLPEP of 10° to 20°.

The parameter combinations based on the large activation-distance showed that a bearing greater than 15° has a degrading effect on the PA. For BLPEP of 5° to 15° the search patterns GGG and GGG produce acceptable PA-values for all four ranges; the minimum value for GGG and GGG is 0.975, which drops to 0.91 for a bearing of 20° at the target range of 36000 m. The employment of an HC-sensor with a bearing error of 20 or even 30 significantly decrease the PA-values for all search parameter combinations over all values of REPTG; with these bearing errors the pattern GGG produces acceptable results only at 10000 m, the others fail at all ranges.

Tables XII to XIV show the influence on the PA of different values for SIGBE at a constant BLPEP-value of 10^0 and a constant aspect-angle of -30^0 . Table XV compares the PA-values for an aspect-angle of 0^0 and SIGBE of 1^0 . The POA has not been shifted.

DDG KRIVAK-CLASS 14-30 KTS NO PCA-SHIFT

1. RLPTG: 32000 M

REPTG	BEPTG	RLPEP	KKK	KKG	KGK	KGG
14000	317	18670	0.46	0.54	0.67	0.82
17000	321	15500	0.44	0.49	0.64	0.75
20000	324	12300	0.37	0.44	0.60	0.71
23000	326	9200	0.36	0.42	0.56	0.66

REPTG	BEPTG	RLPEP	GKK	GKG	GGK	GGG
14000	317	18670	0.97	0.98	0.99	1.00
17000	321	15500	0.94	0.94	0.99	1.00
20000	324	12300	0.90	0.90	0.99	1.00
23000	326	9200	0.84	0.84	0.99	1.00

2. RLPTG: 36000 M

REPTG	BEPTG	RLPEP	KKK	KKG	KGK	KGG
14000	314	23000	0.26	0.44	0.44	0.73
18000	320	18600	0.26	0.43	0.41	0.67
22000	324	14360	0.23	0.36	0.39	0.60
26000	326	10220	0.23	0.36	0.39	0.58

REPTG	BEPTG	RLPEP	GKK	GKG	GGK	GGG
14000	314	23000	0.86	0.93	0.90	1.00
18000	320	18600	0.84	0.91	0.93	1.00
22000	324	14360	0.79	0.83	0.93	1.00
26000	326	10220	0.76	0.81	0.90	0.99

3. RLPTG: 40000 M

REPTG	BEPTG	RLPEP	KKK	KKG	KGK	KGG
14000	310	27240	0.16	0.40	0.28	0.64
20000	320	20650	0.16	0.36	0.26	0.58
26000	325	14340	0.13	0.30	0.22	0.50
32000	328	8160	0.14	0.29	0.25	0.50

REPTG	BEPTG	RLPEP	GKK	GKG	GGK	GGG
14000	310	27240	0.68	0.90	0.75	1.00
20000	320	20650	0.65	0.85	0.73	1.00
26000	325	14340	0.59	0.75	0.74	0.97
32000	328	8160	0.54	0.71	0.72	0.96

Table XII - PA-RESULTS FOR SIGBE OF 10
BLPEP 100/ASPECT-ANGLE -30°

DDG KRIVAK-CLASS 14-30 KTS NO PCA-SHIFT

1. RLPTG: 32000 M

REPTG	BEPTG	RLPEP	KKK	KKG	KGK	KGG
10000	306	23200	0.55	0.64	0.76	0.92
14000	317	18660	0.57	0.67	0.75	0.90
18000	322	14400	0.51	0.61	0.74	0.88
22000	325	10230	0.49	0.60	0.72	0.87

REPTG	BEPTG	RLPEP	GKK	GKG	GGK	GGG
10000	306	23200	0.99	1.00	0.99	1.00
14000	317	18660	0.99	1.00	0.99	1.00
18000	322	14400	0.99	1.00	0.99	1.00
22000	325	10230	0.99	1.00	0.99	1.00

2. RLPTG: 36000 M

REPTG	BEPTG	RLPEP	KKK	KKG	KGK	KGG
10000	301	27650	0.30	0.55	0.50	0.83
15000	315	21820	0.29	0.52	0.48	0.82
20000	322	16460	0.29	0.49	0.50	0.79
25000	326	11250	0.30	0.49	0.45	0.75

REPTG	BEPTG	RLPEP	GKK	GKG	GGK	GGG
10000	301	27650	0.93	1.00	0.89	1.00
15000	315	21820	0.91	0.99	0.91	1.00
20000	322	16460	0.90	0.99	0.89	1.00
25000	326	11250	0.89	0.96	0.91	1.00

3. RLPTG: 40000 M

REPTG	BEPTG	RLPEP	KKK	KKG	KGK	KGG
10000	296	32200	0.13	0.46	0.29	0.71
17000	316	23900	0.13	0.39	0.31	0.68
24000	323	16420	0.17	0.41	0.27	0.66
31000	327	9180	0.14	0.39	0.28	0.65

REPTG	BEPTG	RLPEP	GKK	GKG	GGK	GGG
10000	296	32200	0.71	0.99	0.71	1.00
17000	316	23900	0.72	0.97	0.71	1.00
24000	323	16420	0.73	0.94	0.75	1.00
31000	327	9180	0.66	0.90	0.71	1.00

Table XIII - PA-RESULTS FOR SIGBE OF 2°
BLPEP 10°/ASPECT-ANGLE -30°

DDG KRIVAK-CLASS 14-30 KTS NO PCA-SHIFT

1. RLPTG: 32000 M

REPTG	BEPTG	RLPEP	KKK	KKG	KGK	KGK
14000	317	18700	0.39	0.46	0.57	0.70
17000	321	15500	0.35	0.40	0.53	0.61
20000	324	12300	0.27	0.33	0.48	0.56
23000	326	9200	0.26	0.31	0.44	0.51

REPTG	BEPTG	RLPEP	GKK	GKG	GGK	GGG
14000	317	18700	0.88	0.89	1.00	1.00
17000	321	15500	0.82	0.82	0.99	1.00
20000	324	12300	0.75	0.76	0.97	0.98
23000	326	9200	0.68	0.68	0.95	0.95

2. RLPTG: 36000 M

REPTG	BEPTG	RLPEP	KKK	KKG	KGK	KGK
14000	314	23000	0.24	0.39	0.39	0.62
18000	320	18600	0.22	0.35	0.36	0.56
22000	324	14360	0.18	0.29	0.32	0.47
26000	326	10220	0.16	0.26	0.29	0.44

REPTG	BEPTG	RLPEP	GKK	GKG	GGK	GGG
14000	314	23000	0.78	0.85	0.90	1.00
18000	320	18600	0.72	0.77	0.92	0.98
22000	324	14360	0.61	0.66	0.91	0.96
26000	326	10220	0.58	0.62	0.85	0.93

3. RLPTG: 40000 M

REPTG	BEPTG	RLPEP	KKK	KKG	KGK	KGK
14000	310	27240	0.18	0.37	0.26	0.56
20000	320	20640	0.14	0.30	0.23	0.49
26000	325	14340	0.01	0.24	0.18	0.40
32000	328	8200	0.11	0.22	0.21	0.37

REPTG	BEPTG	RLPEP	GKK	GKG	GGK	GGG
14000	310	27240	0.62	0.82	0.77	1.00
20000	320	20640	0.56	0.72	0.74	0.97
26000	325	14340	0.49	0.61	0.71	0.90
32000	328	8200	0.43	0.55	0.65	0.85

Table XIV - PA-RESULTS FOR SIGBE OF 30
BLPEP 100/ASPECT-ANGLE -30°

DDG KRIVAK-CLASS 14-30 KTS NO PGA-SHIFT

1. RLFTG: 32000 M

REPTG	BEPTG	RLPEP	KKK	KKG	KGK	KGG
10C0C	336	23200	0.65	0.83	0.73	0.99
14C00	346	18700	0.61	0.78	0.77	0.99
18C00	352	14400	0.59	0.75	0.71	0.96
22C0C	355	10230	0.53	0.68	0.71	0.93

REPTG	BEPTG	RLPEP	GKK	GKG	GGK	GGG
10C0C	336	23200	0.98	1.00	0.96	1.00
14C0C	346	18700	0.88	1.00	0.97	1.00
18C00	352	14400	0.97	1.00	0.96	1.00
22C0C	355	10230	0.97	1.00	0.97	1.00

2. RLPTG: 36000 M

REPTG	BEPTG	RLPEP	KKK	KKG	KGK	KGG
10C00	331	27650	0.33	0.65	0.52	0.94
15C0C	345	21820	0.33	0.64	0.51	0.92
20C0C	351	16460	0.29	0.58	0.42	0.87
25C0C	355	11250	0.29	0.56	0.43	0.81

REPTG	BEPTG	RLPEP	GKK	GKG	GGK	GGG
10C0C	331	27650	0.85	1.00	0.81	1.00
15C00	345	21820	0.86	1.00	0.84	1.00
20C0C	351	16460	0.85	1.00	0.83	1.00
25C0C	355	11250	0.85	0.98	0.85	1.00

3. RLPTG: 40000 M

REPTG	BEPTG	RLPEP	KKK	KKG	KGK	KGG
10CCC	326	32200	0.13	0.47	0.29	0.83
1700C	345	23900	0.12	0.44	0.29	0.78
24CCC	353	16500	0.13	0.43	0.27	0.75
31C0C	357	9180	0.16	0.42	0.27	0.69

REPTG	BEPTG	RLPEP	GKK	GKG	GGK	GGG
10C00	326	32200	0.63	1.00	0.62	1.00
17CCC	345	23900	0.65	0.99	0.62	1.00
24C00	353	16500	0.63	0.98	0.61	1.00
31CCC	357	9180	0.61	0.95	0.63	1.00

Table XV - PA-RESULTS FOR SIGBE OF 10

BLPEP 10°/ASPECT-ANGLE 0°

3. PA w/r to POA-shift

A POA-shift also improves the PA-results for all parameter combinations for this targeting-scheme. The results are very similar to those for the UAT-scheme. In particular, the use of the search pattern with the small activation-distance has become more realistic, because PA-values exceeding 0.90 are generated. Following the observed overall trend the use of less accurate sensors generally degrades the PA.

A very important result, however, is that a POA-shift applied with a 2° inaccuracy yields a better PA than obtainable with a 1° inaccuracy without the shift. This is also true for the 3° inaccuracy sensor.

Table XVI and XVII show the PA-values generated by the POA-shift for a SIGBE-value of 1° and 2°, and for BLPEP of 10° and an aspect-angle of -30°. Table XII should be used as a comparison, because those data were obtained without a POA-shift.

DDG KRIVAK-CLASS 14-30 KTS WITH POA-SHIFT

1. RLPTG: 32000 M

REPTG	BEPTG	RLPEP	KKK	KKG	KGK	KGG
10000	306	23200	0.76	0.78	0.95	0.98
14000	317	18700	0.77	0.79	0.93	0.97
18000	322	14400	1.00	1.00	1.00	1.00
22000	325	10230	1.00	1.00	1.00	1.00
REPTG	BEPTG	RLPEP	GKK	GKG	GGK	GGG
10000	306	23200	1.00	1.00	1.00	1.00
14000	317	18700	1.00	1.00	1.00	1.00
18000	322	14400	0.73	0.74	0.91	0.94
22000	325	10230	0.65	0.67	0.90	0.93

2. RLPTG: 36000 M

REPTG	BEPTG	RLPEP	KKK	KKG	KGK	KGG
10000	301	27650	0.72	0.74	0.94	0.97
15000	315	21820	0.65	0.67	0.90	0.95
20000	322	16500	0.62	0.64	0.87	0.91
25000	326	11250	0.60	0.62	0.85	0.88
REPTG	BEPTG	RLPEP	GKK	GKG	GGK	GGG
10000	301	27650	1.00	1.00	1.00	1.00
15000	315	21820	1.00	1.00	1.00	1.00
20000	322	16460	1.00	1.00	1.00	1.00
25000	326	11250	0.98	0.98	1.00	1.00

3. RLPTG: 40000 M

REPTG	BEPTG	RLPEP	KKK	KKG	KGK	KGG
10000	296	32200	0.59	0.62	0.90	0.95
17000	316	23900	0.54	0.57	0.85	0.89
24000	323	16420	0.53	0.56	0.80	0.84
31000	327	9180	0.49	0.52	0.77	0.81
REPTG	BEPTG	RLPEP	GKK	GKG	GGK	GGG
10000	296	32200	1.00	1.00	0.99	1.00
17000	316	23900	1.00	1.00	1.00	1.00
24000	323	16420	0.98	0.98	1.00	1.00
31000	327	9180	0.95	0.95	1.00	1.00

Table XVI - PA-RESULTS W/R TO POA-SHIFT
 SIGBE 10°/BLPEP 10°/ASPECT-ANGLE -30°

DDG KRIVAK-CLASS 14-30 KTS WITH POA-SHIFT

1. RLPTG: 32000 M

REPTG	BEPTG	RLPEP	KKK	KKG	KGK	KGK
14CCC	317	18670	0.59	0.60	0.85	0.87
17CCC	321	15450	0.54	0.55	0.79	0.82
20CCC	324	12300	0.47	0.49	0.74	0.76
23000	326	9200	0.45	0.46	0.70	0.71

REPTG	BEPTG	RLPEP	GKK	GKG	GKG	GGG
14C00	317	18670	0.99	0.99	1.00	1.00
17C00	321	15450	0.96	0.96	1.00	1.00
20C00	324	12300	0.94	0.94	1.00	1.00
23C00	326	9200	0.87	0.87	1.00	1.00

2. RLPTG: 36000 M

REPTG	BEPTG	RLPEP	KKK	KKG	KGK	KGK
14CCC	314	23000	0.56	0.58	0.80	0.84
18CCC	320	18600	0.52	0.53	0.77	0.80
22CCC	324	14360	0.41	0.42	0.68	0.71
26CCC	326	10200	0.40	0.42	0.65	0.67

REPTG	BEPTG	RLPEP	GKK	GKG	GKG	GGG
14C00	314	23000	0.98	0.98	1.00	1.00
18C00	320	18600	0.94	0.94	1.00	1.00
22C00	324	14360	0.89	0.89	1.00	1.00
26C00	326	10200	0.85	0.85	1.00	0.99

3. RLPTG: 40000 M

REPTG	BEPTG	RLPEP	KKK	KKG	KGK	KGK
14C00	310	27240	0.52	0.55	0.77	0.80
20C00	320	20640	0.43	0.45	0.70	0.73
26C00	325	14340	0.35	0.37	0.61	0.63
32000	328	8160	0.36	0.36	0.59	0.60

REPTG	BEPTG	RLPEP	GKK	GKG	GKG	GGG
14C00	310	27240	0.98	0.98	1.00	1.00
20C00	320	20640	0.91	0.91	1.00	1.00
26C00	325	14340	0.82	0.82	0.98	0.98
32C00	328	8160	0.74	0.74	0.99	0.99

Table XVII - PA-RESULTS W/R TO POA-SHIFT
SIGBE 20°/BLPEP 100°/ASPECT-ANGLE -300°

B. CONCLUSIONS/RECOMMENDATIONS

The results obtained reflect the effects of the modified - unclassified - parameters. As already has been pointed out, the various parameters in general have the same effects as observed in the UAT-model; so only especially pertinent additional results will be discussed.

1. Conclusions

1. The sensor inaccuracy requires that the extended platform be placed as near to the target as possible. On the other hand the appearance of an HC or an RPV suggests to the target that a missile attack is imminent. If the target initiates evasive maneuvers, of course the targeting-solution is degraded.

2. The stationing of the extended platform at larger angles than 15° to either side of the estimated bearing from the launch platform to the target degrades the PA for all search patterns. If the tactical situation permits, use of at most 10° is recommended.

3. Bow target aspect-angles generally provide higher PA-values for a constant radar cross section target.

4. The POA-shift appears to be even more productive in an OTH-targeting tactical situation.

5. If the tactical scenario permits "optimum" location of the extended platform, then at these ranges a POA-shift allows the choice of a smaller search sector, and TD can be dramatically improved.

2. Recommendations

1. Execute tactical exercises to assure efficient cooperation between launch platform and extended platform and to reduce delaytimes.

2. Station the extended platform prudently to compromise between screening the presence of a SSM launch platform and increasing the PA.

3. Use the POA-shift to counterbalance the degraded sensor quality of the extended platform. This procedure might even lead to relaxed performance criteria and thereby reduce procurement costs.

APPENDIX A

TARGET-MOTION-ANALYSIS

The purpose of this appendix is to analyze the actual target-motion within a given time-period, and its constraints due to several factors.

After a general derivation of a reachable set of locations, specific analyses are made for certain WPN-surface vessels, which yield the maximum values in crossrange- and downrange-deviations from the assumed target-position at launch-time, the point of aim (POA).

Certain tactical situations prohibit the use of some of the available sector-parameter combinations. Therefore the success of the missile-engagement versus the target(s) can be considered as directly dependent on the envelope of target positions accessible prior to Lock-on (with or without changes in course/speed).

Intelligence reports, and enemy contact reports by coastal radar stations and/or by extended platforms normally assure the identity or at least the type(s) of the enemy force,³ if not even the class(es). With this knowledge and under the assumption that an immediate missile-employment is not necessary, the possible limits of the enemy target-motion should be evaluated based on the last known target-motion and target-position. It is reasonable to assume, that with this procedure an improvement of TA or even TD - avoiding an attack on unintended targets - can be

achieved without reduction of the required high acquisition-probability.

Relevant analyses commonly assume that the target's course is uniformly distributed from 0° to 360° , and its speed is also uniformly distributed within a reasonable range. This assumption leads to the unnecessary inclusion of unrealistic target-motions in the consideration leading to the choice of the relevant search-sector parameters. Even the most modern ships, due to their construction characteristics, are restricted to a turning-rate of not exceeding about 30° /second.

This fact implies that a target ship's course is not uniformly distributed over the above mentioned course range. This simplifying and also disadvantageous assumption means that more area has to be covered by the search-sector than actually necessary to assure the required acquisition-probability.

As already pointed out in section III.C.2, this simulation is designed to investigate the influence of course/speed-changes on the PA. In this context it is reasonable to assume that surface forces under missile attack will use all their capabilities to achieve a maximum turning-rate as well as a maximum acceleration, and thereby maximize own defense-weapon concentration and/or to possibly evade the search-sector of the attacking missiles. These capabilities result in a reachable set of possible positions based on the estimated target course and speed. This set is subject to maximum possible course/speed-changes.

The model for this reachable set is based on the analysis for aircraft in [6] , however modified by the following assumptions concerning the target-motion :

1. Any lateral maneuver in the xy-plane is caused by a constant turning-rate at a constant speed (sea-surface is considered as the xy-plane).

2. Only one turning maneuver is allowed during the relevant time-period.

3. The turning maneuver is made in the beginning of the time-period with maximum turning-rate followed by continued motion in a straight line on the new course at maximum speed.

4. Speed variation due to acceleration is averaged, so that the speed is assumed to be constant throughout the time-period.

5. Average speed and turning maneuvers are assumed to be independent.

The first three assumptions imply that a lateral maneuver must take place on a circular arc and that any movement in the xy-plane is either a straight line or a circular arc with an attached, variable length straight course. These two kinds of maneuvers yield locations on an outer boundary of the reachable set. It satisfies the enemy's requirement to withdraw as far as possible from his position upon which the launch might presumably be based. The time available for this maneuver depends on the time of missile detection, and the expected Lock-on-Time, which, however, can not exactly be determined by the enemy.

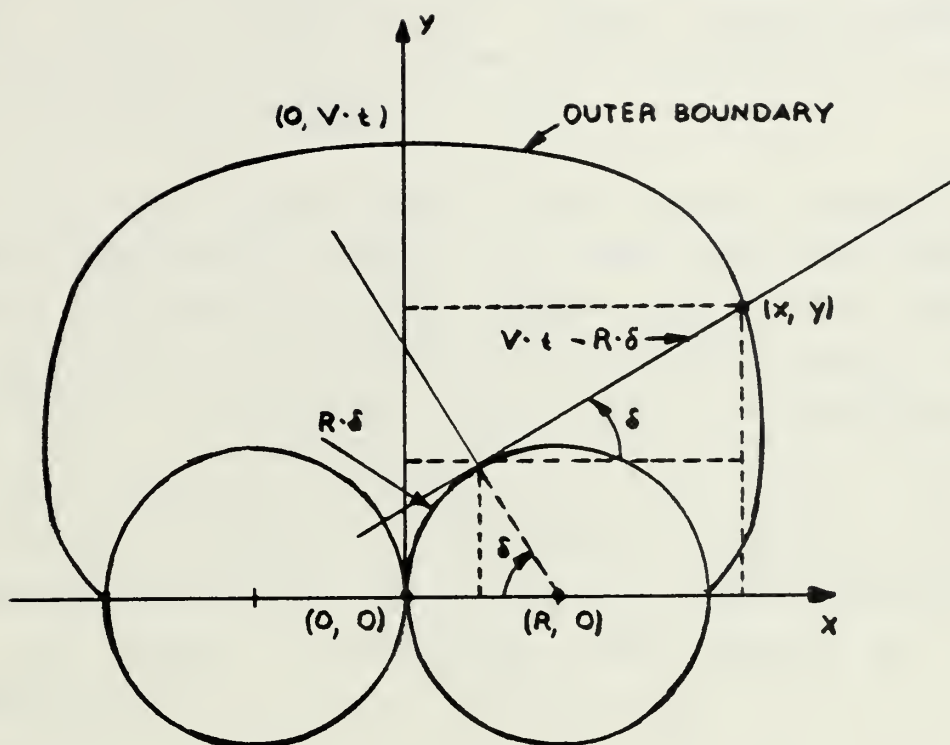


Figure 29 - THE CONSTRUCTION OF THE OUTER BOUNDARY

Assuming the initial velocity vector is pointing along the y-axis, the outer boundary of the reachable set is symmetric about the y-axis, as shown in Fig 30. Δ () is the angle in radians turned through by the target before deciding to proceed on a straight course. The x, y coordinates of half the outer boundary as a function of (δ) are then given by

$$x(\delta) = R*(1-\cos\delta) + (v*t-R*\delta)*\sin\delta, \text{ and}$$

$$y(\delta) = R*\sin\delta + (v*t-R*\delta)*\cos\delta.$$

The maximum length of the distance travelled is $v*t$, where v corresponds to the missile speed, and t is the time, at which the missile locks on the target; R is the minimum turn radius, based on a 90° turn. If the delay due to the assumed reaction-time is to be included, then $y(\delta)$ must be

increased by the additional distance travelled. This outer boundary then represents the maximum possible realistic target-positions within the time from launching the missile until the expected Lock-on.

The TA - analysis has to come up with search-sector parameter combinations, which will cover a maximum number of points of this set as well as points within the position area generated by the boundary - in case the target should not accelerate as expected. Fig 31 shows the comparison of such a set, a circular position area based on the maximum length of the distance travelled as the radius, and the search sector combination GKK without a shift of the POA. Performance data for the DDG target (low initial speed) at a range of 26000 m (RP5-range) are assumed for this illustration.

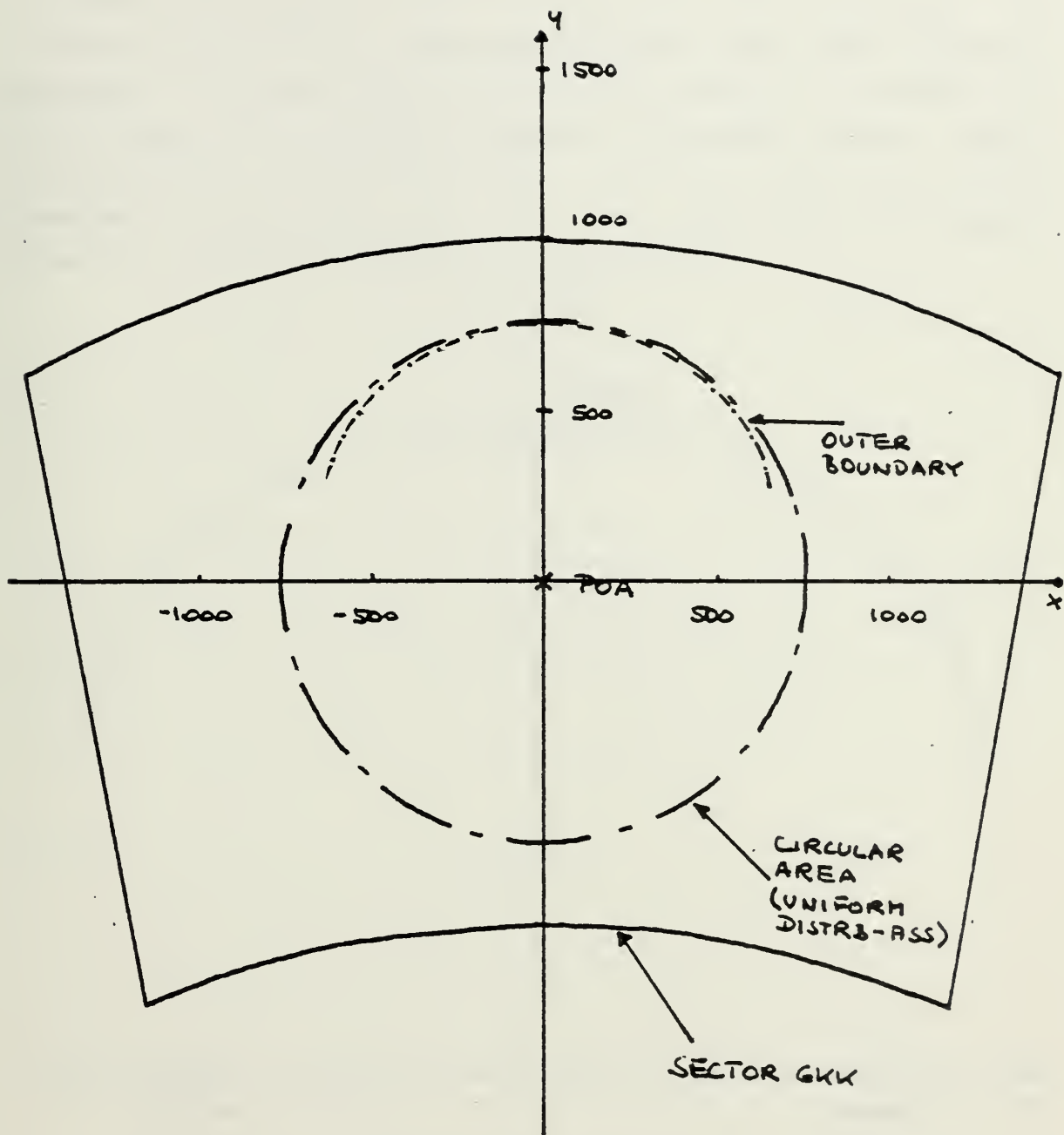


Figure 30 - THE COMPARISON OF TWO POSITION AREAS AND A SEARCH-SECTOR

The outer boundary set only encloses about 60% of the area obtained from the usual analysis; it is also evident that target-discrimination is facilitated by utilizing the reachable set for the analysis. If less time until expected Lock-on is "available", the outer boundary is reduced and vice versa. It is obvious that for the other target types corresponding relations hold. Fig 30 shows an outer boundary for the DDG target at the respective RP1-range, when the activation-distance K is chosen.

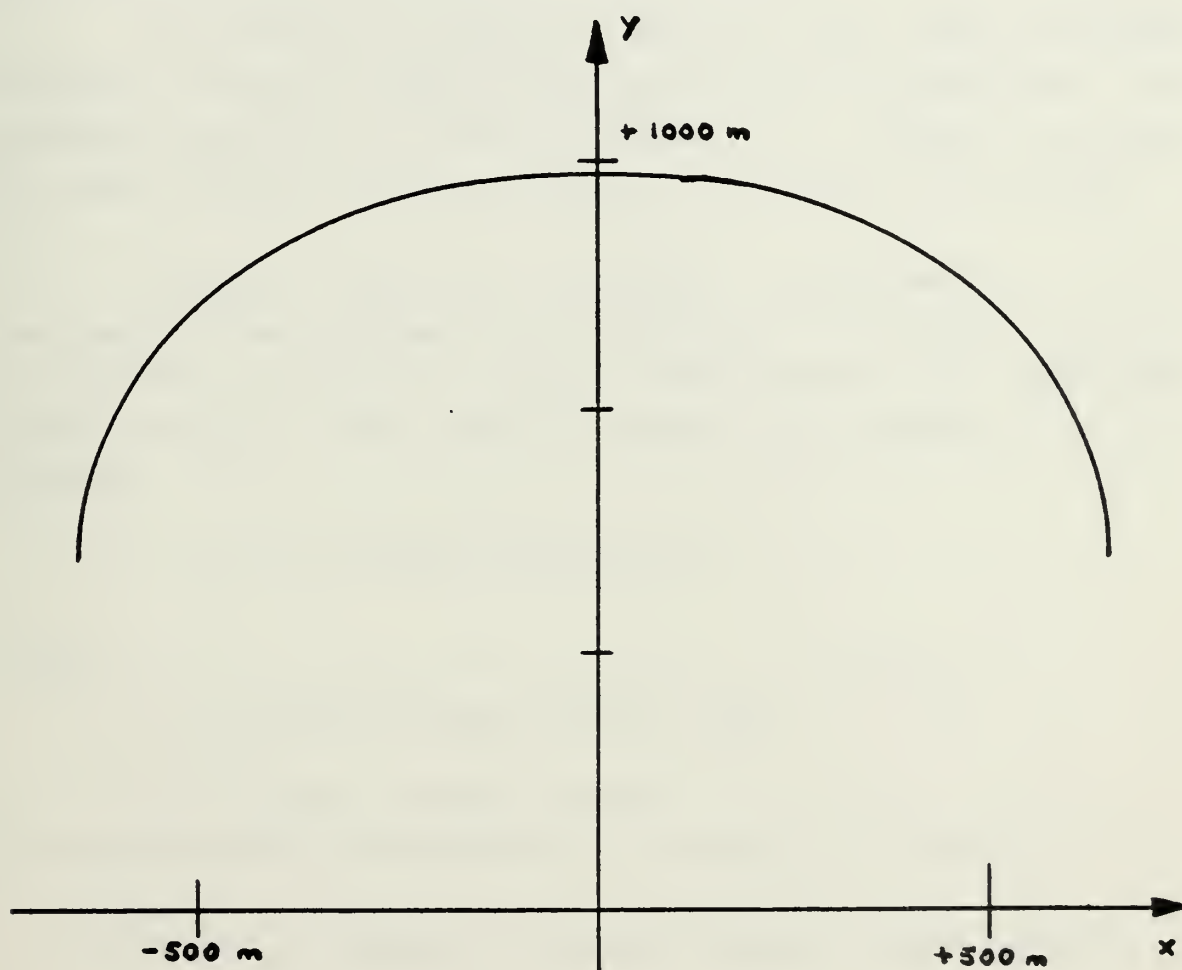


Figure 31 - OUTER BOUNDARY FOR DDG KRIVAK-CLASS

APPENDIX B

ELECTROMAGNETIC RADIATION RANGE PREDICTION

This section provides a method from which various relevant detection ranges were derived for the analysis. As already pointed out in section III.A., no surface ducting or other effects on electromagnetic radiation are assumed.

Typical radar and infrared performance in a non-ducting environment is dependent on sensor antenna height and the amount of target area above the resulting radar horizon. The radar horizon is defined to be (in meters)

$$R_H = 4.115 * (\sqrt{A} + \sqrt{H}) * 1000.0$$

where

A = sensor antenna height, and

H = height of the target.

The probability of detection at range R_H is assumed to be

0.1 when H_1 = height of target's height sensor antenna,

0.5 when H_2 = height of target's bridge, and

0.9 when H_3 = height of target's maindeck.

The respective ranges from the radar horizon formula are denoted as RP1, RP5, and RP9. Pertinent parameters used in

the sensor performance range prediction are [3].

HEIGHT SHIP	A	H1	H2	H3
FPBG-143-	10.7	0.0	0.0	0.0
DDG	21.7	21.7	10.1	4.6
PFG	14.0	14.0	9.8	3.1
FPBG-GSA-	9.2	9.2	4.6	3.1
LSM	17.7	17.7	8.5	3.1

DIMENSION: M

The resulting approximated R_H -values of the FPBG 143-Class towards the WPN surface combattants (radar sensor) are as follows:

TYPE RANGE	DDG	PFG	FPBG	LSM
RP9	22000	20000	20000	20000
RP5	26000	26000	22000	25000
RP1	32000	29000	26000	29000

DIMENSION: M

It is possible that the WPN have sensors available which might detect the attacking missile very early, even

before the SSM actively radiates in its search mode. The radar horizon formula yields the following against a MM 38 missile which is assumed to fly at an average altitude of 10 m. This altitude is considered to be equivalent to the previously defined altitude H_2 .

The resulting R_H -values (RNG5) are as follows:

- DDG...: 31500 m
- PFG...: 28000 m
- FPBG...: 25000 m
- LSM...: 28500 m.

these values are used to determine the possible target reaction-time for the UAT-scheme. R_H -values are based on the line-of-sight condition, which provides a lower bound on electromagnetic radiation performance. The upper bound is a result of ducting, primarily by way of evaporative duct. Reference [7] provides a method of predicting the existence of this duct-type.

APPENDIX C

SIMULATION-MODEL MM38-UAT


```

23C GC TO 240
24C YMAX = VYAVG*TY
C IF (YMAX-L(1))+3.0*SIGRL
C IF (IFLAGP.EQ.0) GO TO 250
C IF (Q.LT.0.0) GO TO 250
C
C *****
C PCA = Q
C GC TO 260
C FCA = 0.0
C *****
C
25C
C
26C RFCAL = SQRT(POA**2+(RANGE1(I))**2-2.0*POA*RANGE1(I)*COS(E1))
C IF (POA.GT.0.0) GO TO 270
C Z1 = 0.0
C GC TO 280
27C Z1 = ARSIN((POA*SIN(E1))/RPOA1)
28C IF (DEG1(K).GT.180.0) GO TO 290
C Z1 = A1(K)-Z1
C GC TO 300
29C Z1 = A1(K)+Z1
30C Z1 = Z1*CF
C
C
C CC 310 KA=1,NA
C
C CC 310 KT=1,NT
C
C CC 310 KL=1,NL
C PC(I,KA,KT,KL) = 0.0
C P(I,KA,KT,KL) = 0.0
C
C
C
C CC 550 ISIM=1,NSIM
C
C CALL NCRML (NCOURS,ZCOURS,1)
C TRUCRS = ESTCRS+ZCOURS*SIGCL
C PSI = TRUCRS*RADIAN
C
C CALL NCRML (NSPD,ZTSPC,1)
C VV = V1+ZTSPC*SIGSL
C IF (ACC.EQ.0.0) GO TO 320
C ACCTIM = (V1MAX-VV)/ACC

```

```

MM381410
MM381420
MM381430
MM381440
MM381450
MM381460
MM381470
MM381480
MM381490
MM381500
MM381510
MM381520
MM381530
MM381540
MM381550
MM381560
MM381570
MM381580
MM381590
MM381600
MM381610
MM381620
MM381630
MM381640
MM381650
MM381660
MM381670
MM381680
MM381690
MM381700
MM381710
MM381720
MM381730
MM381740
MM381750
MM381760
MM381770
MM381780
MM381790
MM381800
MM381810
MM381820
MM381830
MM381840
MM381850
MM381860
MM381870
MM381880

```



```

C 390 CALL RANDOM (NTIME1,UTURN1,1)
      IF (UTURN1.GT.0.9999) UTURN1=0.9999
      IF (T9.GT.TIME1) GO TO 400
      TT1 = UTURN1*T9
      GC TO 410
      TT1 = UTURN1*TIME1
      DELTA1 = TT1*TRNRTE
      CL = DELTA1*RADIAN
C
      TGLX1 = RADIUS*(1.0-COS(DI))+(YR1-RADIUS*DI)*SIN(DI)
      TGLY1 = YY+RADIUS*SIN(DI)+(YR1-RADIUS*DI)*CCS(CI)
      TGLX2 = (-1)*TGLX1
      TGLY2 = TGLY1
C
      TGLX1R = TGLX1*COS(PSI)+TGLY1*SIN(PSI)
      TGLY1R = (-1)*TGLX1*SIN(PSI)+TGLY1*CCS(PSI)
      TGLX2R = TGLX2*COS(PSI)+TGLY2*SIN(PSI)
      TGLY2R = (-1)*TGLX2*SIN(PSI)+TGLY2*CCS(PSI)
C
      TGLX1 = XPOS1+TGLX1R
      TGLY1 = YPOS1+TGLY1R
      TGLX2 = XPOS1+TGLX2R
      TGLY2 = YPOS1+TGLY2R
C
      *****
      ** DECISION FOR TURN-DIRECTION **
      *****
C
      CALL RANDOM (NTURN1,UPOS1,1)
      IF (UPOS1.GT.0.9999) UPOS1=0.9999
      IF (UPOS1.GT.0.5000) GC TO 420
      SIMIX = TGLX1
      SIMIY = TGLY1
      GC TO 430
      SIMIX = TGLX2
      SIMIY = TGLY2
C 420
      *****
      ** TEST FOR TARGET-ACQUISITION **
      *****

```



```

C      C      430      TAL1(KT) = ZETA1-THETA(KT)
      C      TAL2(KT) = ZETA1+THETA(KT)
      C      XTEST1 = SIM1X-XLOCK1
      C      YTEST1 = SIM1Y-YLOCK1
      C      R1 = SQRT(XTEST1**2+YTEST1**2)
      C      G1 = ARSIN(XTEST1/R1)
      C
      C      IF (DEG1(K).LT.090.0) GO TO 450
      C      IF (CEG1(K).EQ.090.0) GO TO 440
      C      IF (DEG1(K).LT.270.0) GO TO 470
      C      IF (DEG1(K).EQ.270.0) GO TO 460
      C      IF (DEG1(K).LE.360.0) GO TO 480
      C
      C      440 IF (SDETBL.GE.0.0) GO TO 470
      C      450 GAMMA1 = G1*CF
      C      GC TO 490
      C      460 IF (SDETBL.GE.0.0) GO TO 480
      C      470 GAMMA1 = (-1)*G1*CF+180.0
      C      GC TO 450
      C      480 GAMMA1 = G1*CF+360.0
      C      490 IF ((GAMMA1.GT.TAU1(KT)).AND.(GAMMA1.LT.TAU2(KT))) GO TO 500
      C      EC TO 530
      C
      C      500 CC 520 KL=1,NL
      C      RTEST1(KL) = ACTIV(KA)-(TDEL(KT)-TLAUN)*VEXCC1+L(KL)
      C      RTEST2(KL) = ACTIV(KA)-(TDEL(KT)-TLAUN)*VEXC+1+L(KL)
      C      IF ((R1.LT.RTEST1(KL)).AND.(R1.GT.RTEST2(KL))) GO TO 510
      C      GC TO 520
      C      510 P(I,KA,KT,KL) = P(I,KA,KT,KL)+1.0
      C      520 CCNTINUE
      C
      C      530 CCNTINUE
      C
      C      540 CCNTINUE
      C
      C      550 CCNTINUE
      C
      C      CC 560 KA=1,NA
      C

```

```

MM3833330
MM3833340
MM3833350
MM3833360
MM3833370
MM3833380
MM3833390
MM3833400
MM3833410
MM3833420
MM3833430
MM3833440
MM3833450
MM3833460
MM3833470
MM3833480
MM3833490
MM3833500
MM3833510
MM3833520
MM3833530
MM3833540
MM3833550
MM3833560
MM3833570
MM3833580
MM3833590
MM3833600
MM3833610
MM3833620
MM3833630
MM3833640
MM3833650
MM3833660
MM3833670
MM3833680
MM3833690
MM3833700
MM3833710
MM3833720
MM3833730
MM3833740
MM3833750
MM3833760
MM3833770
MM3833780
MM3833790
MM3833800

```


APPENDIX D

SIMULATION-MODEL MM38-OTH


```

10R (1 SIGMA) : ,F4.1, DEGREES, //, 15X, SENSOR RANGE ERRCR (1 SIGMM38
2A) : ,F5.1, METERS, //) MM38
15C FCRMAT ( ,0, 15X, TARGET-DATA ACCURACIES (3 SIGMA) BY EXTENDED PLATMM38
160 FCRMAT ( ,0, 15X, COURSE : 10.0 DEGREES, //, 20X, SPEED : 3.0 KN, //) MM38
17C FCRMAT ( ,0, 15X, COURSE LAUNCH-PLATFORM 360 DEGREES, //, 16X, LOCATMM38
18C FCRMAT ( ,0, 15X, COURSE LAUNCH-PLATFORM -15 TO +15 DEGREES, //) MM38
19C FCRMAT ( ,0, 15X, ASPECT - ANGLE : ,F7.1, * ,5X, BEARING : ,F6.1, //) MM38
20C FCRMAT ( ,0, 15X, BEARING LAUNCH-PLATFORM - EXTENDED PLATFCRM : ,F6. MM38
21C FCRMAT ( ,0, 15X, RANGE LAUNCH-PLATFORM - TARGET : ,F8.1, METERS, // MM38
22C FCRMAT ( ,0, 15X, SHIFT OF THE POINT-OF-AIM BY, F6.1, METERS IN DIRMM38
23C FCRMAT ( ,0, 15X, * MISSILE LAUNCHED IN, F6.1, DEGREES AT A RANGE CMM38
24C FCRMAT ( ,0, 15X, ACTIVATION - DISTANCE: K, //, 7X, REPTG, T17, BEPMM38
25C FCRMAT ( ,0, 15X, RLPEP, T38, KKK, T46, KKG, T56, KGG, //) MM38
26C FCRMAT ( ,0, 15X, ACTIVATION - DISTANCE: G, //, 7X, REPTG, T17, BEPMM38
27C FCRMAT ( ,0, 15X, RLPEP, T38, GKK, T46, GKG, T56, GGG, //) MM38
28C FCRMAT ( ,0, 15X, F7.1, T17, F5.1, T24, F7.1, T37, F6.4, T55, F6.4, TMM38
29C FCRMAT ( //) MM38
CALL OVFLOW MM38
NCCURS = 412089 MM38
NSPD = 2301473 MM38
NSPD1 = 7683021 MM38
NDELAY = 753021 MM38
NCET1 = 3658709 MM38
NLCCK = 4321078 MM38
NTIME1 = 7852014 MM38
NTLRN1 = 1425836 MM38
ESTCRS = 0.0 MM38
NSIM = 400 MM38
REAL = NSIM MM38
IFLAGP = 0 MM38
REAC (5,20) THETA(1), THETA(2) MM38
REAC (5,20) ACTIV(1), ACTIV(2) MM38
READ (5,20) L(1), L(2) MM38
READ (5,30) V, VMAX, TRNRTE, ACC MM38
V1 = V*CFS MM38
V1MAX = VMAX*CFS MM38
T5 = 90.0/TRNRTE MM38
WCRAC = WDIREC*RADIAN MM38

```

C C

C C

C


```

C
C
C
ALFAC = A1(K)*RADIAN
ALFAL(K) = DEG1+A1(K)
IF (ALFAL(K).GT.360.0) ALFAL(K)=ALFAL(K)-360.0

C
C
C
DC 650 I=1,NR
RANGE1(I) = (I+7)*400.0
RLFTG1 = RANGE1(I)
TREAC = DEL
Y = V1*TREAC

C
XRNG1 = RANGE1(I)*SIN(DG1)
YRNG1 = RANGE1(I)*COS(DG1)

C
C
DC 640 KK=1,NEPTG1

C
C
DC 620 KX=1,2

C
IF (K.EQ.1) GO TO 280
IF (K.EQ.2) GO TO 280
IF (K.EQ.3) GO TO 290
IF (K.EQ.4) GO TO 300

C
280 SAFETY = 10000.0
GC TO 310
290 SAFETY = 12000.0
RLEMIN = 12000.0
GC TO 310
300 SAFETY = 14000.0
RLEMIN = 14000.0

C
310 CCRAD = PI-ARSIN((RANGE1(I)*SIN(AIRAD))/SAFETY)
BERAD = PI-(AIRAD+CCRAD)
RLEMAX = (RANGE1(I)*SIN(BBRAD))/SIN(CCRAD)
L1FF = RLEMAX-RLEMIN
INCRNG = DIFF/3000.0

C
IF (K.EQ.3) RLEMIN = 12000.0

C
A1(KK) = RLEMIN+(KK-1)*INCRNG*1000.0
C1RAD = PI-ARSIN((RANGE1(I)*SIN(A1RAD))/A1(KK))
C1 = C1RAD*CF
B1RAD = PI-(AIRAD+C1RAD)
E1 = B1RAD*CF
RLPE1(KK) = (RANGE1(I)*SIN(B1RAD))/SIN(C1RAD)

```

```

MM381410
MM381420
MM381430
MM381440
MM381450
MM381460
MM381470
MM381480
MM381490
MM381500
MM381510
MM381520
MM381530
MM381540
MM381550
MM381560
MM381570
MM381580
MM381590
MM381600
MM381610
MM381620
MM381630
MM381640
MM381650
MM381660
MM381670
MM381680
MM381690
MM381700
MM381710
MM381720
MM381730
MM381740
MM381750
MM381760
MM381770
MM381780
MM381790
MM381800
MM381810
MM381820
MM381830
MM381840
MM381850
MM381860
MM381870
MM381880

```



```

C      REPTG1 = AA1(KK)
C      REPTG1(KK) = ALFA1(K)-(180.0-C1)

C      SCRL = SIGRL
C      SEL = SIGBL*RADIAN
C      SCEL = RLPEP1(KK)*TAN(SBL)

C      SCRE1 = SIGRE
C      SCBE1 = REPTG1*TAN(SBE)

C      SDEVBL = Sqrt(SDBL**2+SDBEL**2)
C      SDEVRL = Sqrt(SDRL**2+SDREL**2)

C      TY = (RANGEL(I)-ACTIV(I)+(TDEL(I)-TLAUN)*VMISS)/VMISS
C      VY = V1+ACC*TY
C      VYFIN = AMIN1(V1MAX,VY)
C      VYAVG = (V1+VYFIN)/2.0
C      IF (ACT.GT.TY) GO TO 320
C      YMAX = VYAVG*ACT+(TY-ACT)*VYFIN
C      GC TO 330
C      YMAX = VYAVG*TY
C      Q = YMAX-L(1)+3.0*SDEVRL
C      IF (IFLAGP.EQ.0) GO TO 340
C      IF (Q.LT.0.0) GO TO 340

C      ***
C      ** GENERATION OF ESTIMATED MISSILE LOCK-CN-POSITION **
C      ** W/R TO A SHIFT OF THE PCA **
C      ***
C      FCA = Q
C      GC TO 350
C      FCA = 0.0
C      ***
C      ***
C      FFCAL = Sqrt(POA**2+RLPTG1**2-2.0*POA*RLPTG1*COS(ET1))
C      IF (POA.GT.0.0) GO TO 360
C      Z1 = 0.0
C      GC TO 370
C      Z1 = ARCSIN((POA*SIN(ET1))/RPOA1)
C      36C Z1 = DEGI.CE.360.0) GO TO 380
C      37C ZAI = DGI-Z1
C      GC TO 350

```

```

MM381850
MM381900
MM381910
MM381920
MM381930
MM381940
MM381950
MM381960
MM381970
MM381980
MM381990
MM382000
MM382010
MM382020
MM382030
MM382040
MM382050
MM382060
MM382070
MM382080
MM382090
MM382100
MM382110
MM382120
MM382130
MM382140
MM382150
MM382160
MM382170
MM382180
MM382190
MM382200
MM382210
MM382220
MM382230
MM382240
MM382250
MM382260
MM382270
MM382280
MM382290
MM382300
MM382310
MM382320
MM382330
MM382340
MM382350
MM382360

```


LIST OF REFERENCES

1. W.Schmidt, Fregattenkapitaen FGN, The West German Navy's Class 143 Fast Patrol Boat. The S-148 Class Fast Patrol Boats, Published in International Defense Review, Vol.3-1973, p.337-341, Interavia Switzerland, 1973.
2. Snias, The Antiship Missile Exocet, Published in International Defense Review, Vol.3-1976, p.395-399, Interavia Switzerland, 1976.
3. J.E.Moore, Captain RN, Jane's Fighting Ships 1976-77, Jane's Yearbooks, p.709, 719, 721, and 727, 1976,
4. G.S.Fishman, Concepts and Methods in Discrete Event Digital Simulation, p.16-19, John Wiley Sons, Inc., 1973.
5. M.G.Natrella, Experimental Statistics, Handbook 91 National Bureau of Standards, p.7-4 to 7-5, United States Department of Commerce, 1963.
6. P.J.Wong and A.J.Korsak, Reachable Sets for Tracking, Operations Research Vol.22 Nr.3, p.497-509, 1974,
7. The Analysis and Forecasting of Radar Refractivity, Unclassified, Commander, Naval Weather Service Command, Navair 50-1P-1, July 1967.

INITIAL DISTRIBUTION LIST

	No. Copies
1. Defense Documentation Center Cameron Station Alexandria, Virginia, 22314	2
2. Library, Code 0212 Naval Postgraduate School Monterey, California, 93940	2
3. Department Chairman, Code 55 Department of Operations Research Naval Postgraduate School Monterey, California, 93940	2
4. Professor D.E.Harrison, Jr., Code 61Hx Department of Physics Naval Postgraduate School Monterey, California, 93940	3
5. Assoc.Professor A.R.Washburn, Code 55Ws Department of Operations Research Naval Postgraduate School Monterey, California, 93940	1
6. Bundesministerium der Verteidigung Fue M VII 4 5300 Bonn Federal Republic of Germany	1
7. Amt fuer Studien und Uebungen der Bundeswehr MBOR - Gruppe Seekrieg - Einsteinstrasse	1

8012 Ottobrunn

Federal Republic of Germany

- | | | |
|-----|---|---|
| 8. | Korvettenkapitaen Lueneburg
2.Schnellbootgeschwader
2340 Kappeln-Olpenitz
Federal Republic of Germany | 1 |
| 9. | Marineamt -A1-
294 Wilhelmshaven
Federal Republic of Germany | 1 |
| 10. | Dokumentationszentrale der Bundeswehr
Friedrich-Ebert-Allee 34
5300 Bonn
Federal Republic of Germany | 1 |
| 11. | Commander Naval Surface Forces Pacific
-N 674-
San Diego
California | 1 |
| 12. | Center for Naval Analysis
Att. LCDR J.McCormack 1401 Wilson Boulevard
Arlington, Virginia 22209 | 1 |
| 13. | Bernd Lehmann
Kapitaenleutnant
Seetaktische Lehrgruppe
2940 Wilhelmshaven
Federal Republic of Germany | 3 |

Thesis

169938

L467

Lehmann

c.1

Missile employment
from fast patrol boats.
A computer-based anal-
ysis of the search-sec-
tor parameters.

14 DEC 78

JUL 11 '78

25266

24 APR 81

53091

20 SEP 84

29479

3 FEB 87

51149

Thesis

169938

L467

Lehmann

c.1

Missile employment
from fast patrol boats.
A computer-based anal-
ysis of the search-sec-
tor parameters.



thesL467

Missile employment from fast patrol boat



3 2768 001 03181 8

DUDLEY KNOX LIBRARY